Phase I
Final Report

CRYOGENIC HYDROGEN/HELIUM STORAGE AND SUPPLY SYSTEM
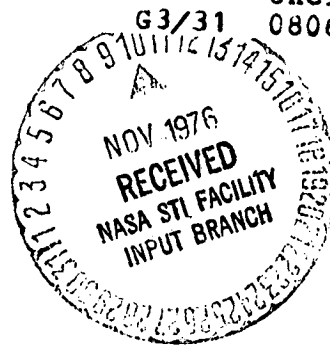
75-11607

February 3, 1976

NOV 1976
RECEIVED
NASA STI FACILITY
INPUT BRANCH

Prepared for

National Aeronautics and Space Administration
George C. Marshall Space Flight Center
Marshall Space Flight Center, Alabama 35812

GARRETT

AIRESEARCH MANUFACTURING COMPANY
OF CALIFORNIA

FOREWORD

The Cryogenic Hydrogen/Helium Storage and Supply System Program, Phase I, was completed under NASA Contract NAS8-30574, by the AiResearch Manufacturing Company of California, a division of The Garrett Corporation. This work was sponsored by the George C. Marshall Space Flight Center, MSFC, Alabama, and administrated under direction of Mr. Eric Haschal Hyde, EP43.

The Phase I program performance period dates from 15 May 1974 to 21 November 1975. This final report was prepared by Mr. R. H. Norman and Mr. R. D. Raynor, who were also responsible for the analytical and development efforts on the program.

ABSTRACT

The Cryogenic Hydrogen/Helium Storage and Supply System Program, Phase I, involved refurbishing an existing cryogenic tank, installing microspheres in the tank annulus, and testing the thermal performance of the unit. The performance data was compared with NRC-2 multilayer insulation and low-emittance aluminized surfaces installed in tanks of the same basic design. Phase II (pending authorization to proceed) is concerned with developing a He-II (superfluid) Joule-Thomson cryostat to provide fractional watt cooling at 2 K, making use of the present tank for storage and supply of supercritical helium.

The cryogenic tank modified during the program was originally designed for the Manned Orbiting Laboratory (MOL) Program, and subsequently modified by vacuum-depositing aluminum on all annulus surfaces and leaving out the NRC-2 multilayer insulation.

A comparison of performance data from all three tanks shows the heat leak of the low-emittance-annulus tank to be almost 40 percent higher than the multilayer-insulated tank, while the aluminized-microsphere-insulated tank heat leak is higher by a factor of 4.8. That same microsphere-insulated tank measured heat leak is 2.5 times higher than is predicted using some of the published data and current theory, while the measured VCS temperature is 69 R lower than predicted. Other recent data agrees quite well with measured tank performance.

It is concluded that the application of aluminized-microsphere insulation is not yet very predictable for tank design purposes, especially at LH_2 temperature and in the presence of a vapor-cooled shield. It is recommended that this tank design be further evaluated and tested with microsphere insulation to determine the reasons for the poor thermal performance, and to provide better understanding of microsphere thermal behavior and application.

CONTENTS

CONTENTS (Continued)

SECTION 1

INTRODUCTION AND SUMMARY

INTRODUCTION

This report describes Phase I of a two-phase program concerned with development of a cryogenic hydrogen/helium storage and supply system for the NASA Marshall Space Flight Center (MSFC). Phase II is to develop a Joule-Thomson cryostat for cooling to 2 K. The Phase I work was conducted for NASA MSFC under NASA Contract NAS8-30574 by the AiResearch Manufacturing Company of California, over the period between 15 May 1974 and 21 November 1975. The issuance of this report concludes Phase I of the program.

The information presented in this report is summarized below.

Section 1, Introduction and Summary, briefly overviews the program activity and summarizes the results of the work accomplished during Phase I.

Section 2, Equipment Description, describes the physical characteristics of the cryogenic hydrogen/helium tank assembly modified and tested during Phase I.

Section 3, Program Task Narrative, discusses the six individual work tasks of Phase I and describes the work performed.

Section 4, Performance and Analysis, presents the test data analysis and performance comparison of three different insulation systems in cryogenic tanks of the same basic (MOL) design.

Section 5, Conclusions and Recommendations, gives conclusions based on the performance and analysis of Section 4, and makes recommendations for future work.

PROGRAM OVERVIEW

The planned work consisted of a six-task effort briefly described below.

Task I--Evaluation and Repair

An evaluation of the second MOL tank built under Air Force contract F04611-71-C-0020 was conducted to determine the location of annulus leakage and the repair method that would render the tank useful for the NASA MSFC program. The tank was disassembled, the leak located, repaired, and leak checked. The leak check showed the tank to be satisfactory for use.

Task II--Instrumentation Installation

Three sensors were installed in the tank to monitor various temperatures:
(1) in the pressure vessel fill port to measure stored liquid temperature;
(2) at the pressure vessel vent port to measure the ullage temperature; and
(3) on the vapor-cooled shield (VCS) surface near the exit of the vent line.

Task III--Tank Modification

During Task III, a preliminary analysis of helium delivery to the cryostat
(for Phase II) was performed. This analysis included: literature search for
helium-II data; performance predictions of the microsphere-insulated tank;
analysis of the J-T process for He-II; and test setup considerations. This
work led to the design of a separate supply line and new outer tank boss
(cryostat adapter). This modification should allow the tank performance
required to deliver cold helium to the Phase II J-T cryostat.

Task IV--Microsphere Insulation

The required amount of microspheres were ordered from The 3M Company, and
inspected for quality. Inspection revealed negligible sphere-breakage, there-
fore no processing was performed to remove broken spheres. Following a tare-
weight determination, the microspheres were installed in the tank annulus, and
the tank with microspheres installed was weighed.

Task V--Annulus Evacuation and Pressure Test

During Task V, the tank assembly was processed for 35 days at elevated
temperature (210 F) and reduced pressure (1×10^{-4} torr) to remove entrapped
gases. The ultimate pressure reached during the last 6 days of the bake-out
period was 3.5×10^{-4} torr.

Task VI--Vented Weight Loss Test

A thermal performance test (vented weight loss) with liquid hydrogen was
conducted at the AiResearch Mint Canyon Remote Test Facility. During testing,
thermal acoustic oscillations were observed giving rise to unanticipated experi-
mentation and procedure changes. The test was significantly extended in order
to compile enough data from which to select suitable periods for analysis
(presented in Section 4).

SUMMARY

The thermal performance of the NASA MSFC tank assembly was compared with
the thermal performance of the first MOL design configuration (employing multi-
layer insulation) and the second (employing low-emittance aluminized annulus
surfaces, without multilayer insulation), both of which were reported under
Air Force contract F04611-71-C-0020.

The original multilayer insulation design exhibited the lowest heat leak; the second configuration exhibited a 40 percent higher heat leak than the first; and the NASA MSFC tank assembly (the third configuration, with aluminized microspheres) exhibited much greater heat leak than the first two, by about a factor of 4.

The predicted performance of the third tank configuration based on recently published theory of microsphere insulation and calorimeter data, did not agree with the test data. Some of the most recent data for aluminized microspheres tended to agree more closely. It was concluded that, at the present time, aluminized-microsphere insulation is not sufficiently predictable for VCS tank design purposes, (especially LH_2 and LHe applications), although more technical information is becoming available.

AiResearch recommends that testing be continued with the NASA MSFC test article to aid in developing improved predictability of the applied thermal performance of aluminized-microsphere insulation.

SECTION 2

EQUIPMENT DESCRIPTION

INTRODUCTION

Equipment modified and tested during Phase I of this contract consisted of a cryogenic hydrogen/helium tank (AiResearch P/N 851240-2-1, modified), mounted in a cryogenic tank handling dolly (AiResearch P/N 956112-1-1). Tank modifications were not formally documented by engineering drawings; engineering sketches were used by manufacturing to perform tank modifications and other work operations.

The cryogenic hydrogen/helium tank assembly was originally designed to store and maintain hydrogen in a supercritical state. In the original design, internal instrumentation consisted of fluid quantity gauging and temperature measurement, with associated electronic signal conditioners (mounted externally). For this application, the instrumentation system was modified to remove the electronic signal conditioning packages, disable the quantity gauging system, and install an additional temperature sensor to monitor the VCS surface temperature. A cross sectional schematic of the tank is shown in Figure 2-1, showing the approximate orientation of the fluid lines and bosses in the normal vent test configuration. The physical characteristics of the tank assembly are given in Table 2-1.

GENERAL DESCRIPTION

The tank assembly (Figure 2-2) is constructed of two concentric, leak-tight spheres. The inner sphere is a pressure vessel which stores approximately 87 lbs of liquid hydrogen, or 150 lbs of liquid helium, in a volume of 20 cu ft. The outer shell provides a vacuum environment for the annular volume which contains a vapor-cooled shield and insulating material. Instrumentation is provided for monitoring temperatures at selected locations.

The insulation system consists of an evacuated annulus, a vapor-cooled shield (VCS), and an insulating material consisting of aluminized glass microspheres. The annulus surfaces of the inner and outer shells and the VCS are covered with vacuum-deposited aluminum, over a resin undercoat. Glass microspheres in the evacuated annulus reduce heat conduction and radiation from the outer shell to inner tank wall. During normal venting, fluid exits from the tank through tubing physically and thermally attached to the aluminum VCS. By this method of fluid delivery the VCS is cooled, removing heat from the annulus and improving thermal performance. The inner pressure vessel and the VCS are supported within the outer vessel by compressed fiberglass support pads that have a low thermal conductivity.

DETAILED DESCRIPTION

Inner Pressure Vessel

The inner pressure vessel is fabricated from forged titanium 5A1-2.5Sn ELI hemispheres which are finished, machined, and welded together. The wall of
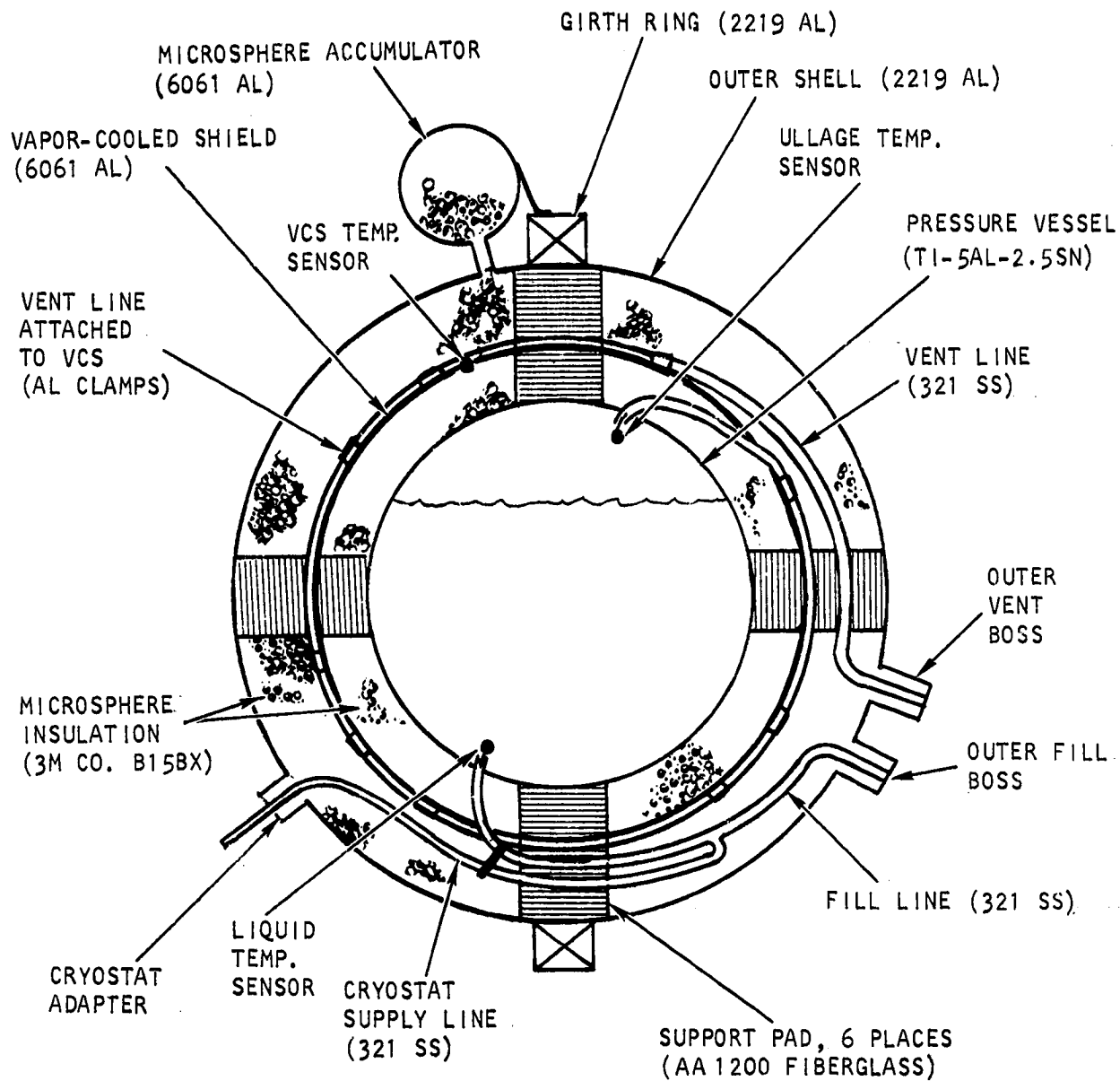
Normal Vent Orientation   S-98020

Figure 2-1.   Cryogenic Hydrogen/Helium Tank Cross-Sectional Schematic

TABLE 2-1

TANK PHYSICAL CHARACTERISTICS

Item	Design Value
Materials	
Pressure vessel	Titanium 5Al-2.5Sn
Vapor-cooled shield	Aluminum 6061
Outer shell and girth ring	Aluminum 2219
Insulation	Microspheres ($\sim$100μ)
Support pads	Fiberglass AA-1200
Dimensions (nominal), in.	
Pressure vessel ID	40.445
Wall thickness	0.045
Vapor-cooled shield ID	41.50
Wall thickness	0.060
Outer shell OD	43.26
Wall thickness	0.055
Volumetric Capacity (nominal), cu. ft.	
At room temperature	20.05
At LH_2 normal boiling point	19.93
Weights (nominal), lb	
Dry weight	160
Liquid hydrogen	87
Liquid helium	150
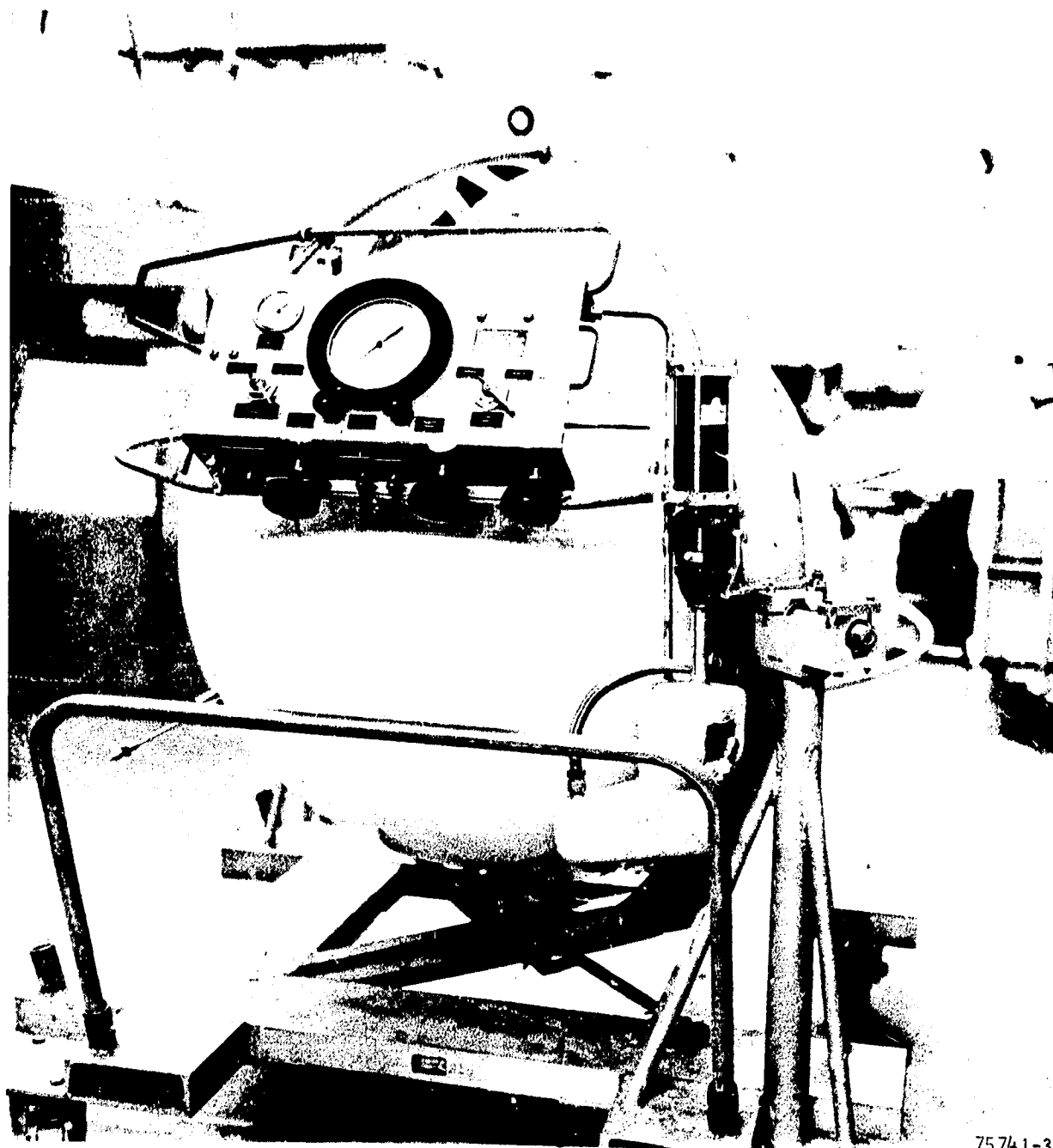
75741-3

Figure 2-2. Cryogenic Hydrogen/Helium Tank Assembly (View 1)
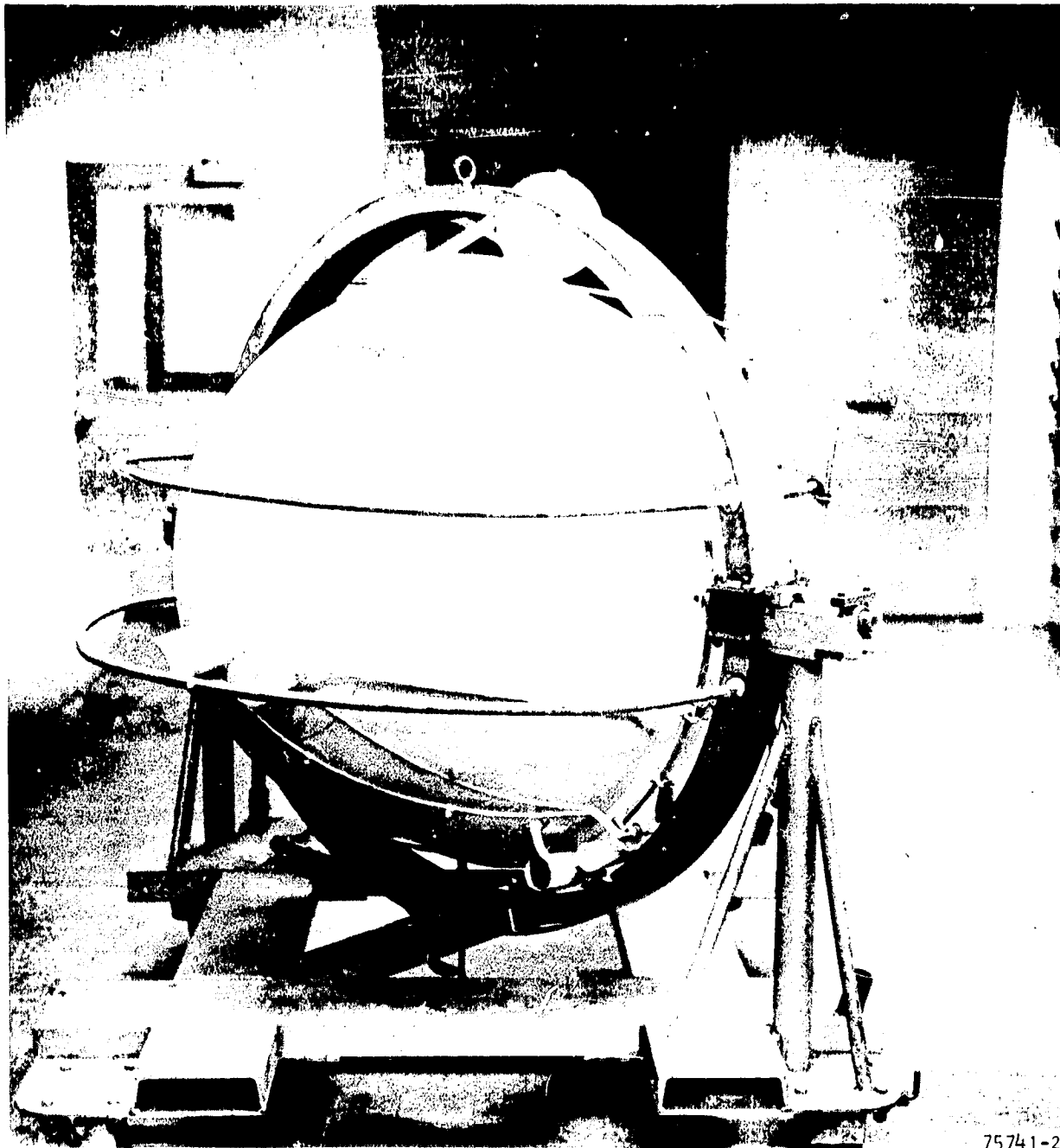
75741-2

Figure 2-2. Cryogenic Hydrogen/Helium Tank Assembly (View 2)

this vessel is designed to withstand both the internal pressure loads and local buckling loads imposed by the compressive support pads. Nominally, the shell is 0.045 in. thick; this wall thickness is designed for the burst pressure of 640 psi (2 times the maximum operating pressure of 320 psi) at 200 R. The wall thickness of the region under the support pads is increased to 0.080 in. to withstand the loads of the supports. The diameter of the thicker wall region is 9.00 in. which is 3.0 in. larger than the diameter of the support pads.

Access Lines for Fill, Vent, Fluid Delivery, and Instrumentation

The access lines (both fluid and instrumentation) to the interior of the inner vessel are routed through the annular space between the inner and outer shells in such a manner that the heat conducted through these lines is minimized. All of the fluid and instrumentation paths are combined into three composite lines: the fill line, the vent (VCS) line and the fluid delivery line to the cryostat. The 3/8 in. fill line (approximately 42 in. long) is attached to the bottom of the inner vessel and contains leads for the stored liquid temperature sensor. The 3/8 in. vent line is attached to the top of the inner vessel, and inside this line are leads for two temperature sensors. The vent line (approximately 16 ft long) is used as the delivery line and is attached to the vapor-cooled shield over most of its length. The outermost 2 feet, or so, of this line is enlarged to 7/16 in. to accommodate the temperature sensor attached to the VCS. This sensor is inserted into a separate 5/32 in. sheath extending about 8 in. from a tee joining the 7/16 in. and 3/8 in. tubing. The ullage temperature sensor sheath extends along the full length of the VCS/vent line terminating inside the pressure vessel at the inner vent boss. The 3/16 in. diameter (0.142 in. ID) cryostat delivery line tees off the fill line about 16 in. from the outer fill boss. This section of line, about 48 in. long, its tee and outer boss (cryostat adapter), represent the major design modification (other than addition of microspheres) to the previously existing MOL tank (P/N 851240-2-1). The reasons for the modifications are discussed in Section 3.

All the annular lines are made of 300 series stainless steel tubing. The dissimilar material joints near the inner vessel and the outer shell are made with sections of coextruded tubes (except for the fluid delivery line to the cryostat): titanium-to-stainless steel coextrusions at the inner vessel, and aluminum-to-stainless steel coextrusions at the outer shell.

Cryostat Adapter

The cryostat adapter is a stainless steel boss on the outer shell of the tank assembly which provides for fluid delivery to the cryostat (Phase II). The boss is located on the outer shell approximately 155 degrees from the existing fill and vent ports. The adapter connects to the inner tank through a 48-in. segment of 3/16 in. tubing which tees into the fill line. The adapter provides for fluid delivery to the cryostat with minimum heat leak.

The 3/16 in. delivery tube connects to a new tee, designed to be assembled around and welded onto the existing fill tube without separating the fill tube from the inner vessel. The completed assembly forms a tee about 16 in. from the outer shell fill boss and about 26 in. from the inner fill boss.

Insulation and Intershell Support System

A 6061 aluminum alloy vapor-cooled shield is located in the 1.3 in. annular insulation space, about 0.5 in. from the inner vessel. The delivery line (vent line) is attached to this shield over most of its length with 29 aluminum U-shaped clamps, 1-3/8 in. wide, each with 6 rivets. The fluid leaving the tank cools this shield and most of the heat being transferred into the insulation from the outer shell will be intercepted before it reaches the inner vessel, which contains the cryogen. Hemispherically-aluminized, hollow, glass microspheres, type B15BX, manufactured by The 3M Company, fill the annular space between the inner and outer shells and serve as annulus insulation.

Six equally-spaced compressed fiberglass pads are used to support the inner vessel and the vapor-cooled shield within the outer shell. The pads are approximately 6.0 in. in diameter and provide a total support area of 170 sq. in. A 6.64-in. diameter hole is cut in the VCS for each pad stack, which contains a contact disc (of 7075 aluminum) located at the same distance from the inner vessel as the VCS when the pads are finally compressed. The contact discs serve to provide a near isothermal extension of the VCS through the fiberglass pads thus intercepting most of the pad heat leak from the outer shell.

Outer Shell

The outer shell of the tank subassembly is made of formed 2219 aluminum hemispheres. The design of the shell is based on resisting the buckling load exerted by the atmospheric pressure on the evacuated outer shell. The tank assembly is supported by a forged and machined girth ring which forms an integral part of the outer shell. Three mounting points are provided on the girth ring to support the tank assembly in the handling dolly. The attachment points are located 90 degees apart, and with the tank in the normal position (the plane of the girth ring vertical), two mounting points are in a horizontal plane and one at the uppermost point of the ring. The girth ring also serves as a mounting base for the external manifold assembly and microsphere accumulator.

Microsphere Accumulator

The microsphere accumulator is a small vessel mounted on the outer shell and opening directly into the tank annulus; it functions to compensate for an increase in annular volume when the inner vessel is filled with liquid helium. The accumulator is a spherical vessel, 8 in. in diameter (256 cu. in. capacity), and fabricated of aluminum 6061-T6. The sphere is welded directly to the outer shell and supported with two struts welded to the tank assembly girth ring (Figure 2-2, Views 1 and 2).

External Manifold Assembly

The external manifold assembly (Figure 2-2, View 2, bottom of tank) consists of a filter subassembly, a vacuum ion pump, and a manual shutoff valve, and is mounted on the girth ring. The manifold assembly functions to enable maintenance and monitoring of the vacuum level in the tank annulus.

The manual shutoff valve allows for connection of a vacuum source directly to the annulus so that any gas within the annulus can be removed. The filter assembly prevents aluminized microspheres from being drawn from the annulus by the pump, or the vacuum ion pump. The vacuum ionization pump is discussed below.

Vacuum Ionization Pump

The vacuum ionization pump is included with the cryogenic tank as part of the external manifold assembly to maintain tank annulus vacuum at low pressure, to assist in maintaining thermal integrity of the tank assembly. Pump operation can be monitored to assess the quality of annulus vacuum. The pump current is proportional to pressure, and by monitoring the current, an adequate determination can be made of the annulus vacuum level.

The actual operating life of the vacuum ionization pump is dependent on the average pressure of the annulus vacuum, with life expectancy directly proportional to the operating pressure of the pump. Using this vacuum ionization pump, the annulus will attain steady-state pressures of approximately 1×10^{-7} torr (if sufficient outgassing has occurred). At this pressure the expected life of the pump is greater than 100,000 hours.

Barostat Regulator

A government-furnished National Bureau of Standards (NBS) Barostat Regulator, P/N D-4828, was used during the thermal performance testing to regulate the tank ullage pressure to very near atmospheric pressure.

Tank Handling Dolly

The tank handling dolly (Figure 2-2, Views 1 and 2) is used to hold the cryogenic hydrogen/helium tank assembly during testing and while being transported.

The tank handling dolly is comprised of two major components: the dolly frame and the yoke. The dolly frame is an open structure consisting of two braced upright supporting members welded to an open square frame. Fork lift provisions are built in as part of the frame. Four swiveling casters and a handle provide for mobility. Two casters have separate foot-operated brakes. The yoke is designed to support a specific cryogenic tank. The yoke consists of two bolt-on channels, a lifting eyebolt on the top channel, a position securing eyebolt on the bottom channel, and a control panel with valves, pressure gages, regulators, and pneumatic fittings.

Additional tubing (Figure 2-2, View 2) was welded to the yoke of the tank handling dolly, to serve as additional protection for the tank during handling.

The overall dimensions of the hydrogen handling dolly (i.e., frame and yoke) are: 59 in. long by 55 in. wide by 69 in. high.

SECTION 3

PROGRAM TASK NARRATIVE

INTRODUCTION

Phase I of the cryogenic hydrogen/helium storage and supply system program was conducted during the period between May 15, 1974 and November 21, 1975. The objectives of Phase I consisted of refurbishing an existing cryogenic tank, installing microspheres in the tank annulus to augment the insulation system, and testing the completed unit. The activities involved with accomplishing these objectives are listed below as Phase I work tasks:

Task I--Evaluation and Repair

Task II--Instrumentation Installation

Task III--Tank Modification

Task IV--Microsphere Insulation

Task V--Annulus Evacuation and Pressure Test

Task VI--Vented Weight Loss Test

Following a Program Review, the work activities are described in chronological order of occurrence.

PROGRAM REVIEW

Program Scope

The NASA MSFC program, conducted under Contract NAS8-30574, is concerned with developing a system for cooling a fractional watt load to a temperature in the region of 2 K. When complete, the cooling system will consist of a cryogenic storage and supply vessel, a Joule-Thomson expansion device, and a counterflow heat exchanger. The storage and supply vessel will hold cryogenic supercritical helium for delivery to the heat exchanger. The Joule-Thomson expansion device/heat exchanger will provide cooling to a specific load in the Helium-II temperature range.

Development of the system will be conducted in two separate and distinct phases. Phase I (the subject of this report) was concerned with preparing the cryogenic fluid storage and supply system. Phase II, if approved by MSFC, will involve development of the Joule-Thomson cryostat.

Historical Background Information

The origin of the cryogenic tank hardware used for this program is of interest and will be discussed below. The discussion traces the design from

the original Air Force Manned Orbiting Laboratory (MOL) Program, through the
Air Force Rocket Propulsion Laboratory programs (Edwards Air Force Base), and
finally to the NASA MSFC program.

1. Air Force Manned Orbiting Laboratory Program

AiResearch, under contract to Douglas Aircraft Corp., was developing cryo-
genic tankage for use in the Manned Orbiting Laboratory atmosphere and reactants
supply subsystem. Although the program was terminated for the convenience of
the government, the cryogenic tankage design was complete, and materials had
been ordered. As a result of this program, sufficient materials were available
to construct several sets of cryogenic tanks.

2. Air Force Rocket Propulsion Laboratory Evaluation Programs

Two cryogenic hydrogen tankage systems, utilizing materials from the
original MOL program, were manufactured by AiResearch for the Air Force Rocket
Propulsion Laboratory, Edwards Air Force Base, California, under contract
F04611-71-C-0020. These were intended for ground test evaluation of thermal
insulation systems. The first test article was nearly identical to the hard-
ware configuration planned for the MOL program, with an insulation system of
multilayer aluminized Mylar (NRC-2) and a vapor-cooled shield. Certain struc-
tural changes were made to reduce cost and make the unit more suitable for
ground handling. This first unit exhibited high thermal performance, verifying
original design predictions, prior to delivery.

The second unit was produced with a different thermal insulation system.
In this unit, the NRC-2 multilayer insulation was eliminated, and all annulus
surfaces were covered with vacuum-deposited aluminum over a resin undercoat.
This coating was intended to reduce heat losses caused by radiated heat enter-
ing the fluid storage vessel. During final testing two failures occurred: (1)
a leak into the tank annulus degraded tank performance, and (2) a short circuit
was observed in the quantity gauging circuits. Due to lack of funding, the
AFRPL program was terminated at this point.

3. NASA MSFC Cryogenic Hydrogen/Helium Storage and Supply System

With the second Air Force MOL tank as government-furnished equipment,
NASA MSFC contracted with AiResearch to repair the unit to use for storage and
supply of cryogenic hydrogen and helium. The cryogenic fluid was to be stored
for delivery to a Joule-Thomson cryostat designed to provide cooling for a
fractional watt load at 2 K. The contract became effective 15 May 1974.

EVALUATION AND REPAIR

Task I involved the evaluation of the cause of leakage, and its method of
repair, with consideration given to incorporating design features to permit
installation of microspheres in the tank annulus. The cryogenic tank and its
associated drawings were reviewed by engineering and manufacturing personnel
for the purpose of establishing manufacturing operations and tooling (MOT)
instructions. MOT's provide the detailed step-by-step manufacturing operations,
in-process tests, and in-process inspections that manufacturing uses to perform

work. In this case the MOT's detailed the exact procedures to be followed in disassembling the cryogenic tank for repair.

Tank Disassembly - Outer Shells Removed

Prior to installing the tank assembly in the disassembly fixture, all external components and associated tubing were removed and stored for future use. After the tank was placed in the disassembly fixture, the outer shells were separated at the girth weld and removed, leaving the inner tank and VCS within the fixture (Figure 3-1). Comparison of the condition of the vacuum-deposited aluminum with photographs showing its condition just prior to assembly in mid-1972, indicated no surface degradation. Visual inspection of the exposed inner tank revealed no obvious defective areas that would have contributed the vacuum degradation.

The tank assembly was attached to a helium mass spectrometer leak detector and evacuated to a pressure of 10^{-6} torr. The leak was located at the entrance of the vent tube into the pressure vessel (Figure 3-2). A fluorescent-penetrant test revealed a series of small cracks in a weld area that had been repaired during fabrication of the pressure vessel.

Rework Activity

After the defective area was reviewed by engineering and manufacturing personnel, rework instructions were prepared. The rework consisted of the following activities:

    (a)   The old weld material in the crack area was routed out to the parent boss material, but not into the boss.

    (b)   A fluorescent-penetrant test was performed to verify removal of the cracks.

    (c)   The area was cleaned with water and a solvent compatible with titanium.

    (d)   During welding, the area to be reworked was bagged so that an Argon purge provided an inert atmosphere to ensure a weld free of contamination.

After completing the rework, a helium mass spectrometer check was performed on the complete inner tank assembly. The unit was surrounded with a plastic bag and the bag pressurized with helium. Leakage was monitored for a period of 60 minutes with no indication of leakage observed. Thus the leak rate was less than 2×10^{-10} scc per sec of gaseous helium, the lowest measurement limit of the helium mass spectrometer.

After completing the leak test, the repaired area was subjected to another fluorescent-penetrant test. This test verified that the weld repair was free of cracks.
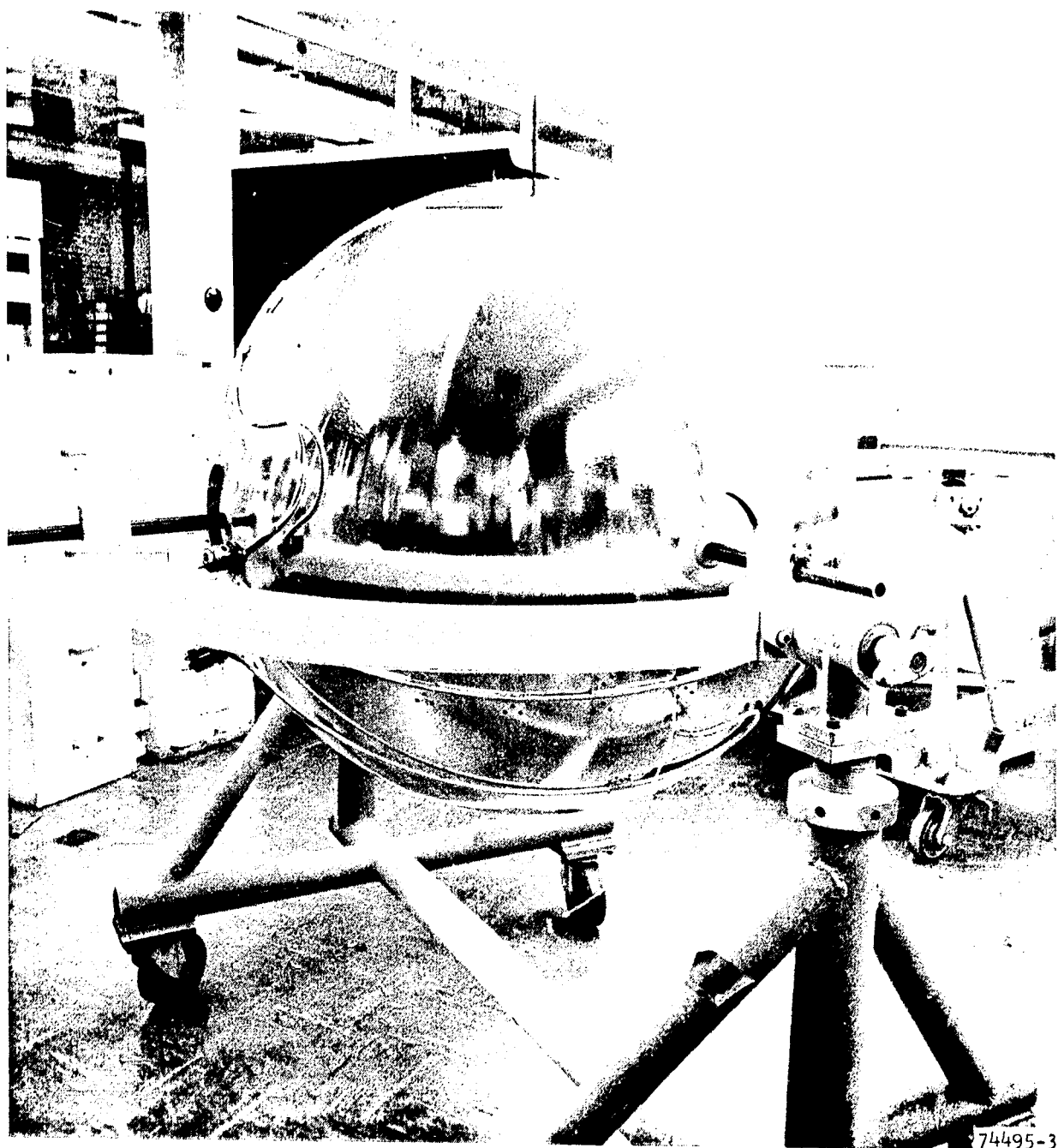
Figure 3-1. Inner Tank and VCS After Removal of Outer Shell

VENT TUBE

REPAIR WELD

CRACKS

INNER TANK

ORIGINAL WELD
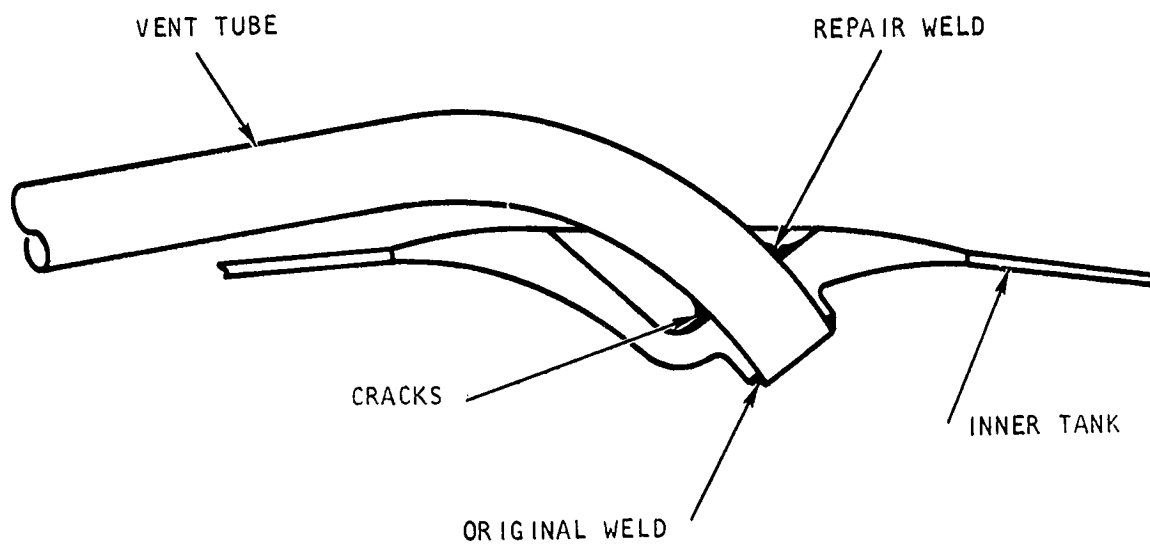
S-88325

Figure 3-2. Pressure Vessel Vent Boss

Temperature Shock and Proof Pressure Tests

Following helium leak test, the inner tank assembly was transported to the AiResearch Mint Canyon Remote Test Facility for the temperature shock and proof pressure tests.* At the test facility, the tank assembly was repositioned in the fixture such that the inner vent boss was located at the bottom of the tank. Thermocouples were attached to the tank in four locations. Liquid nitrogen was then fed into the tank through the vent port. Due to the difficulty of insulating the tank for this test, the minimum temperature obtainable at the inner vent boss was -150 F. The tank assembly was then warmed to 60 F and a repeat of the above test was performed. Following the temperature shock test, the tank was pressurized with precooled nitrogen gas at a rate of less th---
30 psig per minute until a proof pressure of 300 psig was attained, and
average temperature of the thermocouples stabilized at 40 F. Figure 3-3 shows the equivalent proof pressure levels at various combinations of pressure and temperature for this tank. Visual examination of the tank assembly revealed no evidence of deformation or permanent damage. Following the proof pressure test, the inner tank was again subjected to a helium leak test. As there was no indication of leakage, this completed the activities of Task I.

INSTRUMENTATION INSTALLATION

Three temperature sensors consisting of a platinum resistance element wound on an aluminum oxide mandrel were installed in the tank. The leads of the elements are insulated and encased in a flexible sheath, then inserted into dry wells inside the vessel through tubes located in the fill and vent lines. Two of the sensors are located at the inner vessel, one at the fill port to measure the liquid temperature, and the other is at the vent port to monitor the ullage temperature. The third sensor is located on the vapor-cooled shield (VCS) near the exit of the vent line.

Temperature sensor calibration data from the instrumentation vendor, Rosemount Engineering Company, is given in Table 3-1.

TANK MODIFICATION

Phase II Preliminary Analysis

During this portion of the program the proposed method of helium delivery to a J-T cryostat was evaluated. Investigation of this problem at this time instead of in Phase II of the program, appeared desirable in that modifications to the tank could be planned to facilitate installation of the cryostat during Phase II. The analytical work consisted of the following four items.

---

*Test data is given in Appendix A.
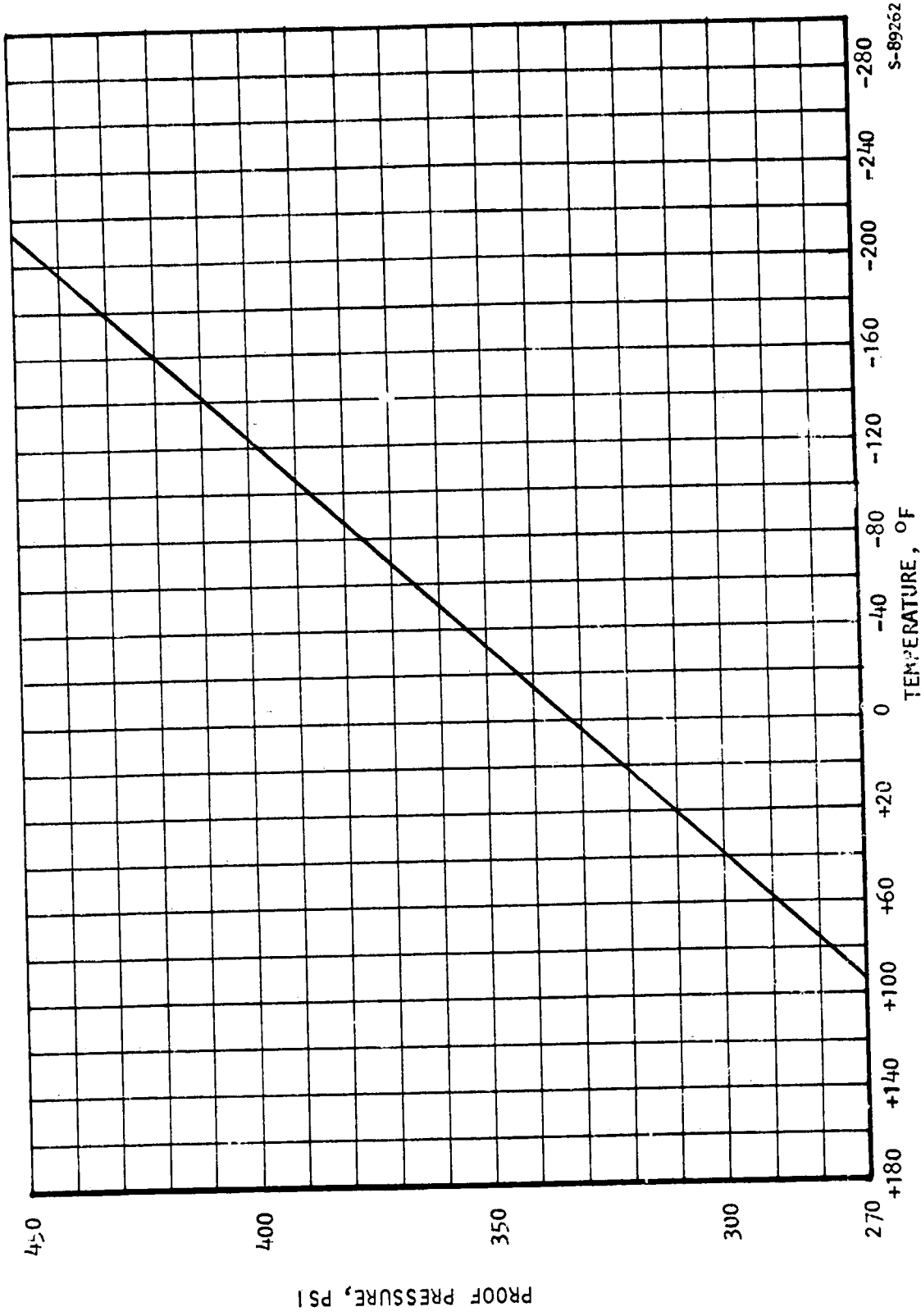
Figure 3-3. Proof Pressure Versus Temperature - MOL Hydrogen Inner Tank Assembly

S-89262

TABLE 3-1

TEMPERATURE SENSOR CALIBRATION DATA

LOCATED ON VAPOR-COOLED SHIELD	ROSEMOUNT ENGINEERING COMPANY TEST REPORT QUALITY CONTROL APPROVED IPTS 1948 MODEL 146DP86 SERIAL 6383 DATE 07 25 73 ACTUAL CALIBRATION POINTS TEMP F — RESISTANCE OHMS 32.0000 — 500.36000 -452.0992 — .57860 -320.7470 — 94.98100 FSC IS 19.584.15600 DRM IS .96775000
LOCATED AT INNER FILL BOSS	ROSEMOUNT ENGINEERING COMPANY TEST REPORT QUALITY CONTROL APPROVED IPTS 1948 MODEL 146DP86 SERIAL 6382 DATE 07 25 73 ACTUAL CALIBRATION POINTS TEMP F — RESISTANCE OHMS 32.0000 — 500.60000 -452.0992 — .56520 -320.7470 — 94.83400 FSC IS 19.59408500 DRM IS .78677000
LOCATED AT INNER VENT BOSS	ROSEMOUNT ENGINEERING COMPANY TEST REPORT QUALITY CONTROL APPROVED IPTS 1948 MODEL 146DP86 SERIAL 6384 DATE 07 25 73 ACTUAL CALIBRATION POINTS TEMP F — RESISTANCE OHMS 32.0000 — 500.13360 -452.0992 — .59040 -320.6247 — 94.89620 FSC IS 19.57482200 DRM IS .76889000

GARRETT

75-11607
Page 3-8

1. **Literature Search for Helium-II Data**

To examine the Joule-Thomson (J-T) process in sufficient de\`u. to define the tank requirements necessary to produce superfluid helium (He-II), it was necessary to conduct a literature search for pressure-enthalpy data which included the two-phase region below the lower lambda point (coexisting He-I vapor and liquid He-II). No such pressure-enthalpy diagram could be found in the Helium literature. The analysis was performed by using the latest NBS publication of helium thermophysical properties (McCarty, NBS-TN-622, 1972) above 1 psia and older published data on heat capacity, latent heat, and vapor pressure of liquid He-II, (Cook, Argon, Helium, and The Rare Gases, Vol. I, Interscience Publishers, New York, 1961).

2. **Performance Prediction of Microsphere-Insulated Helium Tank**

To determine the best method of helium delivery to the cryostat, it was necessary to establish the baseline tank performance (to be derived later from Phase I test results) for supercritical helium operation of the present tank with the addition of microsphere insulation. Using thermal conductivity data for hemispherically-aluminized, 15 to 135 micron diameter glass spheres (from Adv. Cryo. Engrg, Vol. 18, 1973, p. 103) in conjunction with the AiResearch Cryogenic Tank Design and Performance Prediction computer program, the isobaric delivery rate of helium at 50 and 100 psia was determined as a function of helium storage temperature, for two modes of operation: (1) all flow through the vapor-cooled shield (VCS) vent circuit, and (2) all flow through the fill line, not shorted to the VCS which becomes a passive radiation shield. Over the probable temperature range of interest, 5 to 20 R, the vent rate through the VCS averaged about 0.5 to 0.6 lb per hr, while for flow through the fill line (no VCS cooling) about 2.5 to 4 lb per hr resulted. These vent rates were computed for steady-state, constant-pressure operation with the outer shell temperature at 70 F.

3. **Analysis of the J-T Process for He-II**

The J-T process for liquefying helium below the lambda point (0.73 psia, 3.92 R) was analyzed to determine the worst-case tank conditions (maximum temperature at minimum pressure) for which expansion into the He-II region could be achieved. Several important assumptions had to be made in order to begin the study, such as dewar (liquid collector) operating point, heat exchanger high-pressure-side exit temperature, and He-II cooling load (taken to be 1 watt, for reference). Tank pressures (inlet to J-T heat exchanger) of 50 and 100 psia were studied, together with a 1.0 R approach at the cold-end of the heat exchanger (that is, J-T expander inlet temperature of 4.0 R, with He-II dewar operating at 3.0 R, 0.142 psia). The resulting flow rates were on the order of 0.5 lb per hr. The maximum inlet temperature to the J-T heat exchanger (prior to counterflow cooling to the expansion inlet condition, 4 R) was found to vary from 10.5 to 15.0 R, for 50 to 100 psia tank pressure. Somewhat lower temperatures would be required in the tank to allow for cryostat supply line heat leak. A very rough estimation of J-T heat exchanger size was made for the 50 psia, 10.5 R inlet condition. The low-pressure side characteristics (minimal allowable pressure drop and poor heat transfer coefficient) require

significantly larger finned tubing than that, for example, in current use for LN$_2$ cryostats built at AiResearch. Detailed sizing and design will be performed in Phase II.

4. Test Setup and Tank Operating Considerations

The most critical parameter in the operation of a He-II cryostat from the supercritical helium tank is the stored helium temperature, which increases as the tank is depleted. Since the J-T heat exchanger inlet must be very cold to minimize HX size and make liquefaction possible, the transfer losses (heat leak) between the tank and cryostat must be very small. From the J-T process analyzed above and the predicted tank thermal performance, a reasonable operating time of 10 to 20 hrs requires that the temperature rise from tank to HX inlet be held to less than 0.3 R. With a flow of about 3 lb per hr from the tank, this corresponds to a transfer loss of 2 Btu per hr. This level of performance can be achieved if all the tank flow is delivered through a special boss, after which the cryostat flow is split off, and the remaining flow is routed over the boss to provide vapor cooling. In this configuration the tank can deliver about 3 or 4 lb per hr of helium and the pressure will remain constant at 100 or 50 psia due to heat leak, provided that no flow is allowed over the VCS. This special boss and a small line connecting it to the present fill line, near the inner vessel, was recommended as the simplest design modification to the existing tank which could ensure delivery of cold helium to the cryostat.

For Phase I testing with liquid hydrogen (vented-weight-loss test), the effect of this extra line and the removal of the thermal short from the fill line to the VCS, was estimated to be less than a 0.5 percent increase in vent rate.

Cryostat Adapter Design

Using results obtained from the analytical work above, a new tank boss and a "tee" were designed and fabricated. The external boss which is the cryostat adapter, was located on the outer shell approximately 155 degrees from the existing fill and vent ports. The adapter allowed a 3/16 in. diameter supply tube to exit from the fill line, minimizing the heat-leak to the pressure vessel.

A special tee was designed to be assembled around and welded onto the existing fill tube without separating the tube from the pressure vessel. A small hole was machined in the fill tube, about 16 in. from the existing outer fill boss and the tee then welded to the tube. Approximately 48 in. of the 3/16 in. OD tubing (measured ID of 0.142 in.) was required to connect the tee to the external adapter.

Modification of the outer shell was required for the addition of the microsphere fill port and the cryostat supply tube. In addition, a cylindrical 10-micron filter was installed between the annulus evacuation port and the external manifold consisting of an ion-pump and a manual shutoff valve.

MICROSPHERE INSULATION

Purchase and Inspection

Thirty pounds of hemispherically-aluminized, hollow, glass microspheres, type B15BX, were purchased from the 3M Company Special Enterprises Department. Random sampling inspection indicated that the nominal size was 100 microns, with approximately 30 percent of the spheres without aluminum coating (Figure 3-4). A density check of the spheres was performed to confirm the amount required. The packed density of the spheres was 0.063 g/cc.

The original plan of processing the microspheres to remove broken spheres by alcohol floatation was revised.* Inspection of random samples revealed negligible breakage. Therefore, no attempt was made to remove broken spheres.

Transfer of the microspheres to the processing containers was accomplished and the containers were then placed in a vacuum oven. The microspheres were evacuated to a pressure of 1×10^{-4} torr at 300 F for 72 hours. At the end of that time the containers were back-filled with 5 psig, filtered, dry, nitrogen gas and stored for future use.

Microsphere Installation

Prior to installation of the microspheres, the tank assembly was baked out for a period of approximately one week at a temperature of 210 F, while the tank annulus pressure was less than 1×10^{-4} torr.

After tank annulus preconditioning was completed, the system and its holding fixture were mounted on a set of scales and positioned so that the microsphere accumulator fill port was located at the top. This accumulator is part of the tank outer shell and sized to correspond to the equivalent increase in tank annulus volume when the tank is filled with liquid helium. At this point, a system tare weight was recorded.

. A cannister containing the preconditioned microspheres was suspended above the accumulator fill port and connected to the port with a clear plastic tube (Figure 3-5). By alternately pressurizing the microsphere cannister and evacuating the tank annulus, the microspheres were transferred from the cannister to the tank annulus. The tank holding fixture was vibrated during transfer to assure proper packing of microspheres in the annulus. Numerous holes exist in the VCS (where the lines pass through, and in the vicinity of the inner and outer shell bosses) to enable the microspheres to fill the annulus under the VCS.

When the predetermined microsphere fill weight was approached, and visual inspection indicated that the annulus was full, the tank assembly was rotated 180 degrees. The tank was vibrated in the inverted position for a short period. After vibration, the tank was rotated back to the upright position and an additional quantity of microspheres installed in the annulus.

---

*Discussion with Dr. Peter Howell of 3M Co. indicated that the number of broken spheres is usually negligible.

GARRETT AIRESEARCH MANUFACTURING COMPANY
OF CALIFORNIA
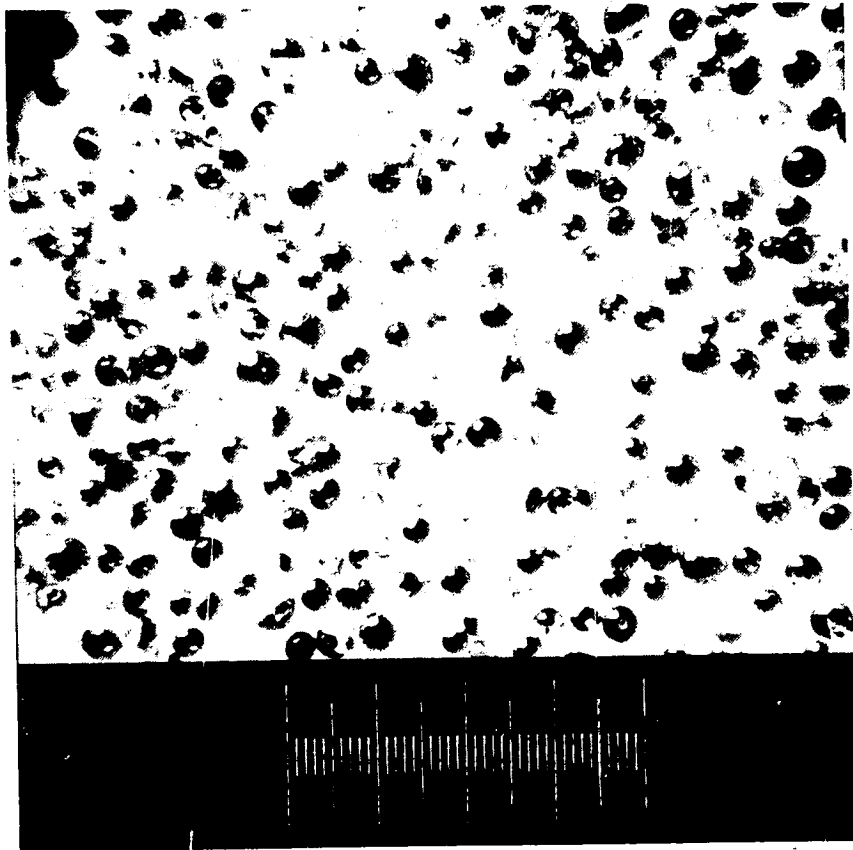
MAGNIFIED APPROXIMATELY 50 TIMES
(EACH MICROMETER DIVISION = 25.4 MICRONS)

Figure 3-4. Microscopic Inspection of Microspheres (Typical)
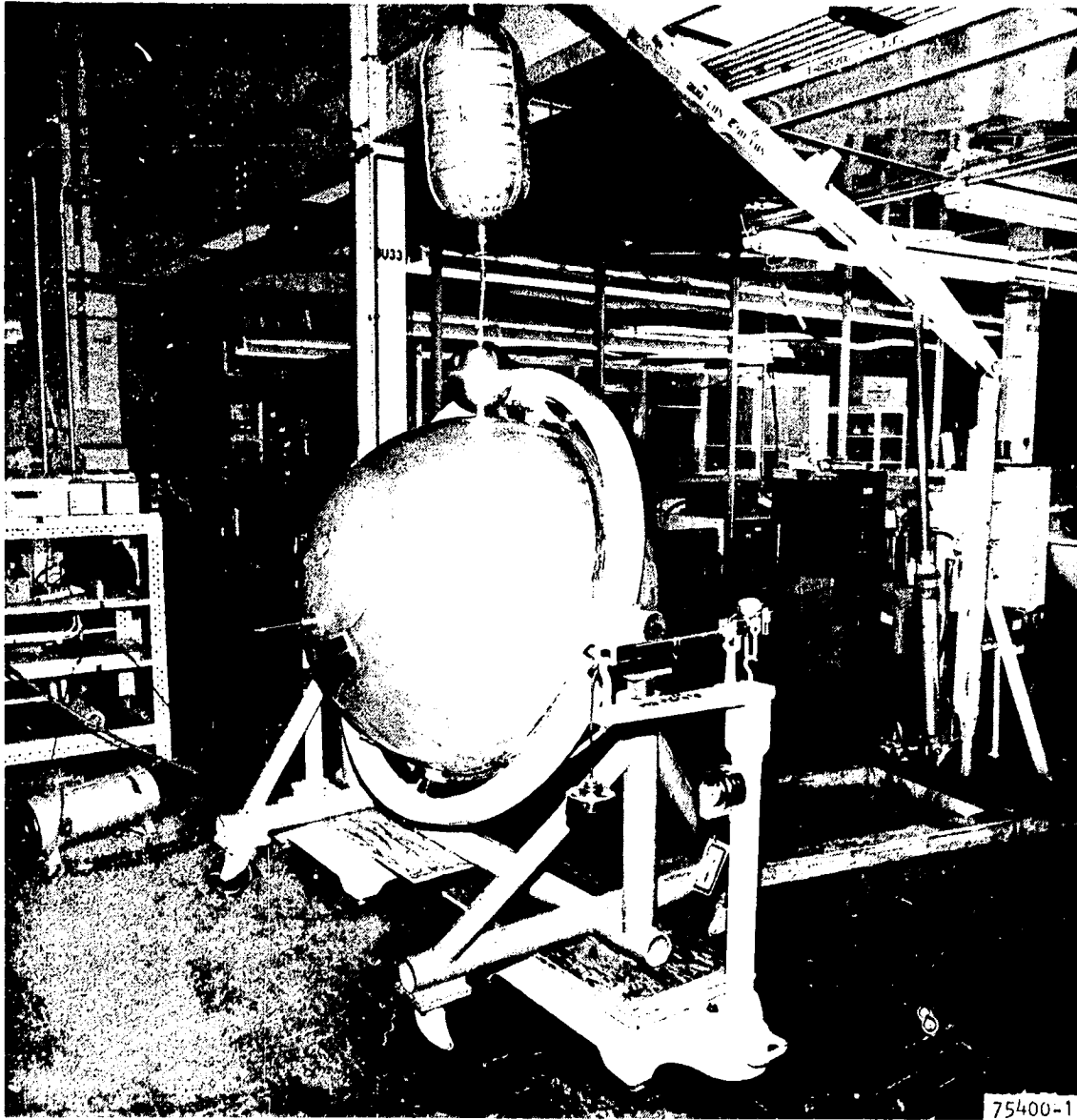
Figure 3-5. Tank Prepared for Microsphere Installation

GARRETT AIRESEARCH MANUFACTURING COMPANY
OF CALIFORNIA

These operations were repeated until visual inspection indicated that the annulus fill was complete. At the completion of fill, the microsphere weight was 16.88 lb,* an installed bulk density of 0.068 g/cc.

ANNULUS EVACUATION AND PRESSURE TEST

When microsphere installation was complete, the fill port was welded closed and a helium leak check performed. This test revealed no leaks.

The tank was installed in an oven and setup for annulus evacuation. It was planned that the annulus be evacuated at a temperature of 210 F until annulus pressure reached a level of less than 1×10^{-4} torr. After an evacuation-bakeout period of 10 days, a static annulus pressure test was performed to aid in predicting the length of the evacuation period*. The test indicated that at least 10 additional days of evacuation at 210 F were required. The evacuation-bakeout period was continued.

At the end of the second 10-day evacuation-bakeout period, a static annulus pressure test was again conducted. This test indicated that there was no appreciable improvement from the continued evacuation bakeout. Investigation of available test data (from previous tests conducted using microspheres as an insulating material) indicated that either a dynamic vacuum approach was utilized, or the annular volume was back filled with CO_2 and allowed to cryopump during the vented weight loss test. As a result, it was proposed that the 30-day static annulus pressure test be run until the pressure builds beyond the upper limit capability of the ion pump (approximately 5×10^{-4} torr). At that point, the pump would be turned on to reduce pressure to 1×10^{-4} torr, or less, and then the test would be continued with the ion pump off.

The evacuation bake-out procedure was concluded after a total of 35 days. During the last 6 days of the test period there was no appreciable improvement noted in the evacuation-system pressure, (3.5×10^{-4} torr), indicating that the ultimate pressure had been reached. A static annulus test substantiated that additional bake-out/evacuation would not improve the condition of the tank annulus.

After stabilizing the tank assembly at ambient temperature and a constant dynamic annulus pressure of 5×10^{-7} torr, the tank was isolated from the pump and the annulus pressure was monitored hourly until a static pressure of 3×10^{-4} torr was reached. The pressure was then monitored twice a day for the remaining 30 days. It was not required to turn on the ion pump, as the annulus pressure did not increase above 4.6×10^{-4} torr during the 30 day test.

VENTED WEIGHT LOSS TEST

The completed system (Figure 3-6) was transported to the AiResearch Mint Canyon Remote Test Facility and prepared for the liquid hydrogen vented-weight-loss (VWL) test. The tank assembly was purged and cooled prior to filling with

---

*Test data given in Appendix A.
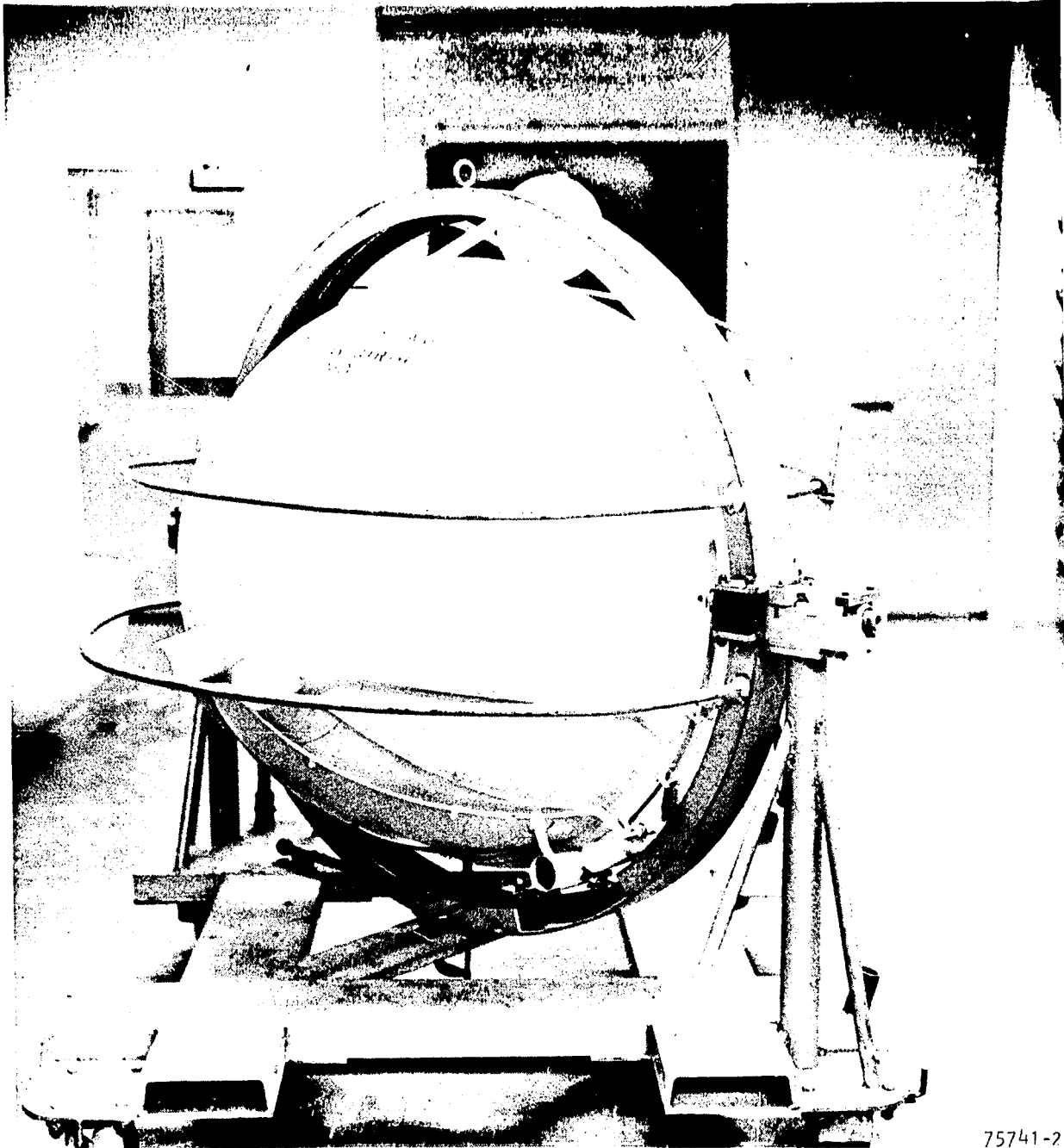
75741-2

Figure 3-6.   Completed Cryogenic Hydrogen/Helium
Storage and Supply System

GARRETT AIRESEARCH MANUFACTURING COMPANY
OF CALIFORNIA

87 lb of liquid hydrogen. After an 18-hour stabilization period the vent port was connected to a wet test meter, through a water saturator. Five days later the NBS barostat and a Baratron pressure readout were installed (Figure 3-7). Two days later Pace dynamic pressure transducers were installed on the fill and vent ports, and an oscillograph was attached. During the WWL test the tank annulus pressure, the fill and vent port pressures, the 3 temperature sensors, the scale and wet test meter were monitored and recorded. (Refer to Figure 3-8 for test schematic.) Oscillograph traces were obtained over several relatively short periods of time.

Pressure oscillations were observed on both the fill and vent pressure gages (scale ranges of 0-30 psig and 0-30 in. Hg, respectively) from the start of testing. Prior to installing the barostat, both the fill and vent port oscillation amplitudes (peak-to-peak) averaged about 0.02 atm; no oscillation frequency was established at this time. With the barostat in the vent circuit, the amplitude of the vent pressure oscillation approximately doubled, with no change in the fill pressure oscillation (gage is less sensitive, however). Suspecting thermal acoustic oscillations (TAO) in the dead-ended cryostat supply line which tees off the fill line, the fill and cryostat support ports were externally connected through an orifice (micrometer valve). The gages showed no change in oscillation amplitude. An oscillograph was then attached to a pair of fast response (time constant of 12 milliseconds) Pace dynamic pressure transducers, one in the fill line and the other in the vent line. The external shunt was then reconnected between the fill and vent ports. Examination of the resulting pressure traces   3 different micrometer valve settings) revealed a steady, constant-amplitu·· vent pressure oscillation of about 0.006 atm peak-to-peak amplitude, with frequency of 8.5 Hz. The fill line pressure was oscillating at a variable amplitude between 0.017 atm and zero, with a frequency of 12 Hz (the period between peak amplitudes was also variable). This reduction in amplitude is not very significant, as it did not significantly reduce the vented weight loss. A calculation of the TAO effect on tank heat leak, based on recently published data, is included in Section 4.

The second attempt to reduce the TAO involved rotating the tank assembly 90° from its normal vent orientation (referring to Figure 2-1, the tank was rotated 90° counterclockwise), such that both inner bosses were out of the liquid phase, and the outer fill and vent bosses were facing upward. In this orientation the fill pressure gage showed no detectable oscillation, while the vent pressure continued to oscillate at about 0.03 atm. At this point in time, the tank contained about 38 percent liquid (by volume) and the ullage gas temperature was about 100 R. The vent line oscillation was finally eliminated by removing the wet test meter saturator, indicating that the vent line oscillation was not thermally induced (no TAO).

Measuring the tank vent rate in the 90° rotated configuration with a low liquid level was undesirable because of the high degree of ullage stratification. Another attempt to eliminate the TAO in the normal vent configuration was made by inserting a ball within the cryostat supply tube, thus blocking off fluid at the tee on the fill line. With the ball in the supply tube, the tank was refilled and subjected to another vented weight loss test. No change was detected in the oscillations, as compared with original testing. (The ball

NEW TARE WEIGHT CONFIGURATION

BAROSTAT INSTALLATION
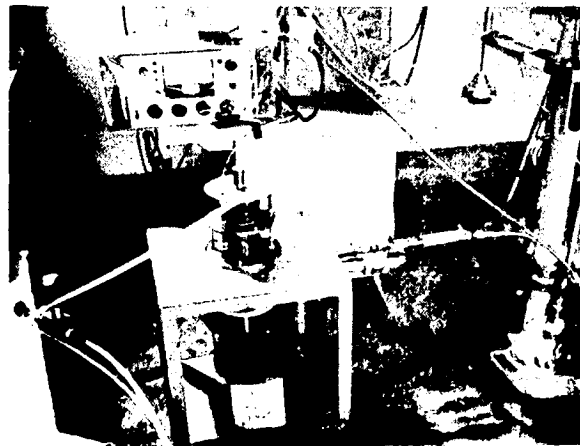
ORIGINAL PAGE IS
OF POOR QUALITY

F-21818

Figure 3-7. Vented-Weight-Loss Test Setup

Figure 3-8. Vented-Weight-Loss Test Schematic

PRESSURE GAGE RANGES

P_1 — 0-100 PSIG

P_2
P_3 } — 0-30 IN. Hg

P_4 — 0-3 IN. Hg

ACCURACY: ±0.25 PERCENT F.S.

VENT TO AMBIENT

WET TEST METER OR EQUIVALENT, ACCURACY ±0.5%

SATURATOR

BAROSTAT (G.F.E.)
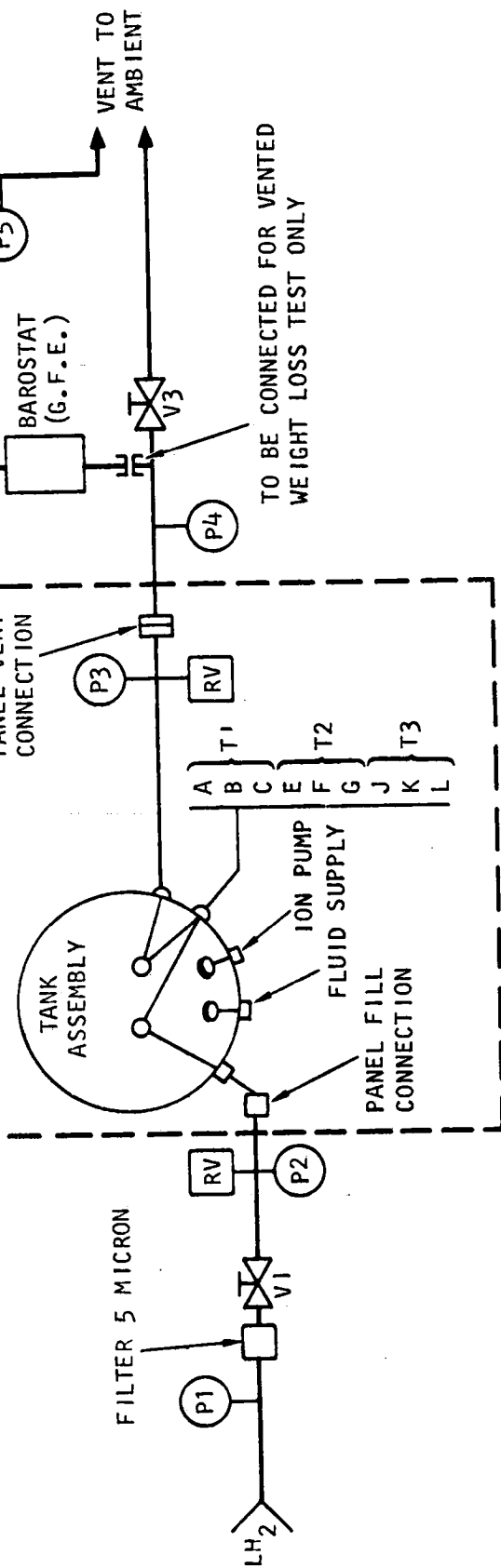
TO BE CONNECTED FOR VENTED WEIGHT LOSS TEST ONLY

PANEL VENT CONNECTION

TANK ASSEMBLY AND TANK HANDLING DOLLY

TANK ASSEMBLY

ION PUMP

FLUID SUPPLY

PANEL FILL CONNECTION

SCALE

FILTER 5 MICRON

LH$_2$

T1 LOCATED IN THE INNER TANK FILL LINE BOSS

T2 LOCATED IN THE INNER TANK VENT LINE BOSS

T3 LOCATED ON VAPOR-COOLED SHIELD

S-98011

could not be made to completely block the opening, it was estimated to be about 85 percent plugged, at best.) About half-way through the test the ball was removed and no change in the WL was detected.

For the final WL determination, the tank assembly was inverted with fluid venting out the cryostat supply line, thus bypassing flow around the vapor-cooled shield. Referring to Figure 2-1, the tank was rotated approximately 170° clockwise from the position shown. In this orientation the inner fill boss is almost exactly at the top of the pressure vessel. A transducer on the vent line showed a pressure oscillation amplitude of about 0.0020 atm during the first 48 hr. From that time on, the oscillation amplitude dropped to 0.0007 atm, for some unknown reason. However, neither of these magnitudes are very significant, and perhaps are not even due to TAO, since the vent line is shorted to the VCS over most of its 16 ft length.

A suitable amount of data was collected to determine the effectiveness of the annulus insulation both with and without flowing through the VCS.

SECTION 4

PERFORMANCE AND ANALYSIS

INTRODUCTION

This section presents a review of the performance data obtained from the two previously tested tanks, a summary of the pre·;nt test data analysis, and a performance comparison of all three tanks. The following tank designations will be adopted for brevity in referring to them henceforth:

- Tank No. 1 - The original MOL hydrogen tank containing 69 layers of crinkled, single aluminized Mylar multilayer insulation (referred to as NRC-2) and a vapor-cooled shield.

- Tank No. 2A - The second tank of the MOL design assembled with all surfaces within the annulus coated with 1500-2000Å of 99.99 percent pure aluminum, vacuum-deposited over a resin undercoat, with finish better than 8 RMS; no multilayer insulation

- Tank No. 2B - The same tank as No. 2A with the addition of a mixture of uncoated and hemispherically-aluminized microspheres (3M Co.) in the entire annulus.

TANK NO. 1 (MULTILAYER INSULATION)

Measured Performance

The MLI-insulated tank , as designed for the MOL Program, was fabricated and tested under contract to the Air Force Rocket Propulsion Laboratory (Edwards Air Force Base, California), and documented by AiResearch Report No. 72-8359, April 14, 1972. The vented weight loss (VWL) test data, using liquid hydrogen, is reproduced in Figure 4-1 (as previously reported on Page 3-17 of Report 72-8359), showing a 213-hour average vent rate of 0.041 lb per hr. At the tank vent pressure of about 13.5 psia, this corresponds to a heat leak to the stored fluid of about 8.0 Btu per hr.

Analytical Performance Prediction

The AiResearch Cryogenic Tank Design and Performance Prediction computer program is briefly described as follows. The function of the program is to determine the steady-state flow rate from a specific tank operating at constant pressure in a constant temperature (outer shell) environment. A heat balance is performed between the various constituents (heat paths) of the insulated annulus, the fluid cooling rate of the vapor-cooled shield (VCS) and the isobaric specific heat input of the stored fluid. The two unknowns, flow rate and VCS temperature, are obtained by simultaneous iteration between the thermodynamics of the stored fluid and the heat transfer rates across each annulus (including the VCS cooling rate). The insulation between either shell and the VCS can be vacuum (radiation only), for which an emittance-versus-temperature table must be provided, or any insulation (evacuated multilayer,
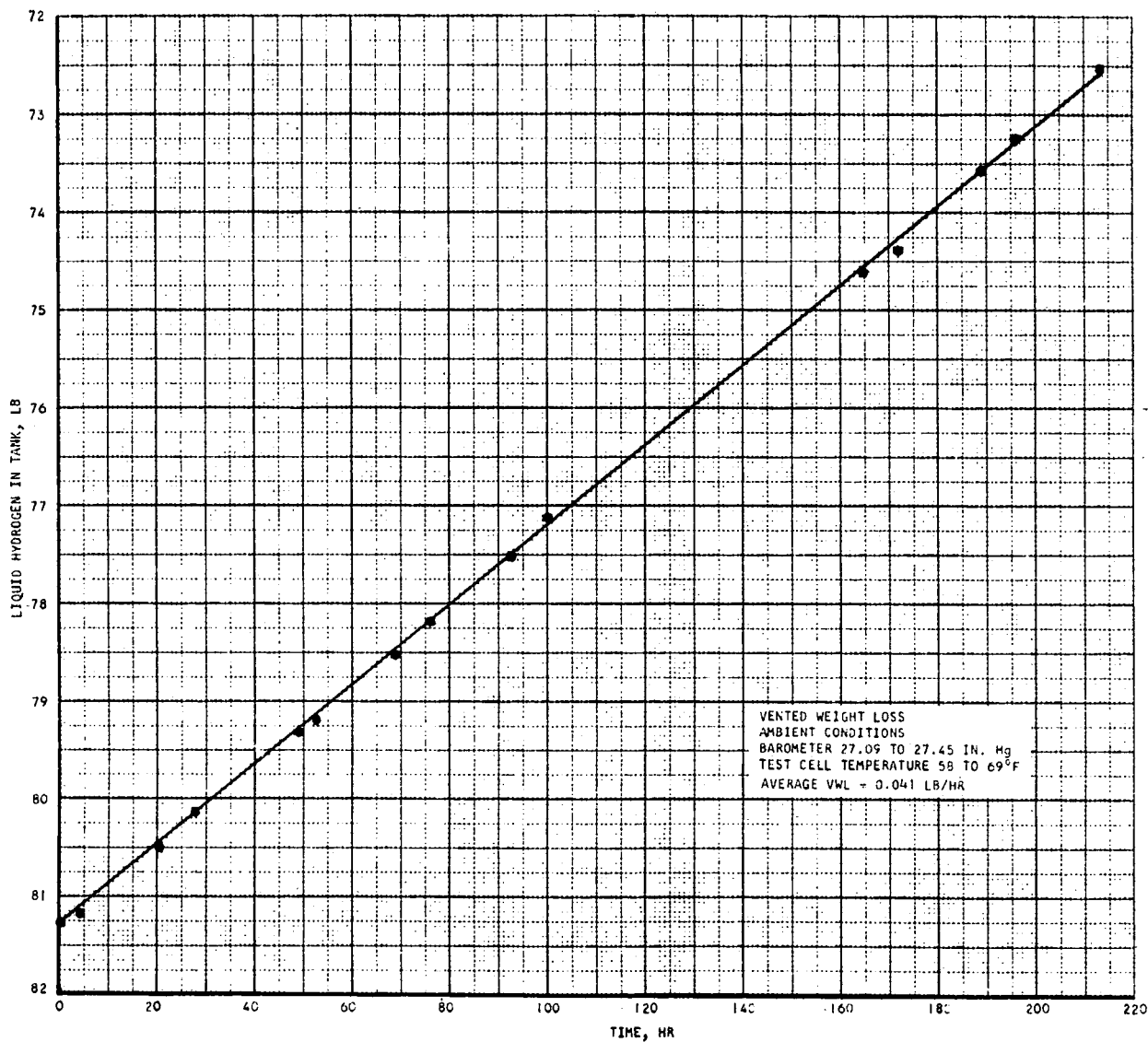
Figure 4-1. LH$_2$ Vented Weight Loss Test — Tank No. 1

fiberglas batt, etc.) for which a thermal-conductivity-integral-versus-
temperature table is provided. Several multilayer insulations are character-
ized by equations dependent on temperature, uncompressed layer density, and
number of layers. The annulus can contain support pads or tension support
struts, or both, and provision is made for stainless steel lines and copper
electrical leads. The program also calculates shell thicknesses and weights
of the tank's major constituents.

The computer printout of the predicted VWL performance was presented on
Page 3-25 of Report 72-8359. The insulation thermal conductivity curve used
for NRC-2 was that derived from Apollo/Lunar Module (LM) supercritical helium
tank test data, representing the thermal performance attained by more than half
the tanks in a sample of 15 tanks of identical design. The predicted vent
flow rate was 0.0399 lb per hr with a tank pressure of 13.5 psia and outer
shell temperature of 70 F. The corresponding heat leak to the stored fluid
is about 7.8 Btu per hr. Thus, the VWL-test-measured thermal performance
was within 3 percent of the analytically predicted performance.

TANK NO. 2A (LOW-EMITTANCE SURFACES)

Measured Performance

A summary of the vacuum-aluminized, low-emmittance-surface-insulated tank
fabrication and testing program was documented by AiResearch Report No. 73-9418,
July 25, 1973, under contract to the Air Force Rocket Propulsion Laboratory.
The thermal performance test (VWL) data sheets were presented on Pages 3A-12
through 3A-18 of that report. The wet test meter flow rate data are presented
here in Figure 4-2, and the various temperature measurements are plotted in
Figure 4-3.

The flow rate data, for the 71-hour test period, show an average vent rate
of 0.0572 lb per hr. Unfortunately, no scale weight data were taken during this
period (due to the removal of the pressure control panel which was leaking) as
a check on the flow rate. The Test Log reveals, however, that scale weighings
were recorded 96.83 hours before and 264.25 hours after the 71-hour test period,
over which time 24.59 lb of hydrogen boiled off. This data yields an average
vent rate of 24.59/432.08 = 0.0569 lb per hr, an excellent corroboration of the
wet test meter data. Therefore, the measured vent rate is taken to be 0.0572
lb per hr, corresponding to a heat leak of 11.18 Btu per hr.

The temperature data appear to be somewhat anomolous, especially the inner
fill boss readings. The average fill boss temperature of about 48 R is 12 R
above the saturated liquid temperature at the tank pressure of approximately
13.5 psia. This discrepancy is greater than should be attributed to instrument
inaccuracy. It is possible that the fill boss temperature sensor tube is
not properly positioned at the inner fill boss opening -- it may be situated
several inches into the tube. The vent boss temperature of 55 R, or about
19 R above saturation, could be due to thermal stratification in the ullage.
This is not unreasonable to expect, considering the very low thermal conductivity
of the thin titanium-alloy vessel wall, and the presence of at least one,
possibly two, fiberglass support pads conducting heat to the hydrogen vapor.
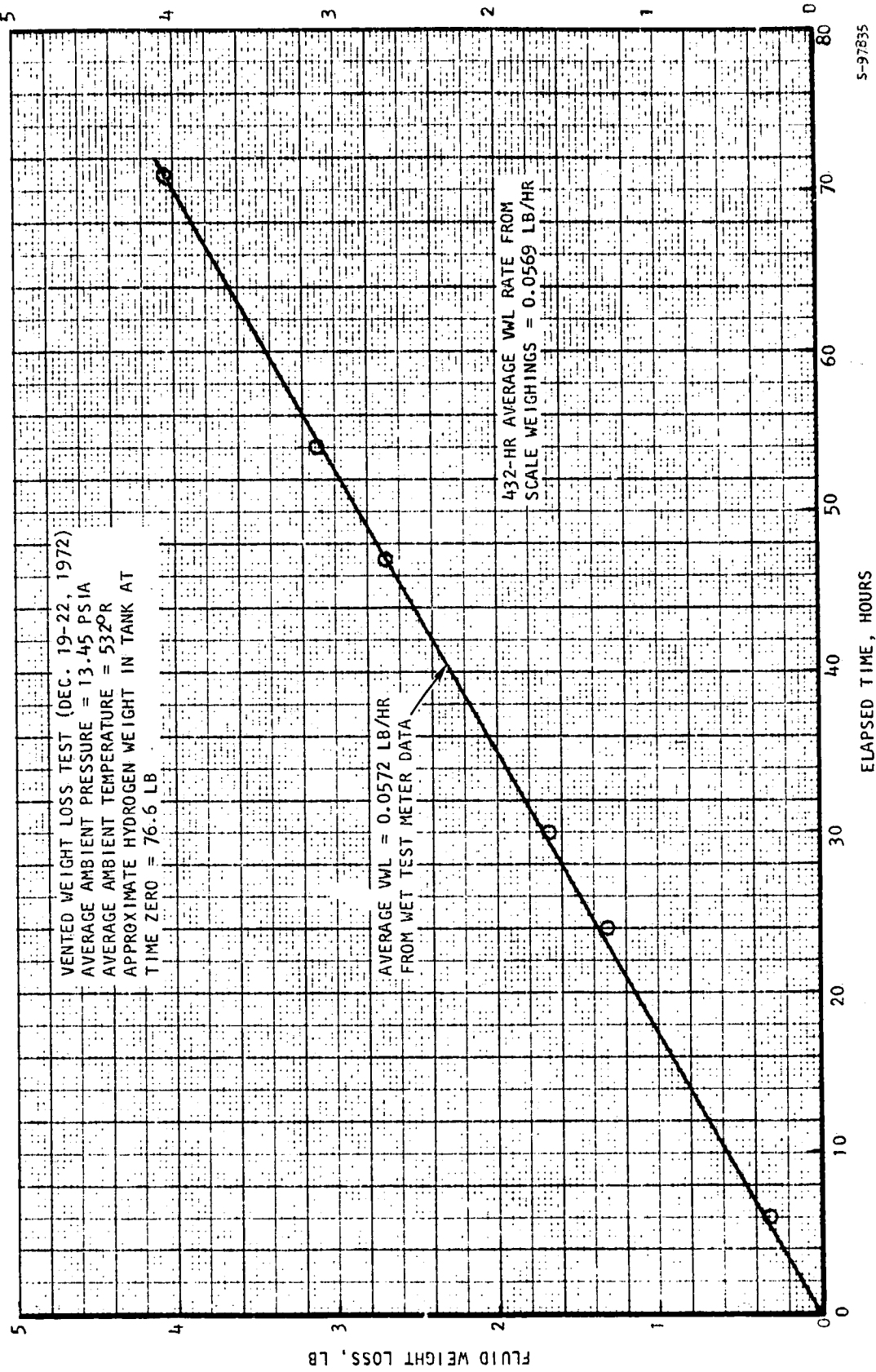
Figure 4-2. LH$_2$ Vented Weight Loss Test – Tank No. 2A

VENTED WEIGHT LOSS TEST (DEC. 19-22, 1972)
AVERAGE AMBIENT PRESSURE = 13.45 PSIA
AVERAGE AMBIENT TEMPERATURE = 532°R
APPROXIMATE HYDROGEN WEIGHT IN TANK AT
TIME ZERO = 76.6 LB

AVERAGE VWL = 0.0572 LB/HR
FROM WET TEST METER DATA

432-HR AVERAGE VWL RATE FROM
SCALE WEIGHINGS = 0.0569 LB/HR

ELAPSED TIME, HOURS

FLUID WEIGHT LOSS, LB
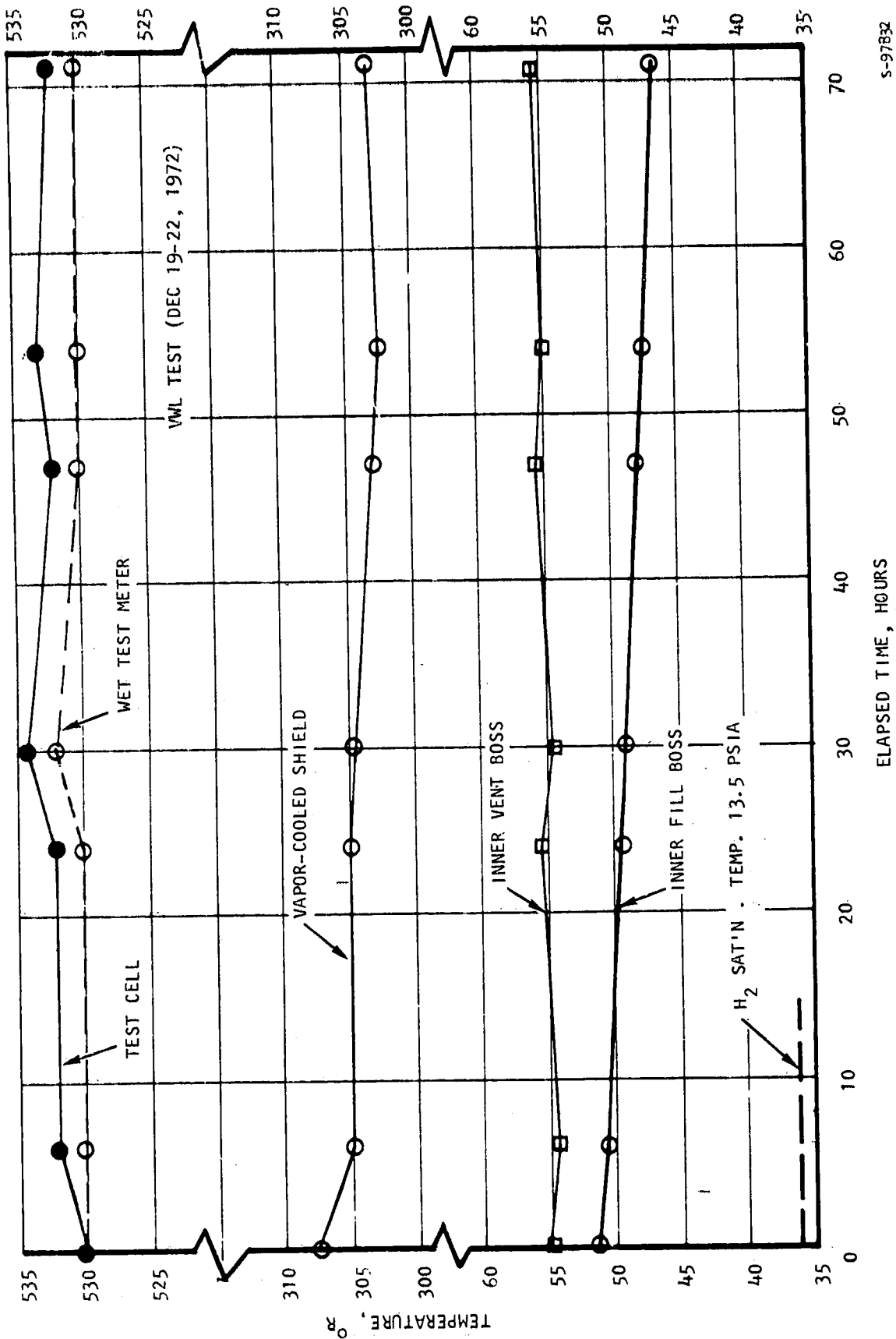
S-97835

Figure 4-3. Temperature Data From VWL Test – Tank No. 2A

The average VCS temperature from Figure 4-3 is taken to be 304 R, and the average ambient (outer shell) temperature 532 R.

Surface Emittance Determination

An analytical prediction of Tank No. 2A thermal performance cannot be made with a high degree of confidence because the total normal emittance of the aluminized vacuum annulus is not known. The best that can be done "a priori" is to assume an emittance versus temperature characterization based on what could be similar surfaces. The difficulty here is that a very wide range of data exists for aluminum surfaces because of the wide range of surface conditions possible. At room temperature, an RMS rating of 33 micro-inches on aluminum 2024-T4 (92.7 percent Al) can exhibit an emittance of 0.09 (and 0.018 at 10 R)*, whereas the aluminized side of crinkled, 1/4-mil, aluminized Mylar can be as low as 0.03. Since radiation is the predominant mode of heat transfer in this tank, a variation like that can give a wide range of heat leak (vent rate) results. The problem is further complicated by the range of possible emittance values to be assigned to the VCS, whose temperature is also an unknown (in the computer analysis). Therefore, it is suggested that the most meaningful analysis to be performed here is to back out an "apparent" emittance characteristic from the test data (both vent rate and VCS temperature) and compare it with data from other aluminum surfaces of known emittance.

Two basic assumptions are made in this method of analysis: 1) the heat transfer through either annular space can be separated into radiation and conduction components, where the conduction contributions are known (that is, they can be calculated independently), and 2) the emittance of all aluminized surfaces is a linear function of temperature, or a constant (an overall average, or effective, value). The first assumption is necessary to do any tank per-formance analysis, the total heat transfer rate being the sum of the individual members' heat leaks. The second assumption is not necessary, but is very conve-nient because there is an infinite number of possible combinations of individual surface emittances that yield the same emittance interchange factor for a given annulus. In this program, the radiation heat transfer rate and emittance inter-change factor are defined as follows:

$$Q_R = \sigma \bar{e} A_1 \left(T_2^4 - T_1^4 \right), \text{ Btu per hr} \qquad (1)$$

$$\bar{e} = \left[\frac{1}{e_1} + \frac{A_1}{A_2} \left(\frac{1}{e_2} - 1 \right) \right]^{-1} \qquad (2)$$

*K. H. Hawks and W. B. Cottingham, "Total Normal Emittances of Some Real Surfaces at Cryogenic Temperatures," Adv. Cryo. Eng., Vol. 16, 1971, page 473.

where $\sigma = 1.714 \times 10^{-9}$ Btu/hr-ft^2- R^4

T = surface temperature, R

A = surface area, ft^2

e = surface emittance (relative to black body = 1.0)

and subscripts "1" and "2" refer to the inner and outer surfaces, respectively, bounding a given annulus.

Using the average test data, as presented in Figures 4-2 and 4-3, for ambient temperature (532 R), VCS temperature (304 R), and vent rate (0.0572 lb per hr); and assuming the actual inner vessel wall temperature to be 36 R, and the VCS effectiveness to be 1.0, the breakdown of heat transfer rates was calculated. The results are presented in Table 4-1. The emittance interchange factors from Equation (1) are then

TABLE 4-1

HEAT LEAK BREAKDOWN CALCULATED FOR TANK NO. 2A FROM TEST DATA

Annulus Space	Heat Transfer Rate (Btu/Hr)			
	Total	Supports	Fill line	Radiation
Below VCS	11.18	3.35	0.56	7.27
Above VCS	59.63	3.42	0.22	55.99

0.0143 and .0125, below and above the VCS, respectively. These emittance results are contrary to the well-known behavior of metallic surfaces, namely, that "emissivity" increases with increase in temperature*. If a straight-line equation were fit to the above interchange factors, the zero temperature value would be 0.0303 and the 530 R value would be only 0.0222; the equation has a negative-slope temperature dependence:

$$e = 0.0303 - 1.53 \times 10^{-5}(T) \qquad (3)$$

The above data analysis depends on an accurate measurement of the VCS temperature. To estimate the effect of VCS temperature on determination of emittance, a computer study was performed to calculate vent rate and VCS temperature as a function of a constant apparent emittance on all annulus surfaces. The results are presented in Figure 4-4, where the sensitivity to VCS temperature is shown to be quite dramatic. A VCS temperature increase of only 6 R raises the vent rate by over 26 percent, and the apparent emittance by almost 32 percent. The measurement of vent rate is considered to be more

---

*W. H. McAdams, Heat Transmission, 3rd Ed., McGraw-Hill, 1954, page 61.
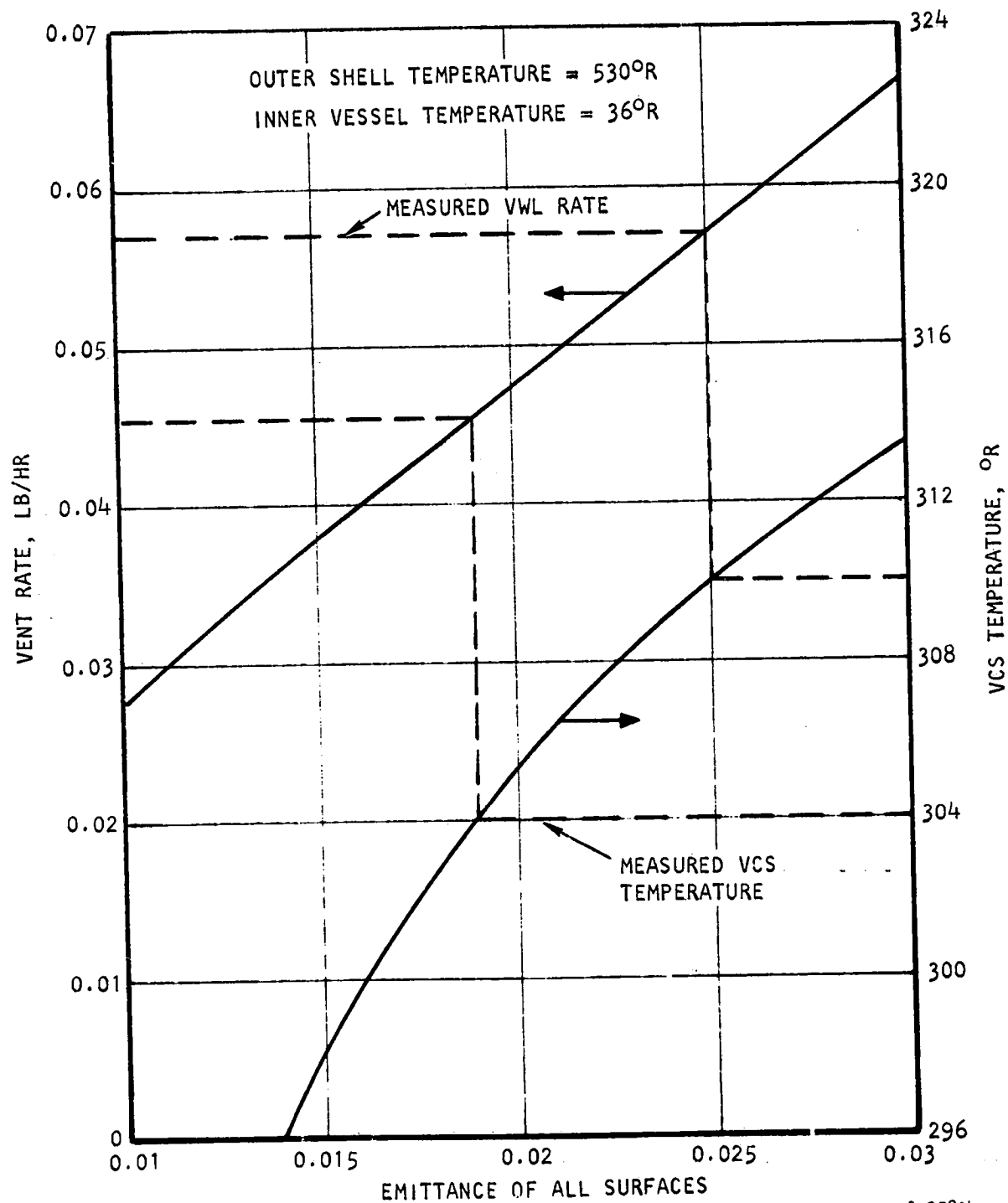
Figure 4-4. Determination of Constant Emittance Required to
Simulate Tank No. 2A VWL Test

accurate, since it is obtained by two different methods. The VCS temperature is less accurately known (only one sensor), and, from Figure 4-3, was found to vary by more than 2 R during the 71-hr test period. Another uncertainty in using the VCS temperature is the assumption that it is a measure of the temperature over the entire shield. Further, the computer study is based on 100 percent effectiveness (i.e., the fluid leaves the VCS at the VCS temperature). This study points toward an apparent emittance of approximately 0.025, if it were independent of temperature. The value of 0.019, which would be required if the VCS were 304 R, is lower than any data in the literature for aluminized surfaces at temperatures above 300 R, and results in a vent rate of only 0.0455 lb per hr.

A possible explanation for the unrealistic emittance temperature dependence of Equation (3), assuming the VCS temperature measurement is correct, may be in the uncertainty in calculating the "known" heat leaks. Table 4-1 shows that the conduction heat leaks are more important below the VCS (35 percent of total) than above it (only 6 percent of the total). If the conduction heat leaks shown in Table 4-1 are too low the radiation heat transfer below the VCS will be less, and by a larger percentage than above the VCS. Hence, it follows that a lower emittance interchange factor could result below the VCS than above it, allowing the possibility of a positive-slope (more reasonable) emittance characteristic.

Another way to evaluate the apparent emittance of the annulus is an extension of the above study, using an emittance characteristic which increases with increasing temperature. This was actually done before the WWL testing in order to estimate the expected vent rate. A linear emittance characteristic proportional to that measured by Cunnington, et.al.* for the aluminum side of single-aluminized Mylar multilayer insulation was used. The best values reported were 0.013 at 113 R and 0.029 at 560 R. A series of computer runs were made with increasing factors applied to the emittance curve. Two printouts were presented in AiResearch Report No. 73-9418, Pages 3-19 and 3-20, with vent rate results bracketing the measured value. A curve 20 percent higher than the base emittance curve gave a vent rate of 0.058 lb per hr (emittance range from 0.012 at 36 R to 0.0336 at 530 R). The predicted VCS temperature, however, was 335 R, or 32 R higher than indicated by the test results.

A summary of the analytical determination of emittance in an attempt to match the vent rate and shield temperature test data for Tank No. 2A is presented in Table 4-2, together with judgments on the validity of the emittance-temperature dependence obtained. In conclusion, it appears that vacuum-deposited, 2000 Å aluminized annulus surfaces exhibit apparent emittances more nearly equal to those of 400 Å aluminized polyester film than polished aluminum plate, especially at room temperature. It also appears that the VCS temperature should be determined more accurately in order to evaluate the annulus emittance, and that for a given emittance characteristic (if available from independent sources) the least accurately predicted parameter would be VCS temperature.

---

*G. R. Cunnington, C. W. Keller, and G. A. Bell, "The Thermal Performance of Multilayer Insulations," Interim Report, NASA-CR 72605, 20 April 1971, page 4-22.

GARRETT AIRESEARCH MANUFACTURING COMPANY
OF CALIFORNIA

TABLE 4-2

SUMMARY OF EMITTANCE ANALYSES FOR TANK NO. 2A

Vent Rate (Lb/Hr)	VCS Temp. (R)	Apparent Emittance		Comments on Temperature Dependence
		36 R	530 R	
0.0572*	304*	0.0297	0.0222	Unrealistic - negative slope
0.0455	304*	0.019	0.019	Constant - too low for 530 R
0.0572*	310	0.025	0.025	Constant - reasonable average
0.050	331	0.010	0.028	} Reasonable - positive slope, dervied from Al-Mylar data
0.058	336	0.012	0.0336	

*Test values

TANK NO. 2B (MICROSPHERE INSULATION)

Measured Performance

The tank insulated with partially-aluminized microspheres exhibited such unusual behavior (as compared with analytical predictions, to be discussed later), that the boiloff test was increased beyond the time usually required to establish a typical vessel steady-state vent rate. Figure 4-5 presents the vented weight loss data** for the entire 31-day test series, and denotes the points at which significant events or procedure changes occurred. Both scale weight data and wet test meter (WTM) integrated data are plotted. In general, over long periods of time, one would tend to place more confidence in the scale weighings, although the wet test meter appears to have responded to some short term events, where the scale did not. The discrepancy between the two is in the right direction (assuming correct calibrations) since plumbing leaks would escape being recorded by the WTM. Vent rates calculated by test segment showed the minimum difference to be 1.6 percent (WTM rate higher than scale rate), and the maximum difference to be 19.8 percent (WTM rate lower than scale rate).

The presence of thermal acoustic oscillations (TAO) with the tank in the normal vent configuration prompted numerous procedure changes and experimentation. Among them were rotating the tank 90 degrees and 170 degrees from the normal, installing a plug (only partial plugging) in the cryostat supply line, and removing the water saturator (upstream of the WTM). Some of these schemes altered the intensity of the oscillations, but since they were of relatively small magnitude,*** examining the entire data set reveals very little change in average vent rate from one time segment to the next, with two exceptions. The obvious one is when the tank is inverted 170 degrees and fluid is vented out

---

**Raw test data from which this curve was constructed is given in Appendix A.
***A quantitative estimate of the TAO effect on tank heat leak is given later in this section.

FOLDOUT FRAME /

Figure 4-5. LH$_2$ Vented Weight Loss Test — Tank No. 2a

The graph legend contains the following numbered items:

1 COMPLETED INITIAL FILL, 87.22 LB H$_2$

2 NORMAL VENT (VCS FLOW) ORIENTATION, COOLDOWN AND STABILIZATION COMPLETE, WET TEST METER INSTALLED

3 BAROSTAT AND BARATRON INSTALLED

4 ATTACHED OSCILLOGRAPH, PRESSURE TRANSDUCERS; INSTALLED MICRO-VALVE BTWN. FILL AND SUPPLY PORTS

5 MOVED MICRO-VALVE TO BTWN. SUPPLY AND VENT PORTS

6 ROTATED TANK 90° (LOST TARE WEIGHT)

7 REMOVED W.T.M. SATURATOR, ADJUSTED BAROSTAT, MISC.

7A ZEROED WET TEST METER

8 TANK ROTATED BACK TO NORMAL, 18.75 LB LIQUID ADDED (APPROX. 25.3 LB IN TANK)

9 TANK ROTATED 170°, FLOW OUT SUPPLY LINE

10 TANK EMPTIED, ROTATED TO NORMAL, INSTALLED BALL-ON-CABLE IN SUPPLY LINE

11 FILL COMPLETED, 85.72 LB H$_2$

12 COOLDOWN AND STABILIZATION COMPLETED

13 BALL-ON-CABLE REMOVED

14 TOPPED OFF TO 86.11 LB, TANK ROTATED 170°, FLOW OUT SUPPLY LINE

15 END OF TEST

JUNE 1975

ELAPSED TIME, HOURS

(528.6)   (737.8)

WEIGHT DATA

METER DATA

NOT GOOD TEST; LESS THAN 7% (VOL.) LIQUID LEFT IN TANK

the fill/supply line, thus bypassing the vapor-cooled shield (VCS). This vent rate is expected to be higher, as was evident from the test data. The other exception is more subtle, and could possibly be due to experimental error: that is, the wet test meter recorded a drop in vent rate of approximately 15 percent when a micro-valve was installed between the fill and supply ports. Since the scale weight data gave the same vent rate as before installing the micro-valve (the tare weight was adjusted for the plumbing change), it is suspected that a small leak may have bypassed the WTM, or there was some error in recording the data.

Two portions of the test sequence were selected for analysis: 1) the last series in the normal vent configuration, where the agreement between scale and WTM data agreed to within 3.5 percent (scale = 0.199 lb per hr; WTM = 0.192 lb per hr); and 2) the last test segment, where the tank was inverted 170 degrees and the flow bypassed the VCS. Vent rate data from the WTM was 17.5 percent lower than from the scale (scale = 0.280 lb per hr; WTM = 0.231 lb per hr). The earlier test data for the inverted tank was not used because the tank was nearly empty and excessive stratification was evident--the vented fluid temperature was 60 -70 R above the liquid temperature.

The temperature data for the selected test periods is presented in Figure 4-6 and Figure 4-7. The various times denoted by circled numbers coincide with the events described on the weight loss curve, Figure 4-5.

The fact that the fill boss temperature now reads within 2 R of 13.5 psia saturated liquid-hydrogen temperature does not preclude the possibility that the temperature sensor is actually in the tube, as was considered in observing the temperature data from Tank No. 2A. The clamp (an unintended thermal short) supporting the supply tube at about 8-10 in. from the inner fill boss could result in the presence of liquid several inches into the fill tube.

The vent boss temperature in Figure 4-6 and the fill boss temperature in Figure 4-7 show a gradual divergence from the corresponding data for Tank No. 2A, Figure 4-3 (inner vent boss temperature nearly constant at 55 R). This is probably due to the much higher heat leak (factor of 3.5 to 4.5 above Tank No. 2A) causing more thermal stratification in the ullage. The slope of the curves could probably be related to the increased rate of liquid level recession in the present tank (No. 2B).

Although the VCS temperature varied gradually over the test period, the following averages are taken for comparison with analysis: 94 R in the normal vent configuration, and 1.2 R with the tank inverted and no flow through the VCS line.

Table 4-3 summarizes the key parameters derived from the selected VWL test periods described above. The uncertainty value expressed for the vent rate is simply the deviation from the mean value between scale and WTM data. The uncertainty expressed for the VCS temperature is the deviation from the average value estimated over the time period. The 24-hr average ambient temperature was estimated to be 529 ±5 R.
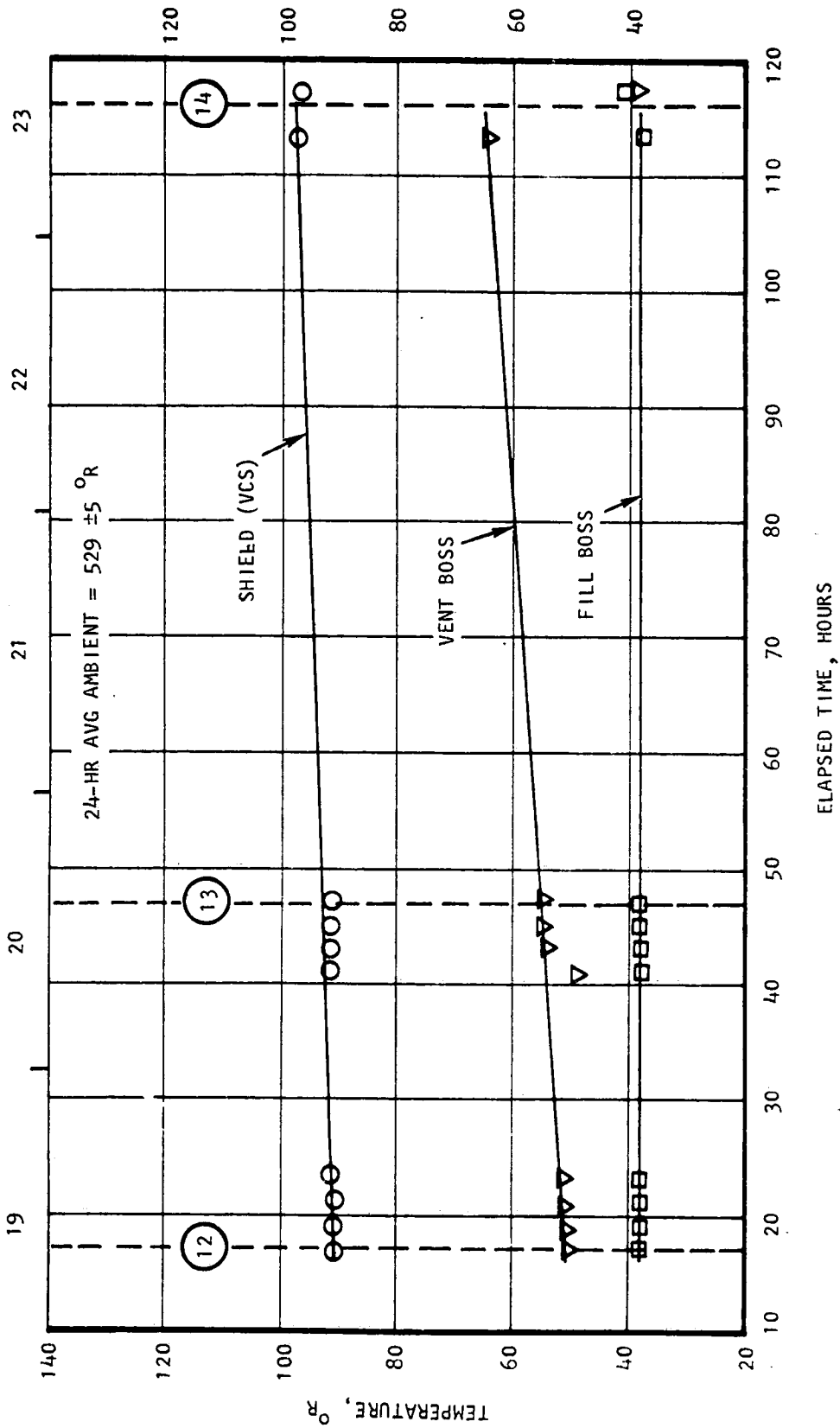
Figure 4-6. Temperature Data for Normal Vent Configuration — Tank No. 2B
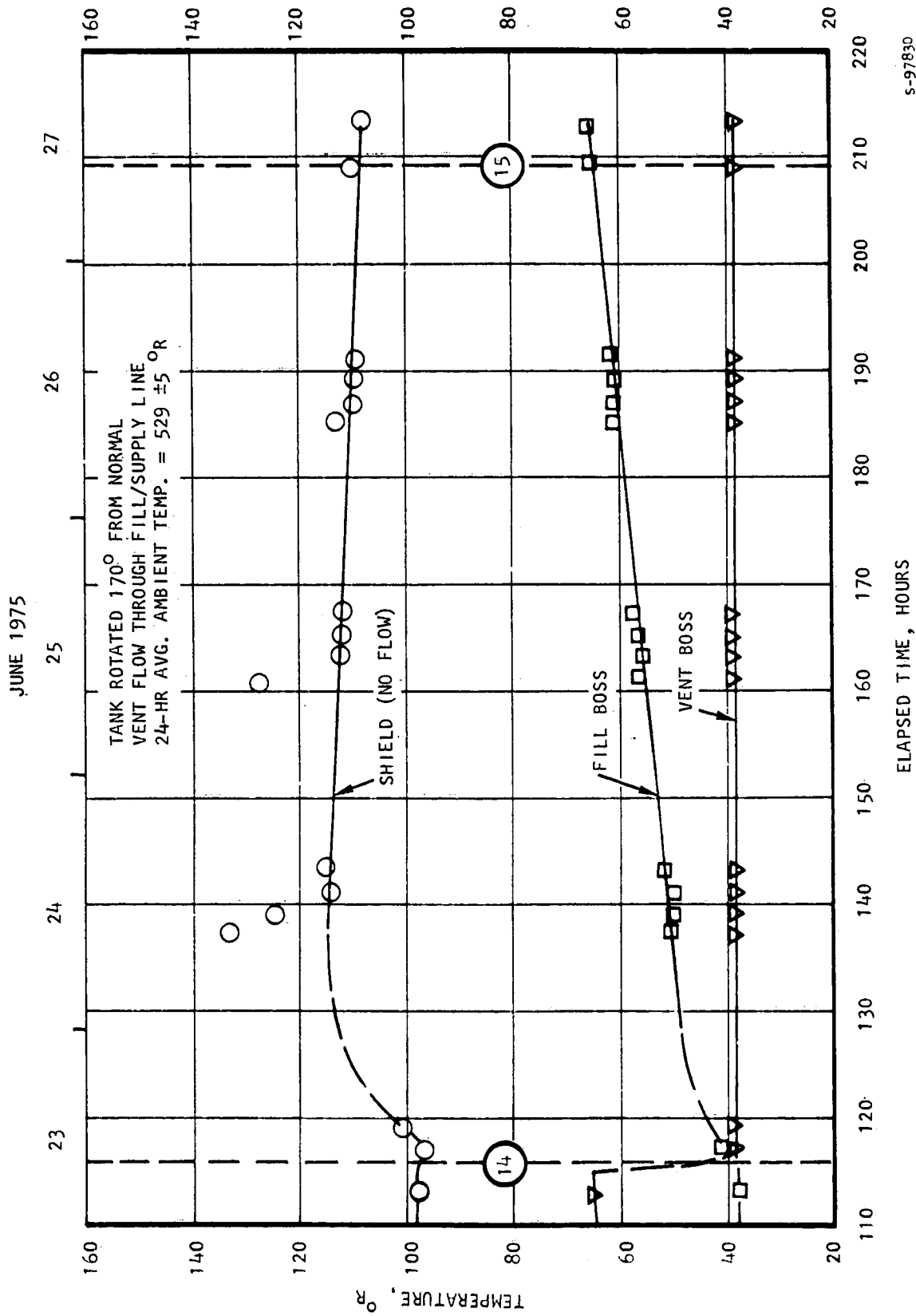
s-97831

Figure 4-7. Temperature Data for Inverted Configuration – Tank No. 2B

TABLE 4-3

MEASURED PERFORMANCE OF TANK NO. 2B

Item	Tank Vent Configuration	
	Normal	Inverted
Average Vent Rate, lb per hr	0.196 ±0.003	0.256 ±0.024
Heat Leak, Btu per hr	38.3	50.0
VCS Temperature, R	94 ±4	112 ±3

Estimated Effect of TAO on Tank Heat Leak

A recently published investigation of thermal acoustic oscillations by Spradley, et. al.* provides an excellent basis for estimating the effect of TAO on tank heat leak. Although this reference work is confined to liquid helium systems and an idealized gas-filled tube geometry, the range of appropriate parameters studied was broad enough to merit applying here.

Our tube configuration is somewhat complicated in that it is a compound line with two different diameters (one line containing 3 tubes within it) with an unknown temperature at the tee joining them. Referring to Figure 2-1, the worst conceivable situation for TAO is suspected to be the path from the cryostat adapter, down the supply line, and into the liquid via the fill line. Using a hydraulic diameter of 0.4456 in. for the fill line gives an aspect ratio of L/D = 58; the cryostat supply line aspect ratio is approximately L/D = 338. Spradley's work does not suggest how to treat a compound line, so assuming aspect ratios are additive, for the total path we obtain an aspect ratio of approximately L/D = 400. The temperature ratio from ambient to LH_2 is T_h/T_c = 15. Using these two parameters the following parameters are obtained from the Spradley model (page No. of referenced work is also given):

$\qquad$ Pressure amplitude, P_A = 0.04 atm (page 43)

$\qquad$ Oscillation frequency, f = 23 Hz (page 85)

$\qquad$ Intensity, $I = \overset{\wr}{(0.04)} (23) = 0.92$ atm - Hz

$\qquad$ Tube heat leak ratio, Q/Q_t = 9 (page 89)

Q/Q_t is defined as the ratio of total tube heat leak (with TAO) to normal conduction heat leak.

---

*L.W. Spradley, W.H. Sims and C. Fan, "Thermal Acoustic Oscillations," Volume II, Final Report, LMSC-HREC TR D390690-II, March 1975.

The predicted Tank No. 2B heat leak breakdown is presented later in the
thermal performance summary, Table 4-6, showing a fill line heat leak (normal
conduction) of 0.27 Btu/hr, and a total tank heat leak of 15.1 Btu/hr. Applying
the above TAO results gives a line heat leak of 2.43 Btu/hr; resulting in a
total tank heat leak of 17.3 Btu/hr, an increase of only 15 percent above the
"no-TAO" predicted value.

If the maximum measured oscillation amplitude of 0.02 atm and frequency
of 12 Hz is used in place of the Spradley prediction based L/D and T_h/T_c,
the resulting Q/Q_t is approximately 2.5 (from an experimental point on page 89,
which grossly exceeds the theoretical value). In this case the total line heat
leak would be 0.68 Btu/hr; resulting in a tank heat leak of 15.5 Btu/hr, an
increase of only 3 percent over the "no-TAO" predicted value.

With a measured tank heat leak of 38.3 Btu/hr, it is concluded that the
fill line TAO effect is negligible, since the line conduction heat leak is such
a small fraction of the total apparent heat leak to the vessel.

Analytical Performance Prediction

Microsphere insulation performance data have been published by Cunnington
and Tien*, where hemispherically-aluminized spheres (among others) were tested
in a flat-plate calorimeter with cold boundary maintained at 78 K. The data
for a 5.84-mm thick layer (average sphere diameter of 84 microns) was curve-
fitted to the following heat flux equation:

$$q = 0.0315 (T_1 - T_2) + 0.0166 \sigma (T_1^4 - T_2^4) \qquad (4)$$

where   q = heat flux, watt/m^2

T_1, T_2 = temperature of the warm and cold boundaries, respectively, K

σ = 5.667 × 10^{-8} watt/m^2- K^4

The conduction term in Equation (4) assumes that the aluminum film thermal
conductivity is constant to temperatures as low as 78 K. This is approximately
correct, but as the cold boundary temperature approaches 36 R (20 K), liquid
hydrogen normal boiling temperature, pure aluminum conductivity rises rapidly,
as shown in Figure 4-8. The constant value implied in Equation (4) is probably
137 Btu/hr-ft- R, as quoted in a paper by Chan and Tien**, which agrees with the
reference used for Figure 4-8. The performance prediction computer program
described earlier was modified to include the characterization of microsphere

---

*G. R. Cunnington and C. L. Tien, "Heat Transfer in Microsphere Cryogenic
Insulation," Adv. Cryo. Eng., Vol. 18, 1973, pp 103-111.
**C. K. Chan and C. L. Tien, "Conductance of Packed Spheres in Vacuum,"
Journal of Heat Transfer, Vol. 95, 1973, pp. 302-308.
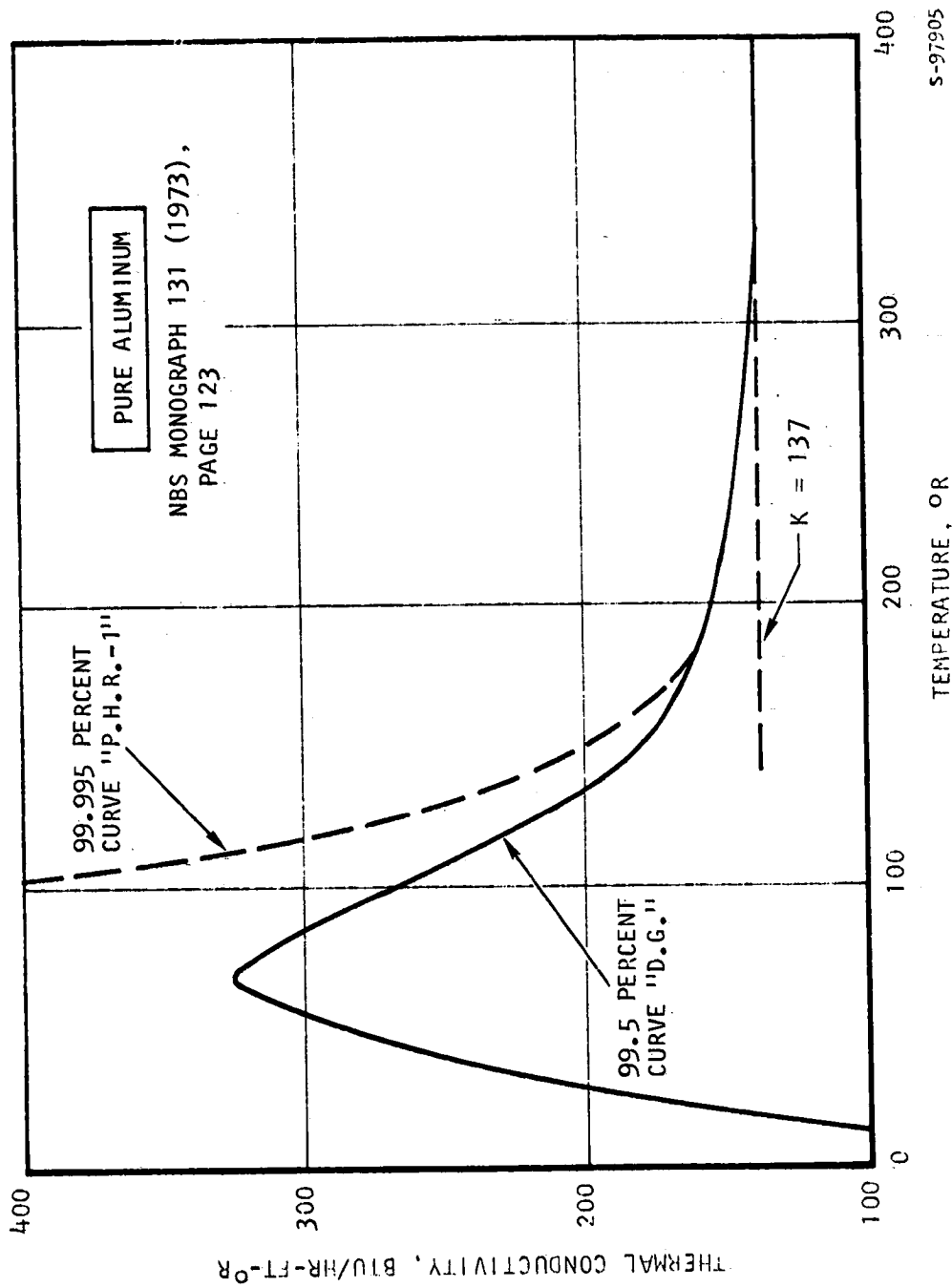
Figure 4-8. Thermal Conductivity of Pure Aluminum at Low Temperature

s-97905

Insulation. The program equation for heat flux has a correction for the thermal conductivity of 99.5-percent-pure aluminum, by making use of a built-in integral curve:

$$\int_{T}^{660°R} k \, dT \text{ versus } T$$

where T is the cold boundary temperature, R. Another correction applied to Equation (4) is an insulation thickness factor, which converts the flux equation into an apparent thermal conductivity equation. According to the theory advanced by Cunnington and Tien, as pointed out in the discussion following their 1973 paper, the conduction heat flux would be proportional to $t^{-2/3}$. (In a more recent paper, by Nayak and Tien, this theory has been slightly revised; it will be examined further below.) In addition, the entire equation is multiplied by t_o, the thickness which applies to the experimental heat flux equation. The heat flux, in general, would then take the following form:

$$q = \frac{q_o t_o}{t} = \left[C_1 (T_1 - T_2) \left(\frac{k_{Al}}{k_o}\right) \left(\frac{t_o}{t}\right)^{2/3} + C_2 \left(T_1^4 - T_2^4\right)\right] \frac{t_o}{t} \qquad (5)$$

where
$$k_{Al} = \int_{T_2}^{T_1} k \, dT \Big/ (T_1 - T_2), \text{ Btu/hr-ft- R}$$

$$t = \text{insulation thickness, in.}$$

This is the microsphere insulation characterization built into the computer program. The constants are determined as follows (T_1 and T_2 remain in degrees Kelvin):

$$C_1 = 0.0315 \, [3.41443/(3.28084)^2] = 0.00999215$$

$$C_2 = 0.0166 \, [3.41443/(3.28084)^2] \, (5.667 \times 10^{-8}) = 2.98408 \times 10^{-10}$$

$$k_o = 137 \text{ Btu/hr-ft- R}$$

$$t_o = 5.84/25.4 = 0.22992 \text{ in.}$$

A more recent paper, by Nayak and Tien*, explores further the influence on microsphere insulation apparent thermal conductivity of the compressive pressure resulting from self-loading (microsphere weight). This effect is expressed in terms of an insulation thickness L. Introducing the concept of lattice conductivity (or conductive component, the radiative conductivity is determined separately) for packed beds of hollow microspheres, experimental data from a spherical calorimeter indicated a relationship of the form:

$$k_c \sim L^{0.66} \qquad (6)$$

---

*A. L. Nayak and C. L. Tien, "Thermal Conductivity of Microsphere Cryogenic Insulation," Paper K-4, 1975 Cryogenic Engineering Conference, Kingston, Ontario.

The revised theory, however, based on the deformation of thin spherical shells under light loads and density stratification, implies an exponent of 0.6. At a mean temperature of 157 K (283 R), the Nayak and Tien data for a 2.3-cm thickness of fully-aluminized microspheres (average diameter of 26 microns) gives $k_c \approx 1.7 \times 10^{-3}$ watts/m- K (9.83 $\times$ 10^{-4} Btu/hr-ft- R). This reference point would give the following relationship:

$$k_c = 5.41 \times 10^{-3} L^{0.66} \tag{7}$$

where k_c = lattice thermal conductivity, Btu/hr-ft- R

          L = insulation thickness, ft

For the MOL tank nominal insulation thickness of 1.3 in., and mean temperature of 283 R, the lattice conductivity from Equation (7) would be 1.25 $\times$ 10^{-3} Btu/hr-ft- R. Using this insulation thickness implies that the VCS is not present. The test data, Table 4-3, for the inverted tank yields an apparent thermal conductivity (which includes the radiation component) of 2.64 $\times$ 10^{-4} Btu/hr-ft- R, which is lower than the Equation (7) value by a factor of 4.7. Therefore, applying this data as if no VCS were present would predict performance to be much poorer than observed. This concept will be pursued in more detail later.

The use of Equation (5) in the computer program gives the tank performance presented in Figure 4-9. Two input variables were examined in the attempt to correlate the test results: 1) VCS effectiveness, and 2) inner-annulus microsphere degradation factor. The effectiveness is a measure of how efficiently the VCS acts as a heat exchanger, that is, how close the fluid exit temperature approaches the average shield temperature (isothermal VCS assumed). The degradation factor is a multiplier (a value of 1.0 means no effect) applied to the heat flux equation for the inner annulus only. This would account for any increased compressive loading on the microspheres, or any other phenomenon which may increase the apparent conductivity of the microspheres at lower temperatures (exclusive of the aluminum conductivity effect and thickness proportionality), or a thermal short between the VCS and inner vessel.

As noted in Figure 4-9, a zero effectiveness shield simulates the inverted tank condition, when the flow by-passes the VCS. The trend toward infinite degradation factor simulates a VCS completely shorted to the inner vessel, thus rendering the inner annulus useless as a heat transfer barrier (VCS temperature and temperature of the fluid in the tank become identical). The tests results for the inverted tank, however, indicate a VCS temperature 205 R lower than predicted (the predicted value is 317 R, off the scale of Figure 4-9). This could be explained by a partially-shorted VCS (shorted to the inner vessel), except that the measured vent rate (from scale data) is even larger than the predicted vent rate if the VCS were completely shorted to the inner vessel (infinite degradation factor). Thus, even if the VCS were shorted, that alone is not enough to explain the disagreement between the microsphere analytical model and the test data for the inverted tank.
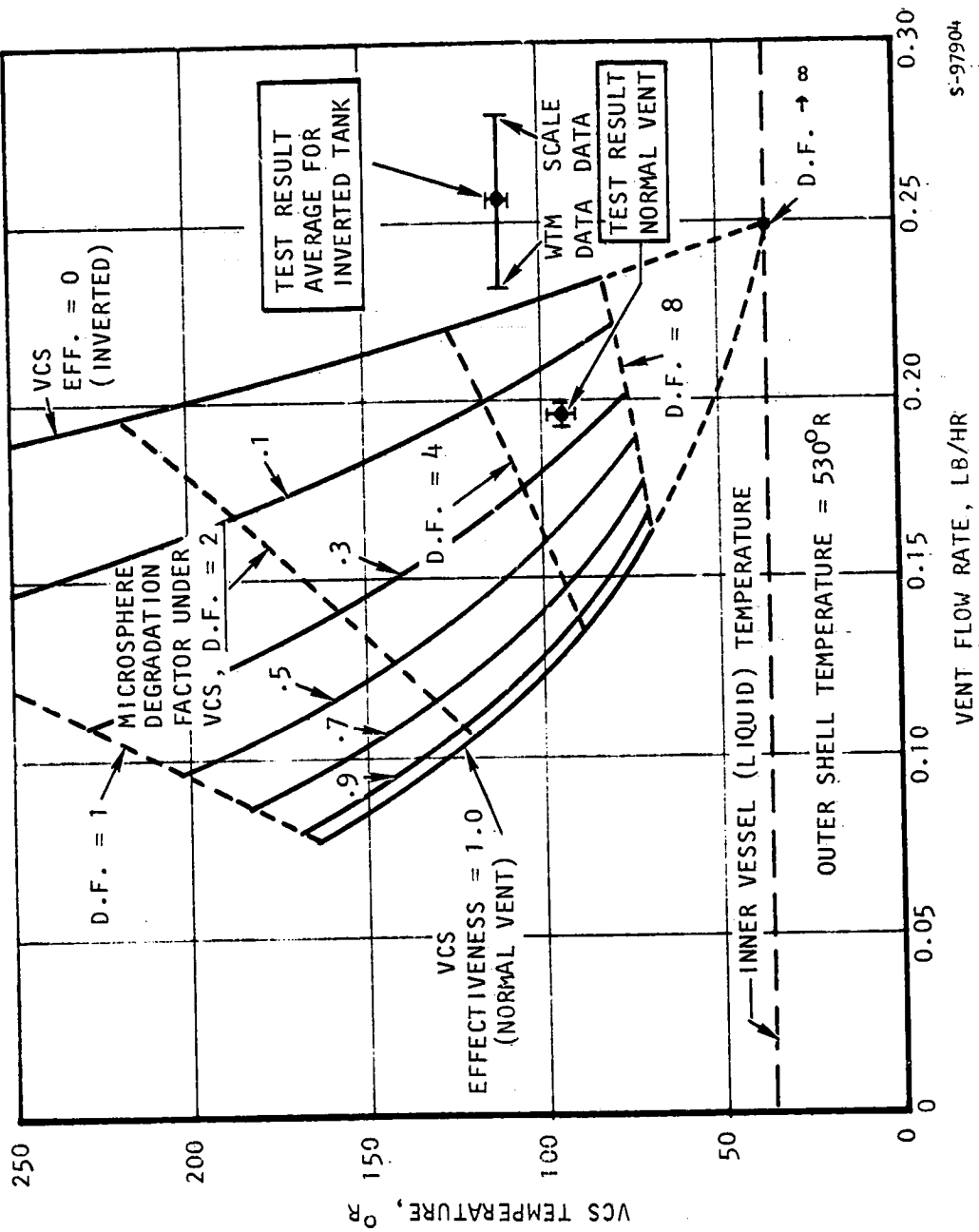
Figure 4-9. Analytical Study of Microsphere-Insulated Tank Performance

s-97904

The normal vent test result could be explained by a grossly inadequate shield efficiency (about 20 percent effectiveness) and a degradation factor of about 6. A degradation factor of this magnitude would not be unusual to apply to idealized equations for multilayer insulation systems, where anisotropic effects can be significant. However, for a near-isotropic media like microspheres, this factor seems to be exceedingly high.

An alternate approach would be to calculate an apparent thermal conductivity from the WWL test results, and compare them with the latest lattice conductivity data of Nayak and Tien, similar to the previous calculation for VCS not present. Using the WWL results, the apparent thermal conductivity is calculated separately for above and below the VCS, assuming that the support pad heat leak is predictable and the VCS effectiveness is 0.9. Then Nayak and Tien's theoretical prediction ($k_c \sim L^{0.6}$) is applied to the tank annulus dimensions and mean temperature. The comparison is presented in Table 4-4.

TABLE 4-4

APPARENT THERMAL CONDUCTIVITY COMPARISON
WITH NAYAK AND TIEN THEORY

| Annulus Region | Insulation Apparent Thermal Conductivity (Btu/hr-ft- R) | | | |
| | Normal Vent Configuration | | Inverted Configuration | |
	From Test	Theory	From Test	Theory
Above VCS	2.29×10^{-4}	7.68×10^{-4}	1.80×10^{-4}	7.79×10^{-4}
Below VCS	7.35×10^{-4}	1.82×10^{-4}	7.37×10^{-4}	2.06×10^{-4}

It is interesting to note that the theory predicts conductivities 3.35 and 4.33 times greater than the test results for the annulus region above the VCS, while the test results are 4.04 and 3.58 times greater than the theory below the VCS. The results are even more conflicting than shown, since the "theory" values do not include radiation (it is negligible below the VCS, only). The aluminum conductivity factor not included in the theory could account for some of the difference below the VCS, but the aluminum factors, (k_{Al}/k_o) in Equation (5), would be only 2.17 and 2.10, for the normal vent and the inverted configurations, respectively. It is apparent that using the new Nayak and Tien ($k_c \sim L^{0.6}$) in the computer program would only result in further divergence between predicted and measured VCS temperature and vent flow rate; that is, for the theory to give higher vent rates (closer to test data), the VCS temperature must be hotter (further away from test data).

More recent data published by Reinker, et. al.* is in much closer agreement with the VWL test results, although it uncovers a potentially serious problem with using hemispherically-aluminized microspheres. It was found that the thermal conductivity was highly dependent on sample history; that is, thermal cycling to LN_2 temperature increased the conductivity significantly. Table 4-5 presents a comparison of the apparent thermal conductivity previously calculated (for the "above VCS" case, an average of the normal vent configuration and inverted configuration from Table 4-4 is used) with data from Reinker at the same mean annulus temperature.

TABLE 4-5

APPARENT THERMAL CONDUCTIVITY
COMPARISON WITH REINKER DATA

| | Apparent Thermal Conductivity (Btu/hr-ft- R) | |
Item	Above VCS T_m = 175 K	Overall Annulus T_m = 157 K
VWL Test	2.05×10^{-4}	2.64×10^{-4}
Reinker Data:		
Uncycled (extrapolated)	1.4×10^{-4}	1.1×10^{-4}
Cycled Once to LN_2	2.5×10^{-4}	2.0×10^{-4}
Cycled Twice to LN_2	3.8×10^{-4}	3.1×10^{-4}

This comparison shows much better agreement than is obtained by using Equation (5), or the Nayak and Tien theory. Note that the VWL test value at 175 K is only 18 percent lower than Reinker's data after one cycle. In the VWL test the insulation was not fully cycled, although some of the microspheres under the VCS were warmed to 260 R (144 K), at 480 hours into the test (see Appendix, page A-14), prior to being rechilled down to LH_2 temperature. This history-dependent behavior of microsphere insulation was reported for the aluminized spheres only; the test data for uncoated microspheres was repeatable after cycling. The conductivity data for the uncoated microspheres fell between the half-aluminized data for one and two cycles.

From the above comparisons it can only be concluded that present theories and experimental (calorimeter) data are inadequate to explain the phenomena observed in the tank VWL tests.

_____
*R. P. Reinker, K. D. Timmerhaus, and R. H. Kropschot, "Thermal Conductivity and Diffusivity of Selected Porous Insulations Between 4 and 300K," Adv. Cryo. Eng., Vol. 20, 1975, pp. 343-354.

PERFORMANCE SUMMARY

The MOL Tank Program and its follow-on programs offer a unique opportunity to compare the performance of three different insulation systems in a production tank of the same basic design, with an evacuated annulus, a vapor-cooled shield, and fiberglass support pads. Table 4-6 presents a performance summary of the three tank configurations tested, and includes the calculated performance based on the best available material data. The reason for the good agreement between test data and calculations (without assumptions) with Tank No. 1 is that AiResearch has more experience with and more technical data for NRC-2 multilayer insulation than the other types.

Figure 4-10 illustrates graphically the relative magnitude of the tank heat leaks tabulated in Table 4-6.

TABLE 4-6

THERMAL PERFORMANCE SUMMARY
OF THREE INSULATION SYSTEMS

Tank No.	1	2A	2B	
Insulation System	NRC-2 Multilayer	Low-Emittance Surfaces	Hemispherically-Aluminized Microspheres	
Test Configuration	Normal Vent	Normal Vent	Normal Vent	Inverted (No VCS Flow)
Test Performance				
Vent Rate (Lb/Hr)	0.0410	0.0572	0.196	0.256
Heat Leak (Btu/Hr)	8.02	11.18	38.3	50.0
VCS Temp (R)	--	304	94	112
Calculated Performance				
Vent Rate (Lb/Hr)	0.0399	0.0572*	0.077**	0.162
Heat Leak (Btu/Hr)	7.80	11.18*	15.1**	31.7
VCS Temp (R)	232	310*	163**	317
Heat Leak Breakdown Calculated (Btu/Hr)				
Insulation***	5.25	7.12	13.69**	27.92
Support Pads***	2.10	3.48	1.09**	3.62
Lines***	0.45	0.58	0.27	0.12
VCS Cooling Rate	21.7	49.6	25.9**	--
Total from Ambient (outer shell)	29.5	60.8	41.0**	31.7

*Assumed emittance of 0.025 on all surfaces.

**Assumed VCS effectiveness of 100 percent.

***Heat leak to pressure vessel.
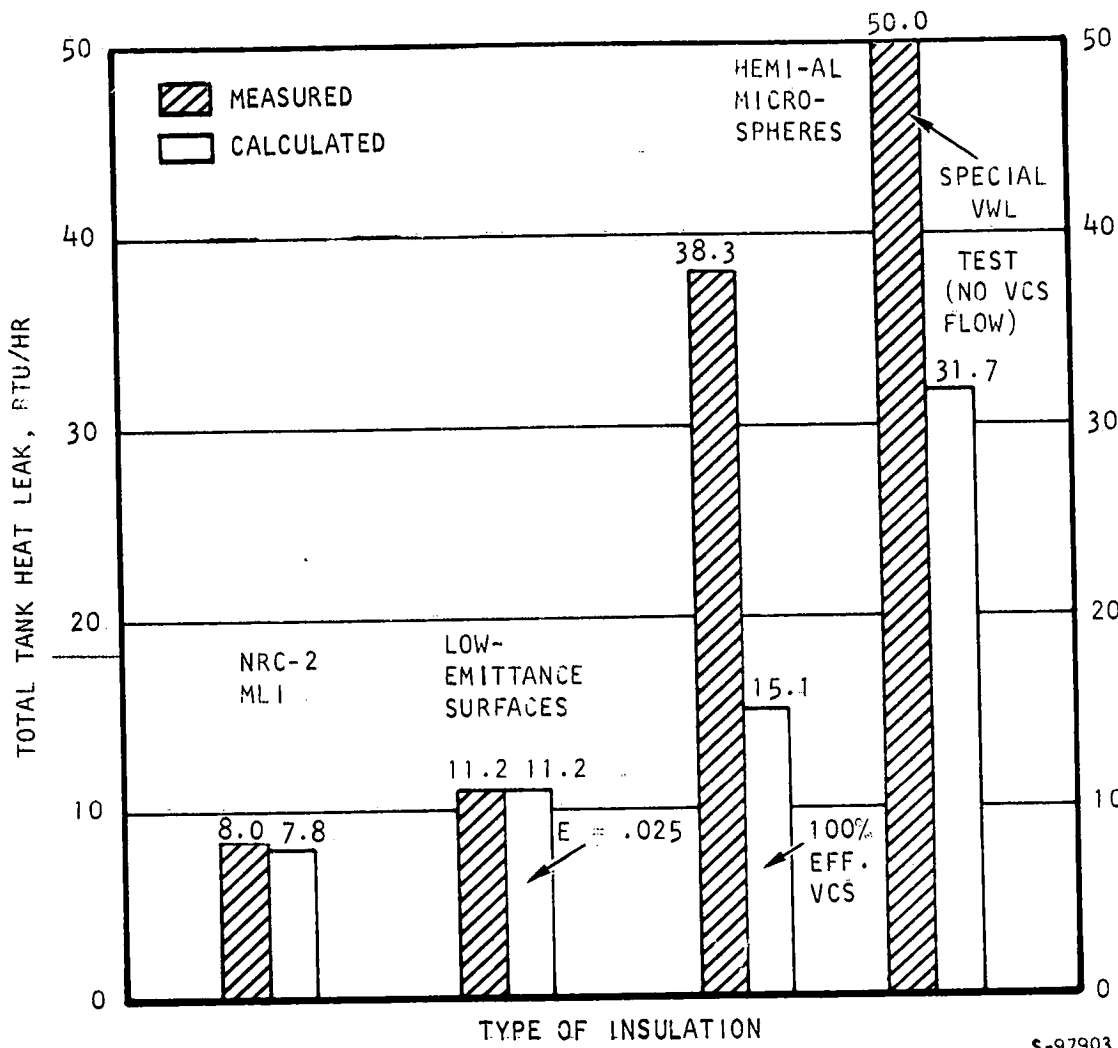
Figure 4-10. Comparison of Three Types of Insulation by
Tank Heat Leak

S-97903

SECTION 5

CONCLUSIONS AND RECOMMENDATIONS

Analytical studies and thermal performance testing of three similar tank configurations with different insulation systems resulted in the following conclusions.

1. Tank No. 1 (Multilayer Insulation) exhibited the lowest heat leak, and its thermal performance was most predictable, due to the extensive experience and tank-installed performance data generated at AiResearch.

2. Tank No. 2A (Low-Emittance Surfaces) demonstrated a heat leak almost 40 percent higher than Tank No. 1.

3. Tank No. 2A aluminized surfaces exhibited (by calculation) apparent emittances very close to aluminized polyester film values, which are about as low as can be achieved.

4. Tank No. 2A data analysis revealed the importance of a very accurate vapor-cooled shield (VCS) temperature determination; a 6 R error in VCS temperature was shown to produce errors of 26 and 32 percent in calculated vent rate and apparent emittance, respectively.

5. Tank No. 2B (Microsphere Insulation) exhibited a much higher heat leak than the other two tanks, by factors of 4.78 (over Tank No. 1) and 3.43 (over Tank No. 2A).

6. Tank No. 2B thermal acoustic oscillations (of low intensity, however) prompted additional experimentation in the vented-weight-loss (VWL) testing, culminating in rotating the tank approximately 170° and venting out the fill/supply line. In the inverted position, the average heat leak increased by about 30 percent.

7. Tank No. 2B VCS and inner vent boss temperatures were observed to slowly drift upward over long periods of time as the tank fluid quantity was depleted (the vent boss was always warmer than the liquid, as in Tank No. 2A); and a gradual decrease in vent rate was detected. These observations indicated ullage stratification; hence, the test periods selected for analysis followed filling or topping-off.

8. The predicted performance of Tank No. 2B, based on published theory and experiments with microsphere insulation (both flat-plate and spherical calorimeters), was in poor agreement with the test data. The measured VCS temperatures were much lower than predicted, while the measured vent rates were much higher than predicted. The best predicted heat leaks were a factor of 2.54 and 1.58 lower than the measured normal and inverted tank values, respectively. The corresponding predicted VCS temperatures were high by 69 R and 205 R, respectively. A comparison of test-data-derived apparent thermal conductivities of the

insulation above and below the VCS with theoretical lattice (conductive only) thermal conductivities of Nayak and Tien between the same temperatures showed contradiction; results varied by factors of 3.4 to 4.3, and in opposite directions above and below the VCS.

9. A low-temperature correction factor for pure aluminum thermal conductivity in the aluminum-coated microsphere theory may account for some of the discrepancy below the VCS; most of the literature data and curve-fitting have been limited to temperatures above 78 K (LN_2 boiling point), where the constant-aluminum-conductivity assumption is valid.

10. A recent paper by Reinker, Timmerhaus, and Kropschot (Adv. Cryo. Eng., Vol. 20, 1975) found that the thermal conductivity of half-aluminized microspheres increased each time the sample was cycled to LN_2 temperature. The apparent thermal conductivity calculated from Tank No. 2B test data, for the insulation above the VCS, was only 18 percent below Reinker's data after one cycle.

11. The Tank No. 2B test results, considered in conjunction with the three previously published calorimeter studies, indicate that perhaps the thermal performance of microspheres (especially the aluminized type) is not as predictable as expected when first proposed as a cryogenic insulation. In addition, for very low temperature cryogens (LH_2 and LHe), its thermal performance may not be competitive with multilayer insulation or low-emittance surfaces, where VCS are employed.

12. A microsphere-insulated tank testing program is recommended to obtain additional performance data on the practical application of microsphere insulation in high performance cryogenic tankage. A suggested tank evaluation and test program would include the following:

   ● Radiographic (X-Ray) examination of the tank annulus to determine the microspheres location (possibly density stratification), and the uniformity of VCS spacing.

   ● Gas analysis of the annulus to investigate the possibility of excessive SO_2 and O_2 (gases inside the microspheres) contaminating the vacuum ion pump leading to potentially erroneous annulus vacuum readings.

   ● Vented weight loss testing and cycling with liquid nitrogen to determine if aluminized-microsphere insulation conductivity increases with cycle time.

   ● Thermal performance testing with supercritical helium, with the addition of temperature measurement and insulation around the cryostat supply adapter, to verify the feasibility of satisfying the Phase II J-T cryostat supply requirements.

APPENDIX A

TEST DATA

This appendix contains test data sheets compiled during testing of the NASA MSFC cryogenic hydrogen/helium storage and supply system. Test data given in this appendix is indexed below.

LABORATORY TEST LOG

ARTICLE ON TEST _H₂/HL SUPPLY TANK_ S/N _____ O1 _____ DATE _8-9-74_

E.W.O/CHGE. NO. _3400-250358-01-0100_ SUPP. _____ I.D. _____

P/N _____ TECHNICIAN _ENGLISH / SALYER_ DATA SHEET _____ LOG SHEET _1_

TIME	
	GN₂ PURGE ON BAG SURROUNDING TANK
	RAN MILLIPORE SAMPLES OF GN₂ & HELIUM
	GAS, SET UP PER E.W.O. SAMPLES OK
9'44	STARTED COOL DOWN TC #1 IS ON TOP
	OF TANK AND TC #2 IS ON THE BOTTOM
10:00	TC #1, 71°F TC #2, 49°F
10:20	TC #1, 62°F TC #2, 30°F
10:40	TC #1, 54°F TC #2, -12°F
11:10	TC #1, 46°F TC #2, -55
11:40	TC #1, 40°F TC #2, -80°F
	AFTER LUNCH BOTTLE HAD WARMED UP TO
	0°F LOST LIQUID FLOW.
1245	LIQUID FLOWING AGAIN
	TC #1, 43°F TC #2, -15°F
1300	TC #1, 46°F TC #2, -40°F
1300¹⁵	TC #1, 48°F TC #2, -74°F
1330	TC #1, 47°F TC #2, -90°F
1340	STARTED TO PRESS WITH He, TC #1, 48°F
1343	TANK PRESS, 30 PSIG TC #1, 46°F
1346	TANK PRESS, 65 PSIG TC #1, 48°F
1352	CHANGED He 'K' BOTTLE
1355	TANK PRESS 140 PSIG TC #1, 43°F

PAGE TIME: _____

TOTAL TIME: _____

LABORATORY TEST LOG

GARRETT
AIRESEARCH

ARTICLE ON TEST H_2/HE SUPPLY TANK   S/N _____ 01 _____   DATE 8-9-74

E.W.O/CHGE. NO. 3400-250 336-01-C/CO   SUPP. _____   I.D. _____

P/N _____   TECHNICIAN ENGLISH   DATA SHEET _____   LOG SHEET 2

TIME	
1400	CHANGED 'K' BOTTLE CONTINUED TO PRESS TANK PRESS 160 PSIG TC #1, 44°F TC #2, -16°F
1405	TANK PRESS 800 PSIG, TC #1, 44°F TC #2, -20°F
1410	TANK PRESS 285 TC #1, 48°F
1412	CHANGED 'K' BOTTLE
1413	CONTINUED TO PRESS, TANK PRESS 290 PSIG TC #1, 46°F TC #2, -18°F
1415	START 4 MIN HOLD TANK PRESS 294 PSIG TC #1, 48°F TC #2, -16
1417	TANK PRESS 295 PSIG TC #2, -16°F TC #1, 46°F
1419	TANK PRESS 296 PSIG TC #1, 46°F TC #2, -12°F °F, END 4 MIN HOLD WAITING AND START WARM UP
1520	TEMP 45°F PURGE STOPPED AND BOTTLE SHIP TO L.A.

PAGE TIME: _____

TOTAL TIME: _____

GARRETT AIRESEARCH MANUFACTURING COMPANY OF CALIFORNIA

FLUID ANALYSIS
TEST DATA SHEET

Part Name _Ha/He Supply TANK (FILTER)_ Para No. _____

Procedure No. _____

Pt and SN _851270 3/b 1_

Date _8-9-74_ Test Engineer _R. RAYOOR_ Technician _ENGLISH_

Inspection _AiResearch Quality Control_ DCAS-QAR

Fluid: _HELIUM GAS_

Parameter		Units	Req	Actual	Remarks
Particle size	Over 500	Microns	0	0	
	350 to 500		2 max	0	
	200 to 350		10 max	3	

Figure 2. Fluid Analysis Test Data Sheet

AIRESEARCH MANUFACTURING COMPANY
LOS ANGELES CALIFORNIA

	DOCUMENT NO.		REV LTR	PG
70210	AT851240			8

GARRETT AIRESEARCH MANUFACTURING COMPANY
OF CALIFORNIA

MINI CANYON)   LAB DATA SHEET

ENG _____ DATE 8-9-74   TEST PURPOSE __ SHOCK AND PROOF PRESSURE

P.O. 201070   BAROM 27.16 "Hg

S/N 1   TEMP 75°F   TEST PERS. ENGLISH

NO.	TIME	2	TC #1 °F	4	TC #2 °F	6	TANK PRESS	8	9	10	11	12	13	14	15	REMARKS
1	13:40		48						STARTED TO PRESS. TANK.							STARTED TO PRESSURE
2	13:43		46				30									PRIOR RUNNING
3	13:46		48				65		CHANGED 'K' BOTTLE.							AT TEMP CT - TEST
4	13:55		43		-16		140									NO TC - R RUNS
5	14:00		44		-20		160									4 MINS PRESS DROP
6	14:05		44				200									
7	14:10		48				285		CHANGED 'K' BOTTLE.							
8	14:13		46		-18		240									
9	14:15		48		-16		244		START 4 MIN HOLD							
10	14:17		46		-16		265									
11	14:19		46		-12		270		END 4 MIN HOLD. END TEST DUMP PRESS.							

75-11607
Page A-5

LAB DATA SHEET

F/C 2400-2S0338-01-0404 DATE 3-4-75   TEST PURPOSE MICROSPHERE FILLING

P/N 956043   BAROM.

S/N 1

TEMP ___   TEST PENS.

MDL TANK TARE	MDL TANK FULL	WT. OF MICRO SPHERES			
DATE WT.	WT.				
3-4-75 502.50	519.38	16.88			

No.	MICRO SPHERE SUPPLY TANKS TARE WT.	EMPTY WT.	WT. LOSS	TOTAL WT. LOSS	REMARKS
1	24.18	18.76	5.42		
2	24.36	19.10	5.26		
3	24.22	19.64	4.58		
4	24.60	22.98	1.62	16.88	

FORM 81390A
AiResearch M..i. Co.

LAB DATA SHEET

EWC 3400-2S0335-01-0526 DATE 4-9-75   TEST PURPOSE VACUUM DECAY

P.N. 956643   BAROM   TEMP 74   TEST PERS. O.J. Boyle

S/N

NO.	DATE	TIME		OVEN TEMP	PURGE TEMP	SYSTEM VACUUM		MANIFOLD VACUUM		HAND VALVE	11	12	13	14	15	REMARKS
1	4-9-75	0805		74	74	1.5×10⁻⁸				OPEN						
2	4-9-75	0840		74	74	1.6×10⁻⁸		3.5×10⁻⁷		OPEN						← ION PUMP ON RANGE
3	"	0845		74	74	1.3×10⁻⁸		1.5×10⁻⁵		CLOSED						CONTROL OFF
4	"	0850		74	74	1.5×10⁻⁸		1.4×10⁻⁵		"						
5	"	0855		74	74	1.3×10⁻⁸		1.4×10⁻⁵		"						
6	"	0900		74	74	1.3×10⁻⁸		1.×10⁻⁵		"						
7	"	1000		75	75	1.3×10⁻⁸		1.1×10⁻⁵		"						
8	"	1010		75	75	1.3×10⁻⁸		1.1×10⁻⁵		"						← ION PUMP OFF
9	"	1015		75	75	1.3×10⁻⁸		7×10⁻⁵		"						
10	"	1020		75	75	1.×10⁻⁸		8.1×10⁻⁵		"						
11	"	1025		75	75	1.5×10⁻⁸		9×10⁻⁵		"						
12	"	1030		75	75	1.3×10⁻⁸		9.5×10⁻⁵		"						
13	"	1035		75	75	1.3×10⁻⁸		1×10⁻⁴		"						
14	"	1040		75	75	1.3×10⁻⁸		1.2×10⁻⁴		"					←	START 1 hour running
15	"	1130		75	75	1.3×10⁻⁸		1.7×10⁻⁴		"						
16	"	1300		75	76	1.3×10⁻⁸		2.2×10⁻⁴		"						
17	"	1400		76	76	1.3×10⁻⁸		2.6×10⁻⁴		"						
18	"	1400		76	76	1.3×10⁻⁸		2.8×10⁻⁴		"						
19	"	1500		76	76	1.3×10⁻⁸		3.2×10⁻⁴		"						
20	4-10-75	0700		74	74			3.1×10⁻⁴		"						
21	4-10-75	0800		74	74			3.1×10⁻⁴		"						

LAB DATA SHEET

FORM #1332A

P.O. 3400-250335-01-0500 DATE 4-9-75

F. 9560/13

TEST PURPOSE _____

BAROM _____ TEMP 74 TEST PERS. _____

NO.	DATE	TIME	3	ENVIR. PORER TEMP/HUM	SYSTEM 5	6	7	MANIFOLD VACUUM 8	MANIFOLD VACUUM 9	HAND VALVE 10	11	12	13	14	15	REMARKS
1	4-9-75	0900		74	74			3.1×10^{-4}		CLOSED						
2	"	1000		76	75			3.1×10^{-4}		"						
3	"	1100		76	76			3.2×10^{-4}		"						
4	"	1200		76	76			2.8×10^{-4}		"						
5	"	1300		76	76			2.1×10^{-4}		"						
6	"	1400		76	76			3.2×10^{-4}		"						
7	"	1500		76	76			3.2×10^{-4}		"						
8	"	1600		76	76			3.2×10^{-4}		"						
9	"	1700		76	76			3.1×10^{-4}		"						
10	4-10-75	0900		76	75			3.1×10^{-4}		"						
11	"	1100		75	75			2.1×10^{-4}		"						
12	"	1400		75	75			3.1×10^{-4}		"						
13	4-13-75	0900		73	73			3×10^{-4}		"						
14	4-14-75	0900		76	76			3.3×10^{-4}		"						
15	4-14-75	1400		74	74			3.7×10^{-4}		"						
16	"	1700		75	75			3.8×10^{-4}		"						
17	4-15-75	0900		76	76			4×10^{-4}		"						
18	"	1200		76	76			4×10^{-4}		"						
19	"	1600		76	76			4.1×10^{-4}		"						
20	4-16-75	0900		75	75			4.1×10^{-4}		"						
21	"	1100		76	76			4.1×10^{-4}		"						

LAB DATA SHEET

WO 3400 250358-07-0500 DATE 4-9-75 TEST PURPOSE VACUUM DECAY

P.R. 9526243

S.N.

TEMP 77 BAROM TEST PERS. C. J. Boyce

NO.	DATE	TIME	ROOM TEMP.	PURGE TEMP.	SYSTEM VACUUM	MANIFOLD VACUUM	HAND VALVE	12	13	14	15	REMARKS
1	4-16-75	1700	76	76	3.8x10⁻⁷	4.2x10⁻⁷	CLOSED					REPLACED 1 CM TUBE
2	4-17-75	0700	74	74	6.4x10⁻⁸	4x10⁻⁴	"					IN SYSTEM VACUUM
3	"	1300	75	75	6.5x10⁻⁸	4.3x10⁻⁴	"					
4	"	1700	75	75	8x10⁻⁸	4.3x10⁻⁴	"					
5	4-18-75	0700	75	75	6.6x10⁻⁸	4.3x10⁻⁴	"					
6	"	1500	75	75	6.6x10⁻⁸	4.1x10⁻⁴	"					
7	4-20-75	0700	74	74		4.2x10⁻⁴	"					
8	"	1230	76	76	3.6x10⁻⁸	4.5x10⁻⁴	"					
9	"	1500	76	76	5.1x10⁻⁸	4.5x10⁻⁴	"					
10	4-22-75	0700	76	76	4.2x10⁻⁸	4.5x10⁻⁴	"					
11	"	1700	76	76	4.2x10⁻⁸	4.4x10⁻⁴	"					
12	4-23-75	0700	75	75	2x10⁻⁸	4.4x10⁻⁴	"					
13	"	1430	76	76	2.1x10⁻⁸	4.5x10⁻⁴	"					
14	4-24-75	0700	74	74	1.4x10⁻⁸	4.4x10⁻⁴	"					
15	"	1525	75	75	2x10⁻⁸	4.5x10⁻⁴	"					
16	4-25-75	0700	72	72	1.7x10⁻⁸	4.4x10⁻⁴	"					
17	"	1500	74	74	1.8x10⁻⁸	4.4x10⁻⁴	"					
18	4-28-75	0700	72	72		3.8x10⁻⁴	"					
19	"	0650	75	75	2.1x10⁻⁸	4.2x10⁻⁴	"					
20	4-29-75	0700	75	75	2.2x10⁻⁸	4.3x10⁻⁴	"					
21	"	1500	76	76	1.9x10⁻⁸	4.6x10⁻⁴	"					

GARRETT AIRESEARCH MANUFACTURING COMPANY OF CALIFORNIA

75-11607

Page 4-7

LAB DATA SHEET

FORM #13273A

No. 3400-25C33S-01-05C3   DATE 4-9-75   TEST PURPOSE VACUUM DECAY

'95-6643

BAROM.

TEMP 74   TEST PERS. A.J. Boyle

DATE	TIME	CENTRIFUGE TEMP.	OVEN TEMP.	5	6	7	SYSTEM VACUUM	MANIFOLD VACUUM	HAND VALVE	11	12	13	14	15	REMARKS
4-30-75	0700	75	75			2X10⁻⁸	4.5X10⁻⁴	CLOSED							
"	1500	77	77			2.2X10⁻⁸	4.6X10⁻⁴	"							
5-1-75	0700	74	74				4.3X10⁻⁴	"							
"	1530	75	75				4.4X10⁻⁴	"							
5-2-75	0700	73	73				7.2X10⁻⁴	"							
"	1530	75	75				4.3X10⁻⁴	"							
5-3-75	0700	72	72				4.1X10⁻⁴	"							
"	1405	73	73				4.1X10⁻⁴	"							
5-5-75	0700	73	73				3.3X10⁻⁴	"							
"	1700	74	74				2.5X10⁻⁴	"							
5-6-75	0700	74	74			3X10⁻⁸	2.8X10⁻⁴	"							
"	1500	76	76			3.3X10⁻⁸	4X10⁻⁴	"							
5-7-75	0700	75	75			1.96X10⁻⁸	7X10⁻⁴	"							
"	1700	77	77			2.2X10⁻⁸	4.4X10⁻⁴	"							
5-8-75	0700	75	75			1.4X10⁻⁸	4.3X10⁻⁴	"							
"	1700	77	77			2.2X10⁻⁸	4.6X10⁻⁴	"							
5-9-75	0700	74	74			2X10⁻⁸	4.3X10⁻⁴	"							
"	1200	75	75			2X10⁻⁸	4.3X10⁻⁴	"							
"	1205	75	75			6.4X10⁻⁸	1.8X10⁻⁶	OPEN							

← OPEN HAND VALVE

⇐ CONTINUE ON FURNACE RECORD SHEET 4

HYDROGEN TANK 851240-
3400-250338-01-0601

			FILL TEMP.				SHIELD TEMP.				
DATE	TIME	ELAPSED TIME	T_1 A-B Ω	T_1 B-C Ω	T_1 AB-BC Ω	T_1 Temp °F	T_2 EF Ω	T_1 FG Ω	T_2 EF-FG Ω	T_2 Temp °F	T_3
MAY 27 73	10:30	—	543.98	1.534	542.446	+70.678	544.75	1.255	543.495	+71.640	547
	15:00	—	UNIT	NOT	STABLE		ENOUGH	FOR	RESISTANCE		
28	08:05	17.1	3.672	.806	2.866	-421	~~27.50~~ 24.550	~~.284~~ .334	~~27.216~~ 27.777	~~-37~~ -411	7.3
	11:11	20.2	3.750	.803	2.947	-421	34.91	.289	34.621	-373	8.1
	13:11	22.2	3.760	.802	2.958	-422.5	29.40	.286	29.114	-379	6.3
	15:11	24.2	3.754	.802	2.952	-422.5	29.40	.283	29.117	-379	7.6
29	08:11	41.2	3.757	.798	2.959	-422	34.80	.285	34.515	-373	8.6
	9:11	42.2	3.760	.799	2.961	-422	36.30	.285	36.015	-372	8.8
	10:11	43.2	3.760	.799	2.961	-422	38.00	.285	37.715	-370	9.2
	11:11	44.2	3.747	.799	2.948	-421	37.798	.283	37.515	-370	9.2
	12:11	45.2	3.760	.800	2.960	-422	38.100	.283	37.812	-370	9.2
	13:11	46.2	3.750	.800	2.950	-422	37.300	.285	37.015	-370	9.5
	14:11	47.2	3.750	.803	2.947	-422	37.800	.285	37.512	-370	9.7
	15:11	48.2	3.750	.804	2.946	-422	34.700	.285	34.412	-373	9.3
	16:11	49.2	3.760	.805	2.955	-422	35.200	.288	34.912	-373	9.4
30	08:11	65.2	3.720	.771	2.949	-422	41.500	.283	41.217	-367	11.4
	9:11	66.2	3.730	.773	2.957	-422	40.400	.284	40.116	-367	11.2
	10:11	67.2	3.730	.777	2.953	-422	39.100	.285	38.815	-368	11.01
	11:11	68.2	3.727	.782	2.945	-422	37.700	.285	37.415	-370	11.0
	12:11	69.2	3.732	.785	2.947	-422	37.870	.288	37.582	-370	11.1
	14:11	71.2	3.729	.785	2.944	-422	38.200	.289	37.911	-370	11.5
	16:11	73.2	3.740	.790	2.950	-422	38.900	.290	38.610	-369	11.8
JUNE 2	08:11	137.2	3.720	.780	2.940	-422	40.479	.294	40.185	-368	16.4
	08:30	137.5	—								
	13:00	142.0	3.515	.781	2.734	-422	39.243	.296	38.947	-369	16.2
	14:15	143.25	3.726	.283	2.943	-422	44.756	.297	44.459	-364	19.2
	16:15	145.25	3.498	.283	3.215	-421	39.994	.297	39.694	-368	16.4
3	08:15	161.25	3.698	.771	2.927	-422	59.398	.299	59.099	-352	24.6
	10:15	163.25	3.710	.776	2.934	-422	53.898	.298	53.600	-357	24.1
	12:15	165.25	3.709	.777	2.932	-422	49.798	.298	49.500	-359	22.6
	14:15	167.25	3.712	.777	2.935	-422	49.499	.299	49.200	-359	22.4
4	16:15	169.25	3.713	.778	2.935	-422	49.264	.300	48.964	-360	22.4
4	08:15	185.25	3.875	.777	2.998	-422	54.800	.302	54.498	-355	26.6
	10:15	187.25	3.706	.779	2.927	-422	51.100	.303	50.797	-357	25.0
	12:15	189.25	3.694	.770	2.924	-422	50.900	.302	50.598	-358	24.6
	14:15	191.25	3.696	.771	2.925	-422	50.100	.303	49.797	-359	24.6
	16:15	193.25	3.687	.765	2.922	422	50.100	.303	49.791	-359	24.8

SHIELD TEMP.			VENT TEMP.				LIQUID WEIGHT					
T_1 FG Ω	T_2 EF-FG Ω	T_c Temp °F	T_3 JK Ω	T_3 KL Ω	T_3 JK-KL Ω	T_3 Temp °F	SCALE # WT.	SCALE #2 WT.	GROSS WT.	TARE WT	LIQUID WT. lbs.	⊗
1.255	543.495	+71.640	547.33	5.240	542.090	+70.351	WARM BOTTLE READINGS.					
ROUGH FOR RESISTANCE			READINGS				299.99	282.00	581.97	494.75	87.22	
.384	27.216	-381	7.353	.374	6.979	-411	294.42	278.10	572.52	—	77.99	
.289	34.621	-373	8.720	.390	8.330	-407						
.286	29.114	-379	6.33	.375	5.955	-412.5						
.283	29.117	-379	7.651	.393	7.278	-409						
.285	34.515	-373	8.62	.376	8.224	-408						
.285	36.015	-372	8.82	.378	8.442	-407						
.285	37.215	-370	9.270	.380	8.89	-407	290.78	276.30	567.08	494.75	72.33	
.283	37.515	-370	9.268	.378	8.89	-407						
.283	37.812	-370	9.260	.378	8.882	-407						
.285	38.015	-370	9.500	.382	9.118	-406						
.285	37.512	-370	9.710	.383	9.327	-406						
.285	34.412	-373	9.360	.380	8.980	-406						
.288	34.912	-373	9.490	.380	9.110	-406						
.283	41.217	-367	11.400	.386	11.014	-403						
.284	40.116	-367	11.220	.336	10.834	-403						
.285	38.815	-368	11.080	.385	10.695	-403	296.96	277.36	574.32	506.87	67.45	
.285	37.415	-370	11.050	.384	10.666	-403						
.288	37.582	-370	11.172	.388	10.784	-403						
.289	37.911	-370	11.520	.390	11.130	-402						
.290	38.610	-369	11.850	.392	11.458	-402						
.294	40.185	-368	16.439	.427	16.012	-396						
							288.41	272.60	561.01	506.87	54.14	
.296	38.947	-369	16.220	.423	15.797	-395	295.27	273.20	568.47	514.50	53.97	
.297	44.459	-364	19.219	.426	18.793	-391						
.297	39.699	-368	16.410	.428	15.982	-395						
.299	59.099	-352	24.651	.458	24.193	-384						
.298	53.600	-357	24.178	.449	23.729	-385	292.60	271.30	563.90	514.50	49.40	
.298	49.500	-359	22.609	.440	22.169	-387						
.294	49.200	-359	22.461	.441	22.020	-386						
.300	48.964	-360	22.473	.442	22.031	-386						
.302	54.498	-355	26.645	.460	26.185	-382						
.303	50.797	-357	25.030	.452	24.578	-383	296.20	269.20	559.40	514.50	44.90	
.302	50.598	-358	24.699	.452	24.247	-384						
.303	49.797	-359	24.695	.451	24.244	-384						
.303	49.797	-359	24.820	.455	24.365	-384						

CONTINUE FRAME 2

DATE	TIME	ELAPSED TIME	Δ TIME	WTM	Δ WTM	BARO. "HGA	BARO.	T °F	T̄	K
MAY 28	09:11	0	~	0.0	—	27.02	—	70°		—
	11:11	2.0	2.0	36.56	36.56	27.01	27.015	70°	70°	.815
	13:11	4.0	2.0	120.00	83.44	27.00	27.00	69°	69.5°	.817
	15:11	6.0	2.0	205.09	85.09	26.99	26.99	69°	69°	.816
29	08:11	23.0	17.0	939.63	732.54	27.06	27.01	68	68.5°	.818
	9:11	24.0	1.0	978.50	40.87	27.07	27.06	69°	69°	.819
	10:11	25.0	1.0	1020.60	42.10	27.08	27.07	68°	68.5°	.821
	11:11	26.0	1.0	1064.45	43.85	27.08	27.08	68°	68	.821
	12:11	27.0	1.0	1108.22	43.77	27.06	27.07	68°	68	.821
	13:11	28.0	1.0	1151.34	43.11	27.05	27.05	68°	68°	.821
	14:11	29.0	1.0	1193.17	41.83	27.05	27.05	68°	68°	.821
	15:11	30.0	1.0	1232.58	39.41	27.04	27.04	68°	68°	.820
	16:11	31.0	1.0	1272.74	40.16	27.03	27.03	69°	69	.818
30	08:11	47.0	16.0	1916.39	643.65	27.10	27.06	62°	65.	.828
	9:11	48.0	1.0	1960.18	43.79	27.11	27.11	62°	62°	.836
	10:11	49.0	1.0	2001.85	41.67	27.10	27.10	63	63	.833
	11:11	50.0	1.0	2042.31	40.46	27.10	27.10	65	64	.831
	12:11	51.0	1.0	2081.70	39.39	27.09	27.09	66	66	.826
	14:11	53.0	2.0	2159.62	38.96	27.07	27.08	65	67	.829
	16:11	55.0	2.0	2239.82	40.16	27.06	27.06	70	69	.819
JUNE 2	08:11	119.0	64.0	4767.58	2527.76	27.04	27.05	61	65	.822

TOOK SCALE WTS. — REPLACED GAGE ON VENT. — INSTALLED BA...
LET UNIT STABILIZE —
1130 RECEIVED & INSTALLED BARATRON PRESSURE READ OUT.

	1300	0	—	0.0	—	22.63	27.03	65°	—	—
	14:15	1.25	1.25	48.01	48.01	27.02	27.02	66°		.82
	16:15	3.25	2.0	123.57	75.56	27.00	27.01	66°		.82
3	08:15	19.25	16.0	837.67	714.10	26.94	26.97	58°	62°	.81
	10:15	21.25	2.0	927.89	90.22	26.93	26.93	59	59	.83
	12:15	23.25	2.0	1006.23	78.34	26.93	26.93	61	60	.83
	14:15	25.25	2.0	1033.40	27.17	26.92	26.92	63	62	.83
	16:15	27.25	2.0	1119.90	76.50	26.90		64		.82
4	08:15	43.25	16.0	1830.05	654.15	26.95		62	63	.82
	10:15	45.25	2.0	1894.4	75.35	26.96				.83
	12:15	47.25	2.0	1962.55		26.97				.82
	14:15	49.25	2.0	2041.16	73.58	26.96		65		.82
	16:15	51.25	2.0	2113.42	72.26	26.95		67		.83

TANK 851240-1 S/N 1

0338-01-0601

$$\bar{\omega} = \frac{K e_{sto} \Delta WTM}{\Delta Time}$$

DATA FROM START OF TEST

°F	$\bar{T}$	K	$\bar{\omega}$
70°	—	—	—
70°	70°	.8151	.0836 * Reading NG
69°	69.5°	.8171	.1912
69°	69°	.8162	.1948
68°	68.5°	.8185	.1973
69°	69°	.8190	.1878
68°	68.5°	.8216	.1941
68°	68.5	.8219	.2022
68°	68°	.8213	.2017
68°	68°	.8210	.1986
68°	68°	.8210	.1926
68°	68°	.8207	.1814
69°	69	.8180	.1842
62°	65	.8281	.1887
62°	62°	.8364	.2055
63	63	.8339	.1950
65	64	.8316	.1883
66	66	.8268	.1827
65	67	.8242	.1796
70°	69	.8190	.1837
61	65	.8275	.1828

— INSTALLED BAROSTAT.

READ OCT.

°F	$\bar{T}$	K	$\bar{\omega}$
65°	—	—	—
66°		.8246	.1777
66°		.8240	.1746
58°	62°	.8139	.2038
59	59	.8373	.2119
61	60	.8329	.1830
63	62	.8304	.1796
64		.8253	.1771
62	63	.8285	.1925
65	63	.8317	.1758
65	—	.8253	.1694
65		.8250	.1703
67		.8201	.1662

ΔTime	ΔWTM	BARO.	$\bar{T}$ °F	$\bar{K}$	$\bar{\omega}$	
HRS.						
0	0.0	—	—	—	—	
2	83.44	-27.00	69°	.8171	.1912	
4	168.53	26.995	69°	.8372	.1979	
21	901.07	27.01	69°	.8174	.1967	
22	941.94	27.02	69°	.8177	.1964	
23	984.04	27.03	69°	.8180	.1963	
24	1027.89	27.04	69°	.8184	.1966	
25	1071.66	27.04	69°	.8184	.1968	
26	1114.78	27.04	69°	.8184	.1968	
27	1156.61	27.04	69°	.8184	.1967	
28	1196.02	27.04	69°	.8184	.1962	
29	1236.38	27.04	69°	.8184	.1958	
45	1879.83	27.05	68°	.8210	.1924	
46	1923.62	27.05	68°	.8210	.1926	
47	1965.29	27.05	67°	.8233	.1923	
48	2005.25	27.06	67°	.8236	.1931	
49	2045.14	27.06	67°	.8236	.1928	
51	2123.06	27.06	67°	.8236	.1924	
53	2203.26	27.06	67°	.8236	.1921	END OF REA...
117	4731.03	27.06	67	.8236	.1869	↓ ...

NEW SET-UP ZERO TIME JUNE 2-75 1900

ΔTime	ΔWTM	BARO.	$\bar{T}$ °F	$\bar{K}$	$\bar{\omega}$
1.25	48.01	27.02	66°	.8246	.1???
3.25	123.59	27.01	66	.8243	.1758
19.25	837.61	26.99	65	.8304	.2027
21.25	927.89	26.98	62	.8323	.2039
23.25	1006.23	26.97	62	.8320	.2020
25.25	1083.40	26.96	62	.8317	.2002
27.25	1159.90	26.95	62	.8314	.1986
43.25	1819.05	26.95	62	.8314	.1962
45.25	1894.40	26.95	62	.8314	.1953
47.25	1964.58	26.95	63	.8291	.1932
49.25	2041.16	26.95	63	.8291	.1928
51.25	2113.42	26.95	63	.8291	.1918

TANK PRESSURES

DATE	TIME	ELAPSED TIME	BARO. "HgA	GAUGES		BARATRON		ION PUMP		
				FILL PRESS. PSIG	VENT PRESS. "Hg	VENT PRESS. "Hg		VOLTS	MICRO AMP	PRESS TORR
MAY 28'25	08:05	19.1	29.02					4000	14	4x10^-6
	11:11	20.2	27.01	.				3900	13	2x10^-6
	13:11	22.2	27.00	—	.9psig			3900	10.5	1x10^-6
	15:11	24.2	26.97	—	.9psig			3950	10.	1x10^-6
29	08:11	41.2	27.06	—	.9			3950	12.	2x10^-6
	08:11	42.2	.					3950	11	1x10^-6
	10:11	43.2	27.08	—	.9			3900	10	1x10^-6
	11:11	44.2	27.08	—	.9			3900	8.8	9x10^-7
	12:11	45.2	27.06	—	.9			3950	7.	7x10^-7
	13:11	46.2	27.05	—	.9			3900	8.	8x10^-7
	14:11	47.2	27.05	—	.9			3950	6.	6x10^-7
	15:11	48.2	27.04	—	.9psig			3900	11.	1x10^-6
	16:11	49.2	27.03	.85	1.5 Hg			3950	12.	2x10^-6
30	08:11	65.2	27.10	183	1.48			3900	4.8	3.8x10^-7
	09:11	66.2	27.11	183	1.48			3900	4.5	4x10^-7
	10:11	67.2	27.10	181	1.45			3710	4.5	4x10^-7
	11:11	68.2	27.10	178	1.41			3950	6.	6x10^-7
	12:11	69.2	27.09	178	1.40			3900	5.5	5x10^-7
	14:11	7..2	27.07	178	1.40			3900	10	1x10^-6
	16:11	73.2	27.06	178	1.40			3950	9	9x10^-7
JUNE 2	8:11	137.2	27.05	172	1.28			3850	8	8x10^-7
	13:15	142.25	27.03	174	1.45	1.3830		3850	8.	8x10^-7
	14:15	143.25	27.02	174	1.40	1.3900				
	16:15	145.25	27.00	175	1.40	1.4090		3900	7	8.5x10^-7
3	8:15	161.25	26.94	.77	1.50	1.4600		3850	6.8	5.5x10^-7
	10:15	163.25	26.93	.78	1.50	1.4630		3850	6.5	5.5x10^-7
	12:15	165.25	26.93	177	1.50	1.4610		3900	5.	5x10^-7
	14:15	167.25	26.92	178	1.50	1.4740		3900	5.5	5.5x10^-7
	16:15	169.25	26.90	179	1.60	1.4940		3900	5.5	5.5x10^-7
4	8:15	185.25	26.95	176	1.45	1.4372		3850	5.5	3x10^-7
	10:15	187.25	26.96	175	1.40	1.4162		3850	5.5	3x10^-7
	12:15	189.25	26.97	175	1.40	1.4110		3850	5.5	5.5x10^-7
	14:15	191.25	26.96	175	1.45	1.4200		3850	6.5	6x10^-7
	16:15	193.25	26.95	176	1.45	1.4361		3850	6.	6x10^-7
5	8:15	209.25	27.03	172	1.40	1.3625		3850	5.	5x10^-7
	10:15	211.25	27.03	.71	1.38	1.3570		3900	3.5	5x10^-7
	12:15	213.25	27.03	171	1.35	1.3520		3900	4.5	3.5x10^-7
	14:15	215.25	27.03	171	1.35	1.3520		3950	5	5x10^-7
	16:15	217.25	27.03	171	1.35	1.3550		3900	5.	6x10^-7

FOLDOUT FRAME 1

HYDROGEN TANK 851240-1 S/N1

3400-250338-01-0601

ION PUMP

Volts	Micro-Amp	Press Torr
4000	14	44×10^{-6}
3900	13	5×10^{-6}
3900	10.5	1×10^{-6}
3950	10.	1×10^{-6}
3950	12.	2×10^{-6}
3950	11	1×10^{-6}
3900	10	1×10^{-6}
3900	8.8	9×10^{-7}
3950	7.	7×10^{-7}
3900	8.	8×10^{-7}
3950	6.	6×10^{-7}
3900	11.	1×10^{-6}
3950	12.	2×10^{-6}
3900	4.8	3.8×10^{-7}
3900	4.5	4×10^{-7}
3710	11.5	4×10^{-7}
3950	6.	6×10^{-7}
3900	5.5	5×10^{-7}
3900	10	1×10^{-6}
3950	9	9×10^{-7}
3850	8	8×10^{-7}
3850	8	5×10^{-7}
3900	7	8.5×10^{-7}
3850	6.8	5.5×10^{-7}
3850	6.5	5.5×10^{-7}
3900	5.	5×10^{-7}
3900	5.5	5.5×10^{-7}
3900	5.6	5.5×10^{-7}
3850	3.5	3×10^{-7}
3850	3.5	3×10^{-7}
3850	5.5	5.5×10^{-7}
3850	6.5	6×10^{-7}
3850	6.	6×10^{-7}
3850	3.	2×10^{-7}
3900	3.5	2×10^{-7}
3900	4.5	3.5×10^{-7}
3850	5.	5×10^{-7}
3900	5.	5×10^{-7}

			FILL TEMP.				SHIELD TEMP.			
DATE	TIME	ELAPSED TIME	T₁ AB	T₁ BC	T₁ AB-BC	T₁ TEMP °F	T₂ LL	T₂ LS	T₃ LL-LS	TEMP °F
JUNE 5	08:15	209.25	3.699	.173	2.926	-42.2	59.400	.307	54.093	-352
	09:15	210.25	—							—
	10:15	211.25	3.696	.760	2.936	-42.2	55.300	.305	54.995	-355
	12:15	213.25	3.565	.614	2.951	-42.2	54.100	.307	53.793	-356
	14:15	215.25	3.548	.607	2.941	-42.2	54.200	.308	53.892	-356
	16:15	217.25	3.548	.604	2.942	-42.2	54.600	.310	54.290	356
6	8:15	233.25	3.551	.604	2.947	-422	61.400	.314	61.586	-363
	9:15	234.25								—
	10:15	235.25	3.566	.609	2.957	-422	57.700	.316	57.580	350
	11:15	236.25	3.565	.606	2.959	-422.5	52.800	.316	58.484	353
	13:45	238.92	ROTATED TANK 90°							
	14:45	239.75	22.336	.769	21.567	-356	48.280	.308	47.972	-362
9	8:45	305.25	49.400	1.052	48.348	-361	70.700	.334	70.366	-340
	11:30	308.5	48.452	.392	48.123	-361	61.600	.328	61.272	-350
	13:30	310.5	49.200	1.087	48.113	-360	61.900	.328	61.572	-349
	15:30	312.5	49.485	1.096	48.389	-361	60.970	.328	60.642	-350
10	8:30	329.5	59.800	1.109	58.691	-350	72.090	.343	71.747	-330
	10:30	331.5	56.509	1.114	55.395	-355	66.470	.340	66.130	-345
	12:30	333.5	55.500	1.117	54.383	-356	66.580	.340	66.240	-345
	14:30	335.5	55.517	1.120	54.397	-355	66.600	.340	66.260	-345
	16:30	337.5	56.200	1.121	55.079	-355	68.300	.341	69.959	-343
11	8:30	353.5	86.221	1.057	85.164	-327	97.201	.377	96.824	-318
	TANK ROTATED BACK TO NORMAL POSITION. REMAINING LIQUID A									
	13:30	358.5	3.757	.809	2.948	-422	49.487	.311	49.676	-359
	15:30	360.5	3.789	.850	2.939	-422	54.589	.319	54.270	-356
12	8:30	377.5	3.803	.868	2.935	-422	66.340	.328	66.012	-345
	10:30	379.5	3.810	.868	2.942	-422	65.100	.329	64.771	347
	ROTATED UNIT APPROX. 170° FLOW THRU SUPPLY PORT									
	12:45	381.75	44.368	.638	43.730	-365	53.088	.587	52.501	-357
	14:45	383.75	46.200	.637	45.563	-363	54.013	.623	53.390	-356
13	8:45	401.75	69.357	.659	68.698	-342	81.172	.653	80.519	-332
	10:45	403.75	61.159	.656	60.503	-350	65.700	.646	65.054	-346
	12:45	405.75	57.616	.650	56.966	-353	66.075	.648	65.427	-346
	14:45	407.75	57.300	.649	56.651	-353	66.000	.648	65.352	-346
16	8:45	473.75	170.70	.82	169.88	-254	214.30	.132	213.48	-215
	10:45	475.75	191.32	.86	190.46	-235	246.83	.66	246.07	-190
	12:45	477.25	211.86	.70	211.16	-217	258.60	.93	257.67	-150
	14:45	479.75	231.70	.76	230.94	-200	330.03	.97	329.06	-113

SHIELD TEMP.   VENT TEMP.   LIQUID WEIGHT

T2 °G	T2 °C	T2 TEMP °F	T3 °R	T3 °KL	T3 °R-KL	T3 TEMP °F	SCALE #1 WT.	SCALE #2 WT.	GROSS WT.	TARE WT.	LIQUID WT. LBS	Ti
.307	59.093	-352	30.600	.482	30.118	-378						
							288.00	269.40	557.40	517.14	40.26	
.305	54.995	-355	28.902	.470	28.432	-380						
.307	53.293	-356	28.820	.472	28.348	-379						
.308	53.892	-356	28.990	.423	28.517	-380						
.310	54.290	-356	29.320	.477	28.843	-379						
.314	61.866	-350	35.770	.510	35.260	-512						
							286.15	266.60	552.75	517.14	35.61	
.316	59.380	-350	33.530	.505	33.025	-325						
.316	58.484	-353	33.510	.499	33.011	-375						
							271.34	256.60	527.94			
.308	47.972	-362	9.580	.431	9.149	-406	270.80	256.10	526.90		33.0	
.334	70.366	-340	36.100	.579	35.521	-375	264.76	249.70	514.46		20.5	
.328	61.272	-350	31.992	.542	31.450	-376	260.37	247.51	507.88		14.0	
.328	61.572	-349	31.520	.539	30.981	-377						
.328	60.642	-350	31.539	.538	31.001	-377						
.343	71.747	-330	42.990	.612	42.378	-365	256.83	247.10	503.93		10.0	
.340	66.130	-345	40.197	.591	39.606	.368						
.340	66.240	-345	39.380	.586	38.794	-370						
.340	66.260	-345	39.600	.589	39.011	-369						
.341	89.959	-343	40.300	.594	39.706	-368						
.377	96.824	-318	61.501	.779	60.722	-350	251.50	248.14	499.64		6.85	
REMAINING LIQUID ADDED							240.31	223.40	463.71	REFERENCE WT. BEFORE FILL		
.311	49.626	-359	25.687	.470	25.217	-383	250.85	231.61	482.46	18.75 ADDED		
.319	54.270	-356	32.589	.506	32.083	-375						
.328	66.012	-345	43.140	.557	42.583	-366	248.60	231.11	479.71		20.0	
.329	65.371	-347	42.150	.555	41.595	-365	245.30	249.19	497.99			
THRU SUPPLY PORT												
.587	52.501	-357	3.788	.857	2.931	-422						
.623	53.390	-356	3.813	.900	2.913	-422						
.653	50.519	-332	3.972	1.062	2.910	-422	247.55	245.95	493.50		18.0	
.646	65.054	-346	3.884	.989	2.895	-422						
.648	65.427	-346	3.825	.991	2.884	-422	246.95	245.60	492.55			
.648	65.859	-346	3.880	.985	2.895	-422						
.182	213.48	-215	4.66	2.07	2.59	-259	240.82	241.00	481.82		3.0	
.186	246.07	-196	4.93	2.34	2.59	-259						
.93	257.67	-150	5.29	2.68	2.61	-261	BACK THRU FILL PORT.					
.97	327.06	-113	5.63	3.00	2.63	-263						

WTM

DATE	TIME	ELAPSED TIME	Δ TIME	WTM	ΔWTM	BARO "H₂A	BARO	T	T	K
JUNE 5	08:15	67.25	16.0	2666.24	552.82	27.03	26.99	63°	65°	.825
	10:15	69.25	2.0	2740.68	74.44	27.03		64°		.829
	12:15	71.25	2.0	2810.87	70.19	27.03		65		.827
	14:15	73.25	2.0	2880.90	70.03	27.03		67		.822
	16:15	75.25	2.0	2950.67	69.77	27.03		68		.820
6	8:15	91.25	16.0	3549.75	599.08	27.10	27.07	64	66	.82
	10:15	93.25	2.0	3615.94	66.19	27.10		66		.827
	11:15	94.25	1.0	3649.86	33.92	27.11		67		.825
	13:45	96.75		TANK ROTATED 90°				WTM READING		21
	14:45	1.0	1.0	61.59	46.33	27.09		70		.817
9	8:45	67.0	66.0	2833.38	2771.79	27.06	27.08	65	67	.824
	10:30	68.75	1.75	REMOVED SATURATOR - CHANGED WEIGHTS ON INST.				64		.830
	11:30	69.75	1.0	32.83	32.83	27.05		64		.829
	13:30	71.25	2.0	97.22	64.39	27.03		64		.829
	15:30	73.75	2.0	164.19	66.97	27.01		64		.828
10	8:30	90.75	17.0	763.36	599.17	27.05	27.03	61	63	.8317
	10:30	92.75	2.0	826.35	62.99	27.05		64		.830
	12:30	94.75	2.0	889.57	62.22	27.06		66		.825
	14:30	96.75	2.0	953.42	65.85	27.03		67		.822
	16:30	98.75	2.0	1018.27	64.85	27.04		67		.8229
11	8:30	114.75	16.0	1613.51	575.24	27.10	27.07	60	64	.8307
		TANK ROTATED		BACK TO NORMAL POSITION. REMAINING LIQUID						
	11:30	0.0	—	0.0	—	—				
	13:30	2.0	2.0	75.35	75.35	27.10		67		.8248
	15:30	4.0	2.0	146.68	71.33	27.08		67		.8242
12	8:30	21.0	17.0	761.94	621.20	27.08	27.08	63	65	.8287
	10:30	23.0	2.0	826.85	64.91	27.08		65		.8257
		ROTATED UNIT APPROX 170°								
	10:45	0.0	0.0	0.0	—	—				
	12:45	2.0	2.0	68.66	68.66	27.10		67		.8248
	14:45	4.0	2.0	131.07	62.41	27.09		67		.8245
13	8:45	22.0	18.0	755.12	624.05	27.13	27.11	61	64	.8319
	10:45	24.0	2.0	825.68	70.56	27.14		64		.8529
	12:45	26.0	2.0	890.81	65.13	27.13		66		.8287
	14:45	28.0	2.0	958.26	67.45	27.14		66		.8284
14	8:45	94.0	66.0	3938.70	2781.88	27.06	27.10	62	64	.8316
	10:45	96.0	2.0	4028.91	70.21	27.06		61		.8320
	12:45	98.0	2.0	4117.14	88.13	27.06		61		.8370
	14:45	100.0	2.0	4201.46	84.32	27.03		61		.8369

$$W^\circ = \frac{K \, C_{std} \, AWTM}{A\,TIME}$$

DATA FROM START OF TEST

°F	T	K	W		A TIME	AWTM	BARO	T °F	K	W
63°	65°	.8259	.1601		67.25	2666.24	26.96	63	.8295	.1845
64°		.8294	.1732		69.25	2740.68	26.96	63	.8295	.1842
65		.8272	.1629		71.25	2810.87	26.97	63	.8295	.1837
67		.8226	.1616		73.25	2880.90	26.97	64	.8275	.1826
68		.8204	.1606		75.25	2950.67	26.98	64	.8279	.1821
64	66	.8262	.1736		91.25	3549.75	26.98	64	.8279	.1807
66		.8271	.1534	SEE LOW SHEET #30	93.25	3615.94	26.99	64	.8282	.1802
67		.8251	.1570		94.25	3649.86	27.00	64	.8285	.1800
M READING	21.26									
70		.8176	.2825							
65	67	.8242	.1936							

WEIGHTS ON BAROSTAT. SET WTM TO 0.0

°F	T	K	W
64		.8301	.1529
64		.8294	.1498
64		.8258	.1557
61	63	.8317	.1644
64		.8301	.1467
66		.8258	.1465
67		.8226	.1473
67		.8229	.1497
60	64	.8307	.1733

MAKING LIQUID ADDED. WTM ZEROED.

°F	T	K	W
7		.8248	.1743
7		.8242	.1650
73	65	.8287	.1699
75		.8257	.1507

*WTM REMOVED FOR 10 MIN. ADDED 5.94 TO TOTAL FLOW FOR AVERAGE.

THRU SUPPLY LINE. WTM ZEROED.

°F	T	K	W
7		.8248	.1589
7		.8245	.1444
71	64	.8319	.1618
74		.8329	.1649
76		.8287	.1514
76		.8284	.1568
72	64	.8316	.1840
81		.8370	.2119
81		.8370	~~2072~~ —
81		.8341	.1975

FLOW THRU FILL PORT.

FOLDOUT

HYDROGEN TANK 851240-1   S/N
3400-250338-01-0601

TANK PRESSURES

DATE	TIME	ELAPSED TIME	GAUGES BARO "HgA	FILL PRESS PSIG	VENT PRESS "Hg	BARATRON VENT PRESS "Hg	ION PUMP VOLTS	MICRO AMP	P
JUNE 6	08:15	233.25	27.10	.68	1.30	1.2910	3900	3.5	2.3
	10:15	235.25	27.10	.80	1.53	1.5250	3900	11.5	3X
	11:15	236.25	27.11	.80	1.50	1.5250	3900	41.5	3X
	14:45	239.75	27.09	.67	1.30	1.3120	3900	50.	4X
	15:45	240.75	—	—	—	—	3900	34.5	2X
9	8:45	305.75	27.06	.69	1.33	1.3310	3900	35.5	2.5X
	11:30	308.5	27.05	7.02 "H2O	.52	0.5405	3900	19.	9X
	13:30	310.5	27.03	7.3 "H2O	.54	0.5515	3850	11.5	0X
	15:30	312.5	27.01	7.4	.55	0.5690	3900	23.	1.5X
10	8:30	329.5	27.05	7.4	.50	0.5210	3900	38.5	2.7X
	10:30	331.5	27.05	7.4	.50	0.5210	3850	19.5	.9X
	12:30	333.5	27.06	7.4	.50	0.5210	3900	17.5	16X
	14:30	335.5	27.03	7.6	.52	0.5485	3900	17.	.6X
	16:30	337.5	27.04	7.5	.52	0.5400	3900	15.	.5X
11	8:30	353.5	27.10	7.0	.47	0.4800	3500	NOT STABL	

TANK ROTATED BACK TO NORMAL POSITION & REF...

DATE	TIME	ELAPSED TIME	BARO "HgA	FILL PRESS	VENT PRESS "Hg	BARATRON VENT PRESS "Hg	VOLTS	MICRO AMP	P
	13:30	358.5	27.10	5.0 "H2O	2.7 "Hg	0.2620	3900	10.	0X
	15:30	360.5	27.08	5.06 "	2.6 "	0.2700	3900	11	0X
12	8:30	377.5	27.08	4.77 "	2.4 "	0.2550	3850	14.	5X
	10:30	379.5	27.08	4.8 "	2.4 "	0.2610	3700	13	3X

TANK ROTATED APPROX 170° FLOW THRU SUPPLY PORT

DATE	TIME	ELAPSED TIME	BARO "HgA	FILL "H2O	SUPPLY "Hg	BARATRON "Hg	VOLTS	MICRO AMP	P
	12:45	381.75	27.10	4.75 "H2O	2.2 "Hg	0.2450	3800	90	9X
	14:45	383.75	27.09	4.86 "	2.3 "	0.2510	3900	19	.9X
13	8:45	401.75	27.13	5.53 "	2.2 "	0.2500	3700	220	4X
	10:45	403.75	27.14	4.56 "	1.9 "	0.2250	3900	32	2X
	12:45	405.75	27.15	4.54 "	1.9 "	0.2190	3850	22	1X
	14:45	407.75	27.14	4.6 "	1.9 "	0.2250	3700	25	.5X
16	8:45	473.25	27.06	8.55 "	.29 "	0.3140	1900	25 MA	1.5
	10:45	475.75	27.06	9.05 "	.29 "	0.3080	1550	29 MA	0X
	12:45	477.75	27.06	.28 "H2O	5.95 "H2O	0.3030	1400	31 MA	
	14:45	479.75	27.03	.30 "	6.10 "	0.360	1300	31 MA	

ION Pump

VOLTS	MICRO-AMP	PRESS. TORR.
3900	3.5	2.3×10^{-7}
3900	11.5	3×10^{-7}
3900	21.5	3×10^{-7}
3900	50.	4×10^{-6}
3900	34.5	2×10^{-6}
3900	35.5	2.5×10^{-6}
3900	19.	9×10^{-6}
3850	11.5	6×10^{-6}
3900	23.	1.5×10^{-6}
3900	38.5	2.7×10^{-6}
3850	19.5	$.9 \times 10^{-6}$
3900	17.5	1.6×10^{-6}
3900	17.	$.6 \times 10^{-6}$
3900	15.	$.5 \times 10^{-6}$
3500	NOT STABLE.	

- SEE LOG PAGE #30 To EXPLAIN TANK PRESSURE RISE

TANK ROTATED.

POSITION + REFILLED WITH LIQUID WE HAD LEFT. 1.5 LBS REMOVED FROM BAROSTAT

VOLTS	MICRO-AMP	PRESS. TORR.
3900	10.	6×10^{-6}
3900	11.	6×10^{-6}
3850	14.	5×10^{-6}
3700	13	3×10^{-6}

RU SUPPLY PORT.			VENT. PORT PRES
3800	90	9×10^{-6}	5.57 H₂O
3900	19	$.9 \times 10^{-6}$	5.68 "
3700	220	4×10^{-5}	6.3 "
3900	32	2×10^{-6}	5.3 "
3850	22	1×10^{-6}	5.3 "
3700	25	$.5 \times 10^{-6}$	5.35 "
1900	2.5 MA.	1.5×10^{-4}	9.30 "
1550	29 MA. OFF SCALE		9.50 "
1400	31 MA " "		5.23 H₂O FLOW THRU FILL PORT.
1300	31 MA " "		5.36 "

DATE	TIME	ELAPSED TIME	$T_1 \frac{A-B}{2}$	$T_1 \frac{BC}{2}$	$T_1 \frac{AB-BC}{2}$	T_1 Temp °F	$T_2 \frac{EF}{2}$	$T_2 \frac{FG}{2}$	$T_2 \frac{EF-FG}{2}$	T_2
6-19-75	08:45	0.0	3.664	.775	2.889	-422	37.500	.283	37.217	
	10:45	2.0	3.673	.765	2.908	-422	39.400	.280	39.120	
	12:45	4.0	3.693	.778	2.915	-422	39.400	.281	39.119	
	14:45	6.0	3.686	.777	2.909	-422	40.066	.281	39.785	
20	8:45	24.0	3.682	.774	2.908	-422	40.310	.282	40.028	
	10:45	26.0	3.700	.786	2.920	-422	40.000	.256	39.714	
	12:45	28.0	3.695	.781	2.914	-422	39.710	.256	39.422	
	14:45	30.0	3.697	.774	2.923	-422	40.490	.288	40.202	
23	8:45	96.0	3.691	.779	2.912	-422	42.031	.297	46.134	
	fill complete 10:05	UNIT	TOPPED OF	WITH	LIQUID	& ROTATED	APPROX	170°		
	12:45	0.0	4.000	.534	3.466	-419.5	46.300	.653	45.647	
	14:45	2.0	3.727	.509	3.218	-421	49.407	.683	48.724	
24	8:45	20.0	7.500	.443	7.052	-409.5	82.000	.712	81.288	
	10:45	22.0	7.530	.460	7.070	-410	77.870	.707	77.163	
	12:45	24.0	7.640	.467	7.173	-409.5	68.425	.697	67.728	
	14:45	26.0	7.930	.467	7.463	-408.5	68.420	.695	67.725	
25	8:45	44.0	10.840	.459	10.391	-405.5	80.300	.708	80.599	
	10:45	46.0	10.520	.462	10.058	-404	63.400	.690	62.710	
	12:45	48.0	11.120	.405	10.715	-40.3	63.605	.634	62.916	
	14:45	50.0	11.326	.413	10.913	-402.5	61.454	.689	60.965	
26	8:45	68.0	12.203	.405	12.798	-39.7.5	61.160	.612	60.465	
	10:45	70.0	13.252	.410	12.842	-399	58.805	.692	58.113	
	12:45	72.0	13.226	.433	13.363	-3.39	59.045	.694	59.001	
	14:45	74.0	14.403	.433	13.640		59.698	.695	59.004	
27	8:45	92.0	16.365	.432	15.933	-394.8	62.102	.690	61.407	
	9:45	93.0	15.532	.440	15.092	-376.3	57.736	.691	57.045	
	12:45	96.0	16.461	.442	16.019	-374.5	58.891	.691	58.200	

FIELD TEMP.   VENT TEMP.   LIQUID WEIGHT

FG	T_2 EF-FG	T_2 temp°F	T_3 JK	T_3 KL	T_3 JK-KL	T_3 Temp°F	SCALE #1 WT	SCALE #2 WT	GROSS WT	TARE WT	LIQUID WT. LB	Δ WT. LB
83	39.217	-369	7.401	.378	7.023	-409.5	279.76	265.60	545.36	468.90	76.46	9.76
80	39.120	-369	7.413	.374	7.039	-409.5						
81	39.119	-369	7.503	.375	7.128	-409						
81	39.785	-368.5	7.666	.376	7.290	-409						
82	40.028	-368	9.061	.379	8.682	-411.5	277.10	263.30	540.40	468.90	71.50	4.96
86	39.714	-368.5	9.282	.382	8.900	-406						
86	39.422	-368.5	9.432	.383	9.049	-405						
88	40.202	-368.3	9.480	.386	9.094	-405	BATT REMOVED 14:20					
297	16.234	-362	16.031	.422	15.609	-395	269.20	256.53	526.23	468.90	57.33	14.17
APPROX 170°	—		—		—	—	285.31	269.70	555.01	468.90	86.11	
53	45.647	-363	3.899	.869	3.030	-421	275.09	275.62	553.71	468.90	84.81	1.30
683	48.724	-360.3	3.947	.909	3.038	-421						
712	55.258	-327	4.125	1.081	3.044	-421	273.29	276.03	549.32	470.10 NEW TARE	79.22	5.59
707	77.163	-325	4.070	1.030	3.040	-421.5						
697	67.728	-345	4.025	.975	3.050	-421.5						
69.5	67.725	-345	4.020	.966	3.054	-421.5						
708	74.595	-332	4.107	1.046	3.061	-421.5	269.44	271.80	541.24	470.10	71.14	8.08
690	62.710	-348	3.963	.948	3.015	-421.5						
684	62.916	-348	3.955	.942	3.013	-421.5						
639	60.965	-348	3.955	.941	3.014	-421.5						
672	60.465	-347	3.960	.949	3.011	-421.5	266.20	268.18	534.38	470.10	64.18	6.36
692	58.113	-350	3.949	.936	3.013	-421.5						
694	59.051	-350	3.943	.945	3.007	-421.5						
683	59.604	-350	3.964	.949	3.015	-421.5						
695	61.407	-350	3.982	.957	3.025	-421.5						
691	57.045	-354	3.934	.936	2.998	-421.5	263.54	265.60	529.14	470.10	59.04	5.74
691	58.200	-357	3.942	.945	2.997	-421.5						

				WTM						
DATE	TIME	ELAPSED TIME	Δ TIME	WTM	Δ WTM	BARO "Hg	BARO	TEMP °F	TEMP °F	K
6-19-25	8:45	0.0	—	1.50	—	27.05	—	64°	—	—
	10:45	2.0	2.0	74.94	73.44	27.08	—	60°	—	.8379
	12:45	4.0	2.0	156.60	81.66	27.08		58	—	.8443
	14:45	6.0	2.0	237.45	80.85	27.08	—	57	.	.8465
20	8:45	24.0	18.0	1080.02	842.57	27.06	27.07	54	56	.8483
	10:45	26.0	2.0	1154.80	74.78	27.16	27.11	56	55	.8515
	12:45	28.0	2.0	1228.77	73.97	27.17		57		.8493
	14:45	30.0	2.0	1303.89	75.12	27.16		58	BALL REMOVED 14:20	.8471
23	8:45	96.0	66.0	3895.14	2591.25	27.15	27.15	61	66	.8421
		—	UNIT	REFILLED		WITH	LIQUID	NITH		
	12:45	0.0	0.0	0.0	—	27.09	—	64	—	—
	14:45	2.0	2.0	90.59	90.59	27.12	—	65	—	.8300
24	8:45	20.0	18.0	1086.02	995.43	27.22	27.17	64_	64	.8338
	10:45	22.0	2.0	1193.95	107.93	27.23		53		.8599
	12:45	24.0	2.0	1292.67	98.72	27.22		55		.8553
	14:45	26.0	2.0	1393.50	100.82	27.20		56		.8525
25	8:45	44.0	18.0	2352.26	958.76	27.27	27.23	53	55	.8556
	10:45	46.0	2.0	2453.08	100.82	27.25		54		.8584
	12:45	48.0	2.0	2544.75	91.67	27.23		56		.8534
	14:45	50.0	2.0	2633.96	89.21	27.20		56		.8481
26	8:45	68.0	18.0	3427.64	793.68	27.14	27.17	55	55	.8470
	10:45	70.0	2.0	3512.09	84.45	27.13		60		.8520
	12:45	72.0	2.0	3576.40	64.10	27.11		65		.847
	14:45	74.0	2.0	3663.91	87.81	27.10		66		.8371
27	8:45	92.0	18.0	4492.16	808.25	27.10	27.10	_61	61	.8283
	9:45									
	12:45	96.0	4.0	4573.88	81.72	27.09		66		.8275

DATA FROM START OF TEST.

TEMP °F	K	ω	ZERO TIME	Δ TIME	Δ WTM	BARO	TEMP	K	ω	TOTAL WT. LB
	—	—		0.0	—	—	—	—	—	
—	.8399	.1730		2.0	73.44	27.08	60°	.8399	.1730	
—	.8443	.1934		4.0	155.10	27.07	61°	.8374	.1822	—
--	.8465	.1920		6.0	235.95	27.07	60°	.8396	.1853	
56	.8483	.2228		14.0	1078.52	27.07	58	.8440	.2128	5.11
55	.8515	.1787		26.0	1153.30	27.08	58	.8443	.2102	
	.8493	.1763		28.0	1227.27	27.10	58	.8449	.2078	
BALL REMOVED 14:20	.8471	.1785		30.0	1302.39	27.10	58	.8449	.2058	
66	.8421	.1855		96.0	3893.64	27.11	56	.8452	.1923	
LIQUID X	ROTATED	APPROX			170°	—	—	—	—	
					—	—	—	—	—	
—	.8300	.2110		2.0	90.59	27.12	65	8300	.2110	
64	.8338	.2587		20.0	1086.02	27.17	64	.8331	.2538	5.08
	.8599	.2603		22.0	1193.95	27.19	61	.8412	.2561	
	.8553	.2369		24.0	1292.67	27.20	59	.8459	.2556	
	.8525	.2411		26.0	1393.50	27.20	59	.8459	.2544	
55	.8556	.2557		44.0	2352.26	27.21	58	.8484	.2545	6.08
	.8584	.2428		46.0	2453.08	27.21	57	.8506	.2545	
	.8534	.2195		48.0	2544.75	27.22	57	.8509	.2531	
	.8741	.2123		50.0	2635.96	27.22	57	.8507	.2515	
55	.8471	.2076		65.0	3427.64	27.21	57	.8506	.2466	5.72
	.8376	.1932		70.0	3512.06	27.20	58	.8481	.2557	
	.8329	.2006		72.0	3598.00	27.19	59	.8473	.2376	
	.8271	.2037		74.0	3683.91	27.17	59	.8456	.2362	
61	.8283	.2101		92.0	4492.16	27.10	61	.8475	.2321	5.57
	.8275	.1895		96.0	4573.88	27.09	66	.8481	.2267	

TIME | TANK PRESSURES | ION PUMP

DATE	TIME	ELAPSED TIME	FILL Press	VENT Press	SUP. Press	BARATRON	VOLTS	MICROAMPS	PRESS TEMP
6-19-75	08:45	0.0	.23	3.5	—	0.2740	3850	30	2X1
	10:45	2.0	6.85 H2O	3.25 H2O		0.3000	3800	40	3.1X1
	12:45	4.0	6.80	3.75		0.2900		21	1.5X1
	14:45	6.0	6.50	3.25		0.2900			.5X1
20	8:45	24.0	6.10	3.13		0.2430			19X1
	10:45	26.0	5.85	3.04		0.2330			2.2X1
	12:45	28.0	5.74	2.92		0.2270			2X10
	14:45	30.0	5.67	2.80		0.2225	BALL PEAKING 14:20 3975	39.9	2.9X1
23	8:45	96.0	6.21	5.20		0.2850			2.3X1
	UNIT REFILLED WITH LIQUID B ROTATED APPROX 110°								
	12:45	0.0	GAGE No. PSIG .23	—	3.37	0.2620	3900	54	1.2X1
	14:45	2.0	.23	—	4.0	0.3050	3850	61	1.5X
24	8:45	20.0	.34	—	4.5	0.3350			1X10
	10:45	22.0	.27	—	3.8	0.2460	3750		10
	12:45	24.0	.22	—	3.25	0.2500		55	1.2X
	14:45	26.0	.20	—	3.22	0.2500			4.6X
25	8:45	44.0	.27	—	3.56	0.2240		57	5X1
	10:45	46.0	.17	—	2.70	0.2110	3900	30	2.2X1
	12:45	48.0	.16	—	2.69	0.2090			2.2X1
	14:45	50.0	.16	—	2.96	0.2250		51	2.4X1
26	8:45	68.0	.18	—	3.50	0.2320			2X1
	10:45	70.0	.17	—	4.0	0.2710		51	2X10
	12:45	72.0	.155	—	3.25				10
	14:45	74.0	.20	—	3.92				X10
27	8:45	92.0	.21		3.75	0.310	3850	72	3.8
	9:45	93.0	.19		2.95	0.270		33	2X1
	12:45	96.0	.10		2.47	0.120			4.5

ION PUMP

VOLTS	MICRONS	PRESS. TORR
3850	30	2.8×10⁻⁶
3800	50	3.1×10⁻⁶
3700	24	1.2×10⁻⁶
3850	47	1.5×10⁻⁶
3800	32	1.9×10⁻⁶
3900	53	2.2×10⁻⁶
3850	43	3×10⁻⁶
3750	27.9	2.9×10⁻⁶
3850	34	2.3×10⁻⁶

APPROX 170°

3900	54	1.2×10⁻⁶
3850	60	4.5×10⁻⁶
3800	22.5	1×10⁻⁶
3950	10	~ 10⁻⁶
3900	25	1.2×10⁻⁶
3800	20	4.6×10⁻⁶
3850	24	2.5×10⁻⁶
3900	30	2.2×10⁻⁶
3950	33.5	2.6×10⁻⁶
3700	27.	1.4×10⁻⁶
3800	70	2.2×10⁻⁶
3700	53	5×10⁻⁶
3850	50	3.8×10⁻⁶
3900	32	2×10⁻⁶
3850	60	4.5×10⁻⁶